

# THE SURFACE ANALYSIS OF PAPER

*Janet Preston*

Imerys Minerals Ltd.

## Contents

1	Introduction	750
2	Chemical structure	756
2.1	Infra Red (IR) spectroscopy	756
2.1.1	Attenuated Total Reflectance IR (ATR-IR)	756
2.1.2	Photo Acoustic Spectroscopy (PAS)	758
2.1.3	Examples of uses of IR spectroscopy in paper	758
2.2	Raman spectroscopy	761
2.2.1	Variants of Raman spectroscopy and examples of use in paper	762
2.3	X-Ray Photoelectron Spectroscopy (XPS)	765
2.3.1	Depth profiling	767
2.3.2	Use of XPS for fibres	767
2.3.3	Use of XPS in determining failure at interfaces	768
2.3.4	The use of XPS to determine surface chemistry of coatings	769
2.3.5	XPS for analysis of paper surface treatments	771
2.4	Secondary Ion Mass Spectrometry (SIMS)	774
2.4.1	Applications of SIMS in paper	777
2.5	UV analysis of surface binder content	782
3	Electron microscopy	783
3.1	Scanning Electron Microscopy (SEM)	783
3.1.1	Examples of SEM use in paper	784
3.1.2	SEM for topography analysis	785
3.1.3	Staining and cross sections	786
3.1.4	SEM and Image analysis	787
3.1.5	Dispersive X-Ray analysis EDX on SEM	790
3.2	Transmission Electron Microscopy (TEM)	791
4	Paper topography	793
4.1	Air leak methods	793
4.2	Profilometry & interferometry	794

4.3	Imaging reflectometry	796
4.4	Confocal laser scanning microscopy	796
4.4.1	Examples of confocal laser scanning microscopy in paper – Topography	798
4.4.2	Examples of confocal laser scanning microscopy in paper – Coating analysis	799
4.5	Atomic Force Microscopy (AFM)	800
4.5.1	Examples of use of AFM in paper	801
4.5.2	Studies of latex coalescence	802
4.5.3	AFM in print evaluations	803
5	Other physical analysis	804
5.1	Optical microscopy	804
5.2	Focussed Ion Beam (FIB)	805
5.2.1	Examples of FIB use in studying coating structure and ink penetration	806
5.3	XRD	809
5.4	Fluid absorption	811
5.5	Mercury porosimetry	811
6	Combination of techniques	814
7	Summary	818
8	Acknowledgements	819
9	Glossary of abbreviations	819
10	References	822

## 1 INTRODUCTION

Paper consists of a network of wood fibres produced by chemically or mechanically processed wood chips, combined with ‘fines’ particles (vessels, ray cells, fibrils, microfibrils and parenchyma cells) and mineral fillers such as kaolin or calcium carbonate. A good description of the wood fibres and chemistry involved is given by Roberts [1]. Paper is made both as an uncoated and coated substrate depending upon the end use requirement. For coated papers the surface fibres are often covered with a thin layer of mineral pigment and polymeric binder to improve its optical properties and ‘printability’. Common minerals for filling and coating include kaolin, calcium carbonate (both natural ground and precipitated) and talc. Filler minerals are often produced as flocculated slurries or containing very low dispersant doses. For coating applications where high solids is important, dispersants such as sodium polyacrylate are always used. For coatings the mineral slurry is combined with a polymeric latex binder and a thickener (usually a modified natural polysaccharide or a synthetic polymer) to form a coating ‘colour’.

The coating colour may contain small quantities of other additives such as biocides, optical brightening agents, lubricants and surfactants. The coating colour is applied to the base paper with an applicator, which may be a roller, rod, blade or jet. The excess coating colour is usually removed with a metering blade or rod, resulting in a uniform coating of controlled coat weight (mass per unit area) to a typical thickness of 8–30  $\mu\text{m}$  depending on application. Pre-metering methods are also used for example: metered size press coating, spray coating and curtain coating. The final coating is a porous layer consisting of pigment, binder and air. The amount and distribution of air within the coating is mainly influenced by the particle packing characteristics of the mineral pigments and the proportion of binder present. The air is present throughout the coating structure as a series of small pores (approx. 0.02–1.0  $\mu\text{m}$  diameter) of different sizes, shapes, and connectivity [2], [3]. A good introduction to paper coating is given by Priest [4].

There are numerous grades of paper which have been developed over many years as the major information transfer medium. These cover a range of grammage, quality and constituents depending upon their end use. For each paper grade, both the surface and bulk properties have been modified and optimised to suit the appearance, optical and printing properties required. Surface analysis techniques are currently used for quality control, production developments and competitive analysis.

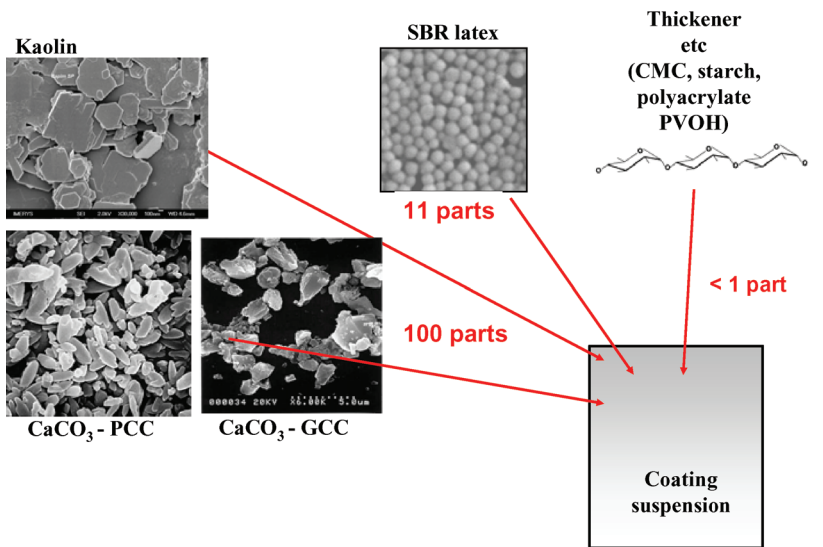
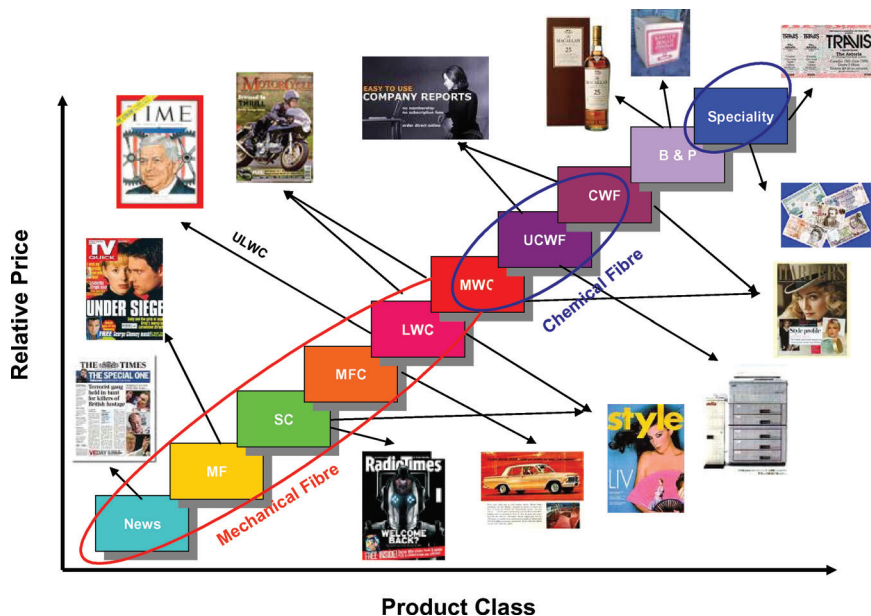


Figure 1. Typical components in a paper coating formulation (J. Husband).



**Figure 2.** There is a wide variety of paper grades available at different qualities, designed to suit their end purpose.

However, more recently rising costs and limited growth in the market have led to over supply of paper and increased competition. The result has been closure and consolidation of paper mills [5]. The growth of the internet is also seen potentially as a problem if advertisers start to prefer electronic media to paper as an information medium. These factors have led to decoupling of the growth of paper from GDP, making future growth in demand difficult to forecast. The industry has responded by cutting costs as much as possible, and also by looking at new innovative ways of using fibre based products. Due to these problems, many companies have responded by developing high value, niche products, in which careful control of the surface is often critical. The accurate determination of surface properties is an important part of facilitating the development of high value products, for example those used in printed electronics, sensors and biologically active printing substrates [6], [7], [8], [9]. This has led to the development of many new techniques in recent years which may be combined to provide a powerful description of the chemical and structural nature of paper.

Surface analysis of paper is often a complex and difficult task. Problems may relate to the use of coating formulations which contain a range of natural products that are very similar in their chemical constituents and therefore difficult to differentiate. The substrate is also inhomogeneous, rough, porous and absorbent. Surface topographical features such as depressions, may sometimes be considered as surface porosity or surface roughness depending upon the technique used to detect and quantify them. Indeed a definition of the surface is not always easy, and the differentiation between surface pores, surface micro-roughness and bulk porosity is often blurred. Chemical signals for example from X-ray Photoelectron Spectroscopy (XPS) or contact angle measurements for surface energy determination are often impacted heavily by the topography and local micro structure of the surface and chemical heterogeneity.

The choice of technique is often governed by the requirements and limitations of the sample. For example the spatial resolution requirements may determine the choice of analysis technique. Some techniques such as Secondary Ion Mass Spectrometry (SIMS) give qualitative or at best semi-quantitative information, whereas others e.g. XPS are quantitative, can be used to determine the amount of chemical constituents in a surface as well as the chemical environment of the elements and give some idea of spatial resolution. There may also be physical constraints on analysis of certain samples. Many instruments operate under a strong vacuum, but this is not suitable for samples which have a highly volatile component, or which are in solution.

A good summary of the criteria for selection of analysis technique was given by Ernstsson and Warnheim [10];

- Analysis depth requirements – how surface sensitive do you need?
- What chemical information is required e.g. elements, functional groups?
- Qualitative or quantitative, or semi quantitative?
- Lateral resolution – do you need to be able to map the distribution of the components?
- Other information required, for example do you need to know the topography of the samples as well as the chemical composition?
- Physical requirements for sample analysis – for example some samples need to be smooth and homogeneous, some need to have a conducting surface and samples which require an ultra high vacuum need to be dry and not in solution.

Table 1 summarises some of the techniques discussed in this review in terms of their analysis area and the information they provide.

A good overview of the basic operating principles of many different surface analytical techniques together with examples of how these can be used to

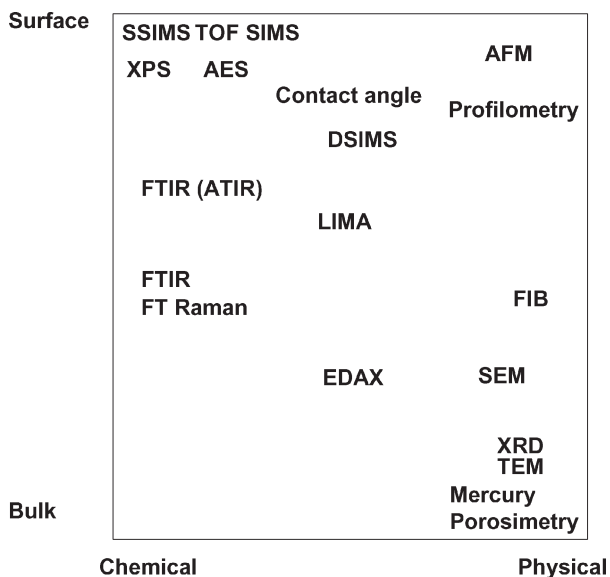


**Figure 3.** Schematic of different analytical techniques included in terms of the nature of their analysis (surface or bulk, chemical or physical – Adapted from Swift and West Ceram).

analyse organic coatings is given by Perry and Somorjai [12]. These include a range of techniques used to a lesser extent in the paper industry such as High Resolution Energy Electron Loss Spectroscopy (HREELS), an electron scattering technique which is ideal for studying surface mono-layers and Ultra-violet Photoelectron Spectroscopy (UPS), which probes the valence bands of materials and the density of the electronic states, and can fingerprint organic materials. Auger Electron Spectroscopy is only really useful in determining chemical structure on conducting samples, and its relevance to paper and printing is limited, as a result it will not be discussed further here. A good review of techniques to probe the optical appearance of paper is given by Dube *et al.* [13] and a good general text for the use of surface analysis in the field of paper and printing is given by Connors and Banerjee [42].

This review mainly covers the chemical analysis of paper, but a short section on physical analysis including mercury porosimetry and topography is also included for completeness, as physical characteristics often affect the same phenomenological properties as paper chemistry. A glossary of abbreviations is appended to this review.

**Table 1.** Summary of different analysis techniques (Adapted from Swift and West [11] and Ernstsson and Warmheim [10]).

<i>Technique</i>	<i>XPS/ESCA</i>	<i>Static SIMS</i>	<i>Dynamic SIMS</i>	<i>ToF-SIMS</i>	<i>FT-IR (ATR)</i>	<i>EDX</i>
<b>Type of sample</b>	Solids and low vapour pressure liquids	Solids and low vapour pressure liquids	Solids	Solids and low vapour pressure liquids	Solids & Liquids	Solids
<b>Species in / analysed</b>	X-rays/electrons	ions or atoms / ions	ions / ions	ions/ions	Photons/Photons	Electrons/X-rays
<b>Sampling depth</b>	1–10 nm	> 1nm	0.5nm–5 µm	1–2 nm	0.5–5 µm	0.5–5 µm
<b>Analysis area</b>	40µm–1cm diameter	50 µm–1 mm diameter	10 µm–1 mm diameter	50 µm–1 mm diameter	1mm <sup>2</sup> –8cm <sup>2</sup>	2µm <sup>2</sup> –3mm <sup>2</sup>
<b>Imaging</b>	Yes, <10µm resolution	Yes, 0.5 µm resolution	Yes, 1 µm resolution	Yes, 0.5 µm resolution	No	Yes, 0.1 µm resolution
<b>Elements detected</b>	All except H, He	All	All	All	All	All except Na down
<b>Info-gained</b>	Elemental, oxidation state, functionality	Elemental molecular structure	Elemental, simple molecular	Elemental, molecular, Functional Groups, Isotopical	Molecular, functional groups	Elemental Map
<b>Quantification</b>	Good	Semi	Good with standards	Semi	Semi	Semi
<b>Sensitivity</b>	1000 ppm	ppm-ppb	ppm-ppb	ppm-ppb	1%	0.1–0.5 wt.%
<b>Destruction</b>	Low	Negligible	High	Negligible	Negligible	Some at High Beam Current

## 2 CHEMICAL STRUCTURE

### 2.1 Infra Red (IR) spectroscopy

IR spectroscopy is a widely available and commonly used laboratory tool. In the paper industry, IR spectroscopy is used for identification of individual components, studies of binder migration [14], [15], identification of any contaminants that may be present in the paper product [16] and sometimes for competitive analysis. Fourier Transform Infra Red (FTIR) is the most commonly used example of IR spectroscopy and has been used to study laboratory prepared uncoated papers [17]. Details of the theory [18] and sample preparation [19] techniques can be found elsewhere. IR spectroscopy primarily gives information about molecular vibrations which are characteristic of molecules and functional groups. Infra red light is absorbed by the molecular species, and the absorbance of this radiation is plotted either as transmittance or absorbance as a function of the wave number (1/wavelength). The technique is generally used to identify unknown organic or inorganic species, by comparing the resulting spectrum to libraries of different spectra; for example  $-\text{COOH}$  and  $-\text{OH}$  groups are readily detected. Studying the relative areas of the peaks can give some quantification of ratios of different components in a mixture for example, as long as there is no overlap in the peaks used. However if fully quantitative analysis is required a series of standards must be available, using known amounts of the components in the sample.

The degree of surface sensitivity is controlled to a large extent by the type of accessory used to hold the sample. Measurements from the bulk can be obtained by using transmission spectra of thin films. The attenuated total reflectance set up, gives information from the top few microns and if a grazing angle infra-red reflection absorption spectroscopy (IRAS) attachment is used, the depth is only nanometres [10]. This is particularly useful for the study of thin surface films or contamination; however care must be taken that migration of soluble species into these upper layers does not mislead the researcher. A diffuse reflectance sphere attachment is used for study of the spectrum from rough or highly scattering surfaces. The scattered IR radiation is collected by the sphere and a system of mirrors before passing into the detector. The best lateral resolution that can be obtained is around  $5\mu\text{m}$  [20].

#### 2.1.1 Attenuated Total Reflectance IR (ATR-IR)

ATR-IR is one of the most commonly used systems in the field of paper science, as the preparation of the samples is very quick and easy. IR radiation is passed through an ATR-IR crystal which has a higher refractive index than

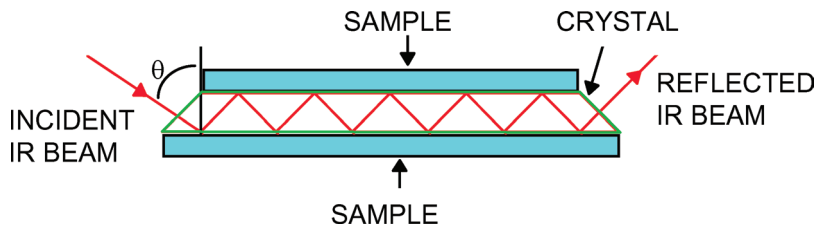


**Figure 4.** The multiple internal reflection ATR-IR crystal (from ref. [230]).

that of the sample being measured (Figure 4). With the correct geometry and crystal refractive index, the IR beam is totally internally reflected within the ATR crystal. When a coated paper sample is contacted with the surface of the ATR crystal, the light is repeatedly reflected from the crystal surfaces in contact with the coating. The evanescent wave exists at the boundary between the sample and the crystal and penetrates into the sample with an intensity that decreases with distance; this results in an IR spectrum with peaks which can be assigned to different components [21]. The ATR method measures approximately 8 cm<sup>2</sup> sample for each measurement. The technique is non-directional in an XY plane and therefore measures an average both the machine and cross machine directions in the case of paper.

The depth of beam penetration,  $d_p$ , is defined as the distance from the crystal-sample interface where the intensity of the evanescent wave decays to 1/e of its original value (~ 37%) [22] and is given by:

$$d_p = \lambda / (2\pi n_1 (\sin^2 \theta - n_{21}^2)^{1/2}) \quad [1]$$

Where  $\lambda$  is the wavelength,  $n_1$  = refractive index of ATR crystal (2.37 for a thallium bromide iodide crystal KRS5 crystal),  $n_2$  is the refractive index of the sample, and  $n_{21}$  is the ratio of the refractive index of the sample to the refractive index of the crystal.  $\theta$  is the angle of incidence of the IR radiation.

One problem with ATR-IR is that the quality of the spectra obtained depends greatly on pressure applied to the sample. This means that without pressure control the data quality may be poor [23]. More recently a single reflection ATR set up using a diamond crystal has been used by some authors [29]. This allows a more constant amount of pressure to be applied to the sample, and this set up is applicable for many different sample types. However the area of sample assessed with this is much less than for the KRS5 crystal described above.

### 2.1.2 Photo Acoustic Spectroscopy (PAS)

Photo Acoustic Spectroscopy (PAS) is another useful variant of IR spectroscopy. This method involves almost no sample preparation and is a completely non-destructive technique. The technique involves the application of a modulated IR beam to the sample surface, which results in a modulated temperature change on the sample. This causes the gas inside the chamber to expand and contract causing pressure waves which are subsequently recorded by a microphone. More detailed information can be found elsewhere [24]. This technique is used for coat weight determination, however, problems can occur for more accurate depth profiling if effects such as light scattering and coating homogeneity are not taken into account.

### 2.1.3 Examples of uses of IR spectroscopy in paper

Rousu [25] used FTIR to study the separation of offset ink oils on thin layer chromatography plates which had been coated with different pigments and binders. She found it possible to detect the carbonyl functionality present in vegetable oils which was absent in mineral oils. Wickman [26] also used FTIR analysis to detect the proportion of alkyd resin remaining in a model ink after laboratory Prufbau printing onto different substrates. In this work an absorption peak at  $1736\text{ cm}^{-1}$  was used to detect the alkyd resin and a peak at  $1464\text{ cm}^{-1}$  present in both the alkyd and heatset oil was used to obtain a calibration curve for alkyd resin proportion. Vikman and Sipi [27] used FTIR-ATR and Raman spectroscopy as methods to determine the lightfastness of prints made with dye based inkjet inks. Both techniques proved useful for this as systematic changes in the spectra could be observed as the papers were exposed to light.

Hiorns *et al.* [28] used the ATR-IR technique to determine the relative ratio of pigment to latex or plastic pigment in the top  $0.5\text{ }\mu\text{m}$  of coated paper surfaces. Peaks characteristic of the latex ( $760\text{ cm}^{-1}$  &  $970\text{ cm}^{-1}$ ) and the plastic pigment ( $760\text{ cm}^{-1}$ ) were identified and were compared to a normalised peak from the calcium carbonate ( $712\text{ cm}^{-1}$ ) present in the coating layer (Figure 5). A series of standards were first prepared with known ratios of calcium carbonate and binder and a calibration curve constructed (Figures 6–9). This was then used to determine the surface binder levels of coatings containing carbonates of different particle sizes.

Analysis of surface binder content may be important in printing, where the absorbency of the coating surface can be critical in determining ink setting rate, fount solution absorbency, picking, etc. The technique can also be used to evaluate if differential migration of binders occurs when different

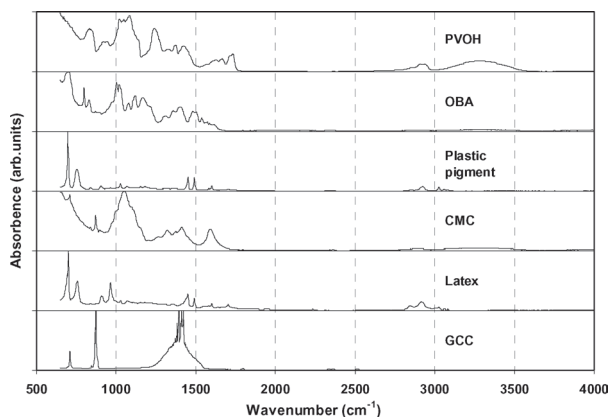


Figure 5. IR Spectra of coating components.

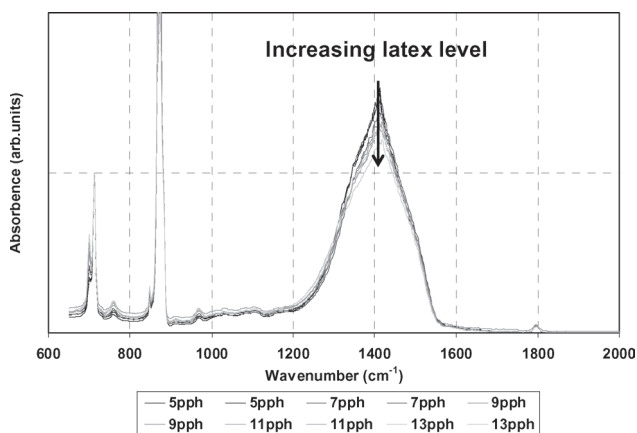


Figure 6. Spectrum of coated paper.

pigments of widely varying particle size or shape are used together. The technique was less useful for determination of components used at lower levels in the coating formulation such as CMC and OBA, as the peaks were rather obscured by noise in the data or by peaks from other components.

A similar study was carried out by Halttunen *et al.* [29], who also used FTIR/ATR spectroscopy to determine surface latex content of different coatings. A diamond ATR-IR crystal was used with an IR microscope, and this allowed mapping of the samples surface, with a lateral resolution of 60µm.

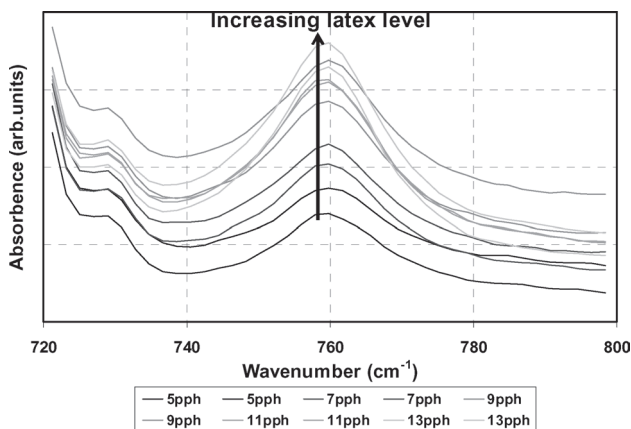


Figure 7. IR spectrum for different latex levels 760 cm<sup>-1</sup> peak.

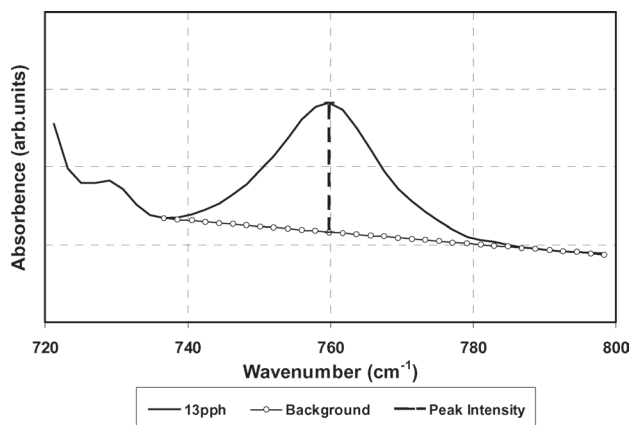
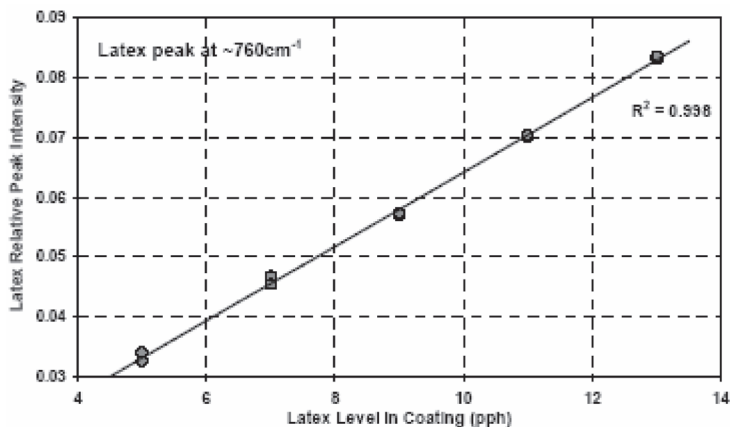


Figure 8. Removal of the background from the peak.

Maps of 400 spectra at 50  $\mu\text{m}$  steps allowed the binder coverage of a base-paper to be assessed.

Another example of ATR-IR use is for the determination of the surface particle alignment of kaolin particles in a paper coating [30]. In this work a penetration depth of approximately 0.5–0.6  $\mu\text{m}$ , was calculated using equation [1] and a KRS5 crystal with  $\theta = 45^\circ$ . Kaolin particles have two absorption wavelengths resulting from -OH stretching at 3695 and 3620  $\text{cm}^{-1}$ . The band at 3695  $\text{cm}^{-1}$  is due to vertically orientated particles, and the stretch at



**Figure 9.** Calibration curve for latex level in the colour and relative peak height for different latex levels (from Hiorns *et al.* [28]).

3620  $\text{cm}^{-1}$  due to horizontally orientated particles. A ratio of these two peak heights ( $\beta$ ) gives a measure of the alignment of the kaolin platelets in the coating [230]. ATR spectra for the samples were collected and the ratio  $\beta = I_{3695}/I_{3620}$  measured, using the peak heights. This technique was used by Preston *et al.* to show the change in particle alignment which occurred on calendering a kaolin containing paper, with increase in calender pressure [30]. The total  $-\text{OH}$  signal is related to the degree of contact between the crystal surface and the paper. In Figure 10, this increases as the calender pressure increases, and the paper becomes smoother and has improved crystal contact.

## 2.2 Raman spectroscopy

The Raman effect was first discovered in 1928 and was initially used to study the vibrational states of simple molecules. With the development of lasers in 1960, Raman spectroscopy was increasingly used to solve a variety of problems. The main drawback of the technique was laser-induced fluorescence (LIF) which overwhelms the Raman signal. However with the development of near IR FT Raman spectroscopy LIF is less of a problem [31]. The use of longer wavelengths also reduces the probability of fluorescence. In the field of paper, fluorescence generally derives from optical brighteners and lignin.

Raman spectroscopy is a very similar technique to IR spectroscopy. There are however, differences between the two. For example Raman spectroscopy

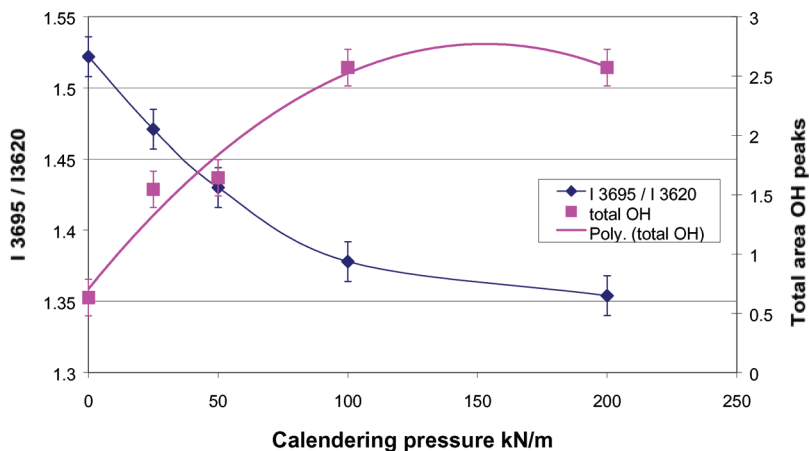


**Figure 10.** Variation in Particle Alignment of Coated Surfaces with Calendering Pressure ATR Ratio of peaks I 3695 / I 3620 from Preston *et al.* [30].

is sensitive for non-polar molecules whereas IR spectroscopy is only sensitive to polar species making the techniques complimentary [32]. Raman spectroscopy also uses a single wavelength laser light to excite the sample. This lower wavelength, more intense light, enables better focussing and therefore superior spatial resolution can be achieved. Swerin *et al.* [33] suggest that a resolution can be obtained down to the optical diffraction limit  $\sim 200$  nm. Raman spectroscopy is also insensitive to water (useful for analysis in the paper industry), and there is reduced overlapping of peaks. Raman spectroscopy requires almost no sample preparation and the technique is mostly non-destructive [23].

### 2.2.1 Variants of Raman spectroscopy and examples of use in paper

Apart from conventional Raman spectroscopy there are also many other adaptations available:

- Confocal Raman Microscopy [34]: This combines the techniques of Raman spectroscopy and confocal microscopy and allows chemical assessment in the z direction. The resolution is set by the wavelength of the light and also the aperture of the microscope objective and is 200nm in the x-y direction and roughly double this in the z direction. This has been used by Vyorykka *et al.* [32] to study distribution of binder and pigment in coatings and also under a layer of printed ink (Figure 12). Vyorykka [35] also developed an immersion technique for studying pigment / binder dis-

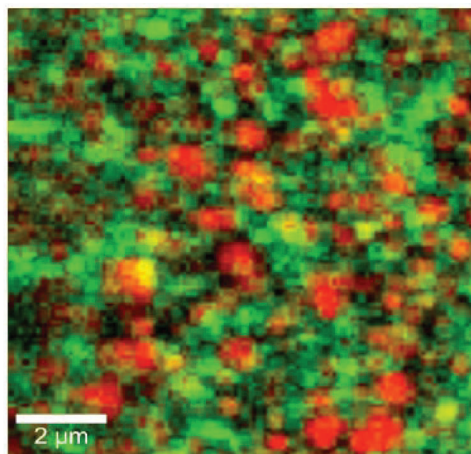


**Figure 11.** Raman mapping of SB latex (green),  $\text{CaCO}_3$  (red), cmc (black) Image courtesy of YKI.

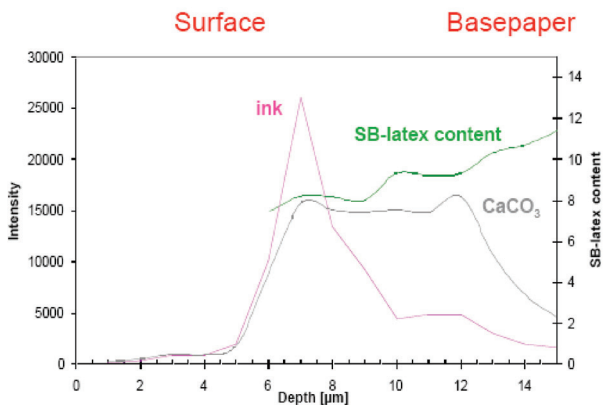


**Figure 12.** Raman Depth profiling by cross section and analysis.

tribution throughout the bulk of the coating which was necessary due to the light scattering of the coating layer. The combination of two microscope objectives allowed both surface and bulk analysis of the GCC/SB latex distribution to be obtained. Vikman and Sipi [27] also used depth profiling Raman to study the lightfastness of dye based inkjet inks.

- Resonance Raman Spectroscopy: This is where the laser wavelength coincides with the electronic spectrum of the molecule which gives a much enhanced signal ( $\sim \times 10^6$ ). One example is where a UV laser of wavelength 244 nm has been used to enhance the spectrum from butadiene, due to its conjugated double bonds. Fluorescence was also less of a problem as the fluorescence and Raman spectrum did not overlap [23].
- Surface-enhanced Raman Spectroscopy: In this variant the molecules of interest are absorbed on metal surfaces, or conversely, metal colloidal particles e.g. silver or gold are absorbed onto the sample surface, both causing a significant enhancement of the signal. However, problems do exist; for example the colloidal metal may cause burning of the sample, and the spectra are less straightforward to interpret [23].
- Kerr-gated resonance Raman spectroscopy: In this technique, the fluorescence is separated from the Raman spectrum, by using a high frequency laser pulse. A Kerr gate accepts the Raman signal which scatters within a few pico seconds, but the fluorescence emission takes place much more slowly and is therefore separated from the signal of interest. This method was successfully used by Vikman *et al.* [36] in determining inkjet ink / paper chemical interactions in the study of lightfastness of inkjet printed papers.
- Raman spectroscopy combined with atomic force microscopy (AFM): This technique has the advantage of being able to obtain both chemical and topographical information from the sample at the same time.

Advancements in the Raman technique not only allow determination of unknown compounds, but now allow it to be used to detect differences in crystallinity, for example the separating of calcite and aragonite in a calcium carbonate sample. One example of this in the paper industry is shown by Santos *et al.* [37]. In this work PCC and GCC of different particle size distributions were made into coating colours as sole pigments and as blends. Uncalendered papers were measured and papers calendered under two different conditions. A range of techniques including Raman spectroscopy, scanning electron microscopy (SEM) and atomic force microscopy (AFM) were used to determine the relationship between the topography and sheet gloss. Shifts in the peaks were observed with different calendering conditions and due to differences in the particle packing of the different morphology pigments.

The technique can also be used in the identification of components of recycled paper pulp [38]. One major advantage is that Raman spectroscopy can separately detect styrene, butadiene, acrylate and acrylonitrile allowing different latices to be distinguished [23], [32].

Swerin *et al.* [33] used confocal Raman spectroscopy to depth profile inkjet

inks into different inkjet coating layers. For every ink / paper combination peaks were selected for the ink which had no significant overlap with the other paper components (Epson 1290–1376  $\text{cm}^{-1}$ , Canon 1117–1207  $\text{cm}^{-1}$  and HP 1057–1160  $\text{cm}^{-1}$ ). The Full Width Half Max (FWHM) of certain peaks were analysed for each. The inks were shown to be held within the coating layers in all instances. The deepest penetration of the ink occurred for the sample coated with a mixture of kaolin and amorphous silica, which also had the lowest % of small pigment pores.

### 2.3 X-Ray Photoelectron Spectroscopy (XPS)

The surface analytical technique XPS (also known as ESCA, or Electron Spectroscopy for Chemical Analysis), was first developed in the mid 1960's by Siegbahn *et al.* [39], but is based upon the photoelectric effect discovered by Einstein. It is a powerful tool for chemical surface analysis. The development of the technique of XPS from 1900 to 1960 has been reviewed by Jenkin [40]. More recent texts describing XPS are given in [41] and in relation to paper in reference [42] & [43].

The main strengths of this technique are that it is extremely surface sensitive (top 2–10 nm of the surface), it is quantitative and reasonably easy to interpret, and there is not only elemental information for all of the elements (apart from hydrogen and helium), but also information concerning the chemical environment of that element (chemical state, bonding etc). The lateral resolution of the technique is improving with time and is now around  $3\mu\text{m}$  which makes mapping of some paper constituents and contaminants possible.

The basic principle of XPS involves irradiating a sample surface with mono-energetic soft X-rays and analysing the emitted electrons according to their kinetic energy. The whole process takes place under a high vacuum, as the mean free path of the emitted electrons is very small. Istone [89] cites the work of Ahmed *et al.* [44] showing the importance of using a monochromatic X-ray source. A standard X-ray source was shown to cause cellulose to degrade, whereas a monochromatic X-ray source did not cause this.

If an atom is exposed to a photon of energy which is greater than the binding energy of the electrons in the atomic orbitals, then electrons can be ejected. The photoelectrons have kinetic energies which can be given by:

$$\text{KE} = h_p \nu - \text{BE} - \phi_{\text{XPS}} \quad (2)$$

where  $h_p$  is Planck's constant,  $\nu$  is the frequency of the exciting radiation (X-ray beam), KE is the kinetic energy of the photoelectron, BE is the binding energy of the electron in its orbital and  $\phi_s$  is the spectrometer work function.

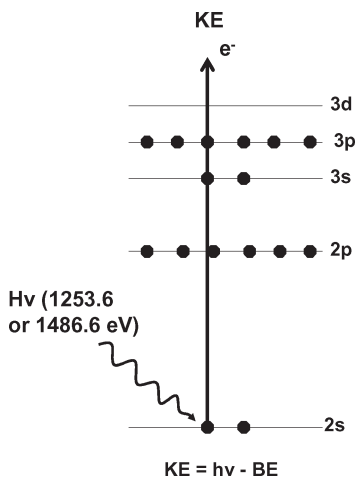


**Figure 13.** The XPS photoelectron emission process (reproduced from 11).

The XPS spectrum consists of a series of lines, indicative of the binding energies of the electrons being ejected. They are generated for electrons from different orbitals, (which have different binding energy levels) and also from different spin states within each orbital. The binding energy can be described as the energy difference between the initial and final states after the photoelectron has left the atom [45]. There is a variety of possible final states for the atoms and therefore there will be a spread in the kinetic energies of the emitted electrons, leading to a number of different peaks. There is also a range of probabilities of achieving each end state, which results in different peak intensities. Peaks from the core electrons are the most intense and are usually diagnostic for each element; measurement of their intensities can be used for quantification. Only the outermost electrons retain all of their kinetic energy and are analysed, the lower electrons experience energy loss and their signal becomes part of the background signal. The kinetic energy of the ejected electrons is very small (0–1500 eV), and therefore they cannot travel large distances through matter, hence the surface sensitivity.

Each element has a unique spectrum which is affected by the immediate chemical environment of that element. The chemical environment and the polarisability of the element will give rise to certain shifts in the binding energies (known as chemical shifts), which can be up to around 8 eV in magnitude. These chemical shifts can be useful for determining the chemical state of the elements being analysed. For example C–C has a 1s core line at

285.00 eV, whereas C=C has a 1s core line at 284.73 eV. A CO<sub>3</sub> (carbonate ligand) has a carbon 1s line at 290.44 eV.

### 2.3.1 Depth profiling

Some depth profiling information is possible using two different methods.

Angle resolved depth profiling allows some limited depth information of planar surfaces between 1 and 10 nm depth. The surface sensitivity is increased by decreasing the angle between the sample and analyser thus allowing the depth measurement of 1 nm to be achieved.

Depth profiling can also be achieved by etching, for example by using an argon ion beam (2 μA), and then reanalysing the surface using XPS. This approach was used by Dalton *et al.* [46] who used depth profiling over an etch area of 5 × 5 mm followed by analysis with the XPS (Figure 14). After etching, a measurement was taken over an area of 4 × 3 mm. A calibration of the depth of etching of an ink film printed onto a non-porous substrate (Melinex™) was carried out using AFM, which showed the etch rate to be approximately 1 nm min<sup>-1</sup>.

### 2.3.2 Use of XPS for fibres

A good review of the use of several surface analysis techniques is given by Koljonen[47] as part of her thesis on the effect of fibre surface properties on

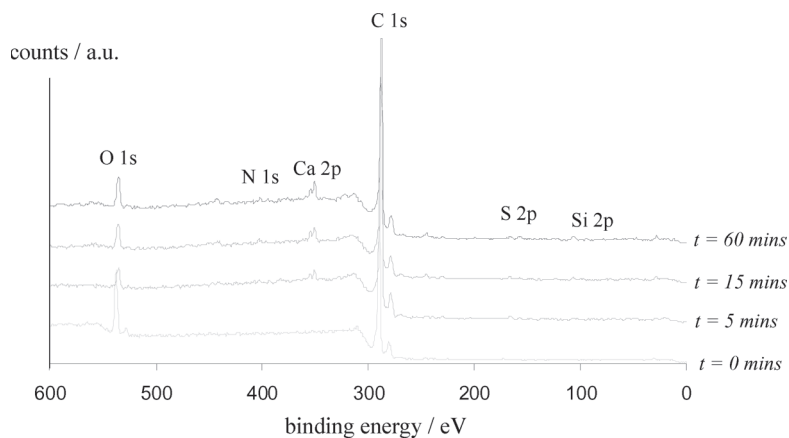


**Figure 14.** XPS wide spectra of clay coated paper with a 0.33 μm printed ink film thickness. Spectra taken at different time intervals after etching with Ar<sup>+</sup> ion beam [46].

paper properties with mechanical and chemical pulps. In this work XPS has been utilised with solvent extraction to evaluate the surface lignin and extractives contents on the pulp surface. As part of this work Johannsson *et al.* [48] describe two methods of analysis to monitor the pulp surfaces: the oxygen-to-carbon ratio (O/C) measured from the wide spectrum and aliphatic carbon (C1, C–C) measured from high resolution spectra. Both methods of analysis turned out to be consistently good indicators of surface lignin content for a variety of extracted pulps.

Heijnesson, Hulten *et al.* [49] compared different XPS techniques in analysis of fibre surfaces. Three different methods of analysis were compared using the XPS instrument; based on the O/C atomic ratio, C1 carbon content, and Hg amount for Hg treated lignin. The sensitivity, reproducibility and stability of the 3 methods were assessed. The work showed that the surface of the fibres was richer in lignin and extractives than the bulk of the fibre. Of the 3 methods the mercury was found to be the most reproducible, although some degradation occurred during the XPS analysis. This method gave the same result for surface lignin content of thermo-mechanical fibres as the other methods, but found a lower surface lignin content for the kraft pulp fibres, possibly because of contamination due to adventitious carbon, which would be seen with the O/C and C1 methods. The O/C and C1 methods were also sensitive to the method of sample drying.

The experimental procedure for XPS determination of pulp extractives was studied by Johannsson *et al.* [50] who carried out a round robin study on a series of pulp samples with varying lignin content in 5 different laboratories. They suggested that although XPS had been used extensively, little attempt had been made to standardise the procedures, despite the often complex and variable nature of the fibre based materials studied. The results showed that despite minor differences in analysis methods, reproducible results could be obtained. These were further improved if the X-ray exposure was restricted and from a monochromatic source. Carefully controlled sample handling procedures and comparison with a paper based reference also improved the validity of the data obtained.

### 2.3.3 Use of XPS in determining failure at interfaces

XPS can also be used to determine the chemical nature and position of both visible and invisible defects in a coating. When dealing with a visible defect it is often difficult to determine if the defect is on the surface of the coating or between the fibre surface and coating. If the defect lies on the surface, then the XPS spectrum for defect and non-defect areas will differ. If the defect is beneath the coating then both XPS spectrums should be identical. Such

defects are usually caused by contamination on rolls, dryer, or contaminants falling onto the sheet (e.g. grease, oils, and graphite). Knowing the location of the defect often allows the problem to be easily fixed as shown by Istone *et al.* [51].

Hemminger [52] described the use of XPS in determining chemical changes occurring at the paper surface after coating and also gives an example of surface wax distribution and wax bloom from wax additives present with developmental latices. In areas of wax bloom an increase in the surface carbon was observed and a decrease in the latex base peaks such as Cl, Na and S.

A number of applications for XPS have been summarised by West and Stevenson in reference [53]. Amongst these examples are the study of the surface coatings of TiO<sub>2</sub> pigments, where the amount and distribution of an alumino-silica coating layer can be assessed, and the study of plasma treated packaging prior to its printing. Angle resolved XPS was also used to study surface degradation. The XPS was used at several angles of incidence, with respect to the detector, allowing the depth of detection to be varied between 1 and 10 nm. As an example both sides of an interface where failure had occurred were analysed and were found to be rich in amine. It was shown that the amine species had migrated to the interface from the top coat of a paint, displacing oxygen.

Andersson *et al.* [54] used XPS to study the surfaces of a precoated paper before and after application of a barrier coating. The coating was also fractured after heat sealing and the technique used to look at the failure, to see if it was a cohesive or adhesive failure occurring. In the fibrous areas of failure, a cohesive failure within the board was mainly the cause. In the coated areas, both adhesive and cohesive failure had occurred, and it was suggested that an intermediate, surfactant rich layer with low adhesion was present. The XPS data showed an enrichment of latex near the barrier coating surface, so that there was a surface area fraction of more than 95% in the surface layers compared to 75% in the bulk of the coating.

Swift and West [11] have used XPS to look at the degradation of colour from a coating layer. The technique was able to determine that the colour fade was linked to a decrease in the polysulphide concentration and an increase in the sulphate concentration. The fading was due to a decrease in the NaS<sub>x</sub> chromophore as the sulphide radical was oxidised to the sulphate state.

### *2.3.4 The use of XPS to determine surface chemistry of coatings*

Strom *et al.* [55] used XPS to determine the surface composition of coated papers containing different mineral compositions (clay and calcium carbonate)

and different types of latex binders. They used a variable angle technique (decreasing the angle between the paper and the analyzer) to sample the surface to different depths and established that no thin over layer of carbon existed on the surface of these paper coatings. Their work also gave valuable insights into the surface composition of the paper coatings and the degree of latex that was present. Decreasing the pigment particle size increased the specific surface area and resulted in less binder at the coating surface.

Brungard and Cleland [56] used XPS to determine relative pigment concentrations in the surface layers of coated papers containing kaolin, calcium carbonate and  $\text{TiO}_2$ . The technique was reliable in estimating these concentrations, although the  $\text{TiO}_2$  had to be present at over 5wt.% concentration. Calendering, coat weight and the use of two different binder types did not impact the results significantly. Tomimasu *et al.* [57] also studied the pigment / binder content of the surface of coated papers and agreed that calendering had little impact on the pigment / binder ratio. They used XPS to determine the coating surface binder content and study the impact of pigment composition, particle size of latex and its functional groups and drying conditions. They suggested that latex selectively migrates to the surface more than starch, but this is a finding which is not generally accepted by other authors [15].

Seppanen *et al.* [58] explored the relationship between surface energy, topography, wettability and surface chemistry using XPS for a set of pilot coated papers. They found that there was a good correlation between the surface energy of the coated papers found by using a sessile drop, contact angle technique and the surface chemistry of the coatings determined using the XPS. They showed that the surface energy decreased with increasing amount of latex near the paper surface, and also that the paper topography had little impact on the result when droplets of  $1.7\mu\text{l}$  or larger were used.

Al-Turaif and Lepoutre [59] have used XPS to study the surface structure and chemistry of pigment and latex coatings during drying. Samples of SB latex and kaolin were prepared at a wide range of pigment volume concentrations (PVC) and were then freeze dried during various stages of drying. Microscopy, gloss, XPS and surface energy measurements were used to study the changes in the surface occurring with drying time. They found that the SB/clay ratio increased at the surface with drying time. The surface energy, especially the polar component decreased during film formation. The interaction between the latex and the pigment differed below and above the Critical Pigment Volume Concentration (CPVC). Above the CPVC, the latex continues to coalesce even above the second critical concentration (when air is introduced into the coating), whereas below the CPVC the coalescence is complete by this point.

Al-Turaif & Lepoutre [60] reported the use of XPS to study the impact of sintering on the surface chemistry of pigment and latex coatings. Sintered coatings formulated below the critical pigment volume concentration (CPVC), dried in the absence of water, had a higher SB latex:pigment ratio on the surface of the coating, and a lower surface energy than a standard wet coalescence process. When the systems were formulated above the CPVC, no significant differences were seen compared to the wet drying process.

In a later publication Al-Turief [61] carried out a study looking at kaolin and PCC blends combined with styrene butadiene acrylonitrile (SBN) latex. XPS was used to characterise differences in surface composition when these coatings were applied to both porous and non-porous substrates. It was seen that as the proportion of prismatic PCC particles increased, so did the proportion of SBN latex at the surface. The author suggested that this was due to the PCC disrupting the surface giving more pathways to the surface allowing more latex movement. In addition the PCC was suggested to enhance latex spreading on the surface.

Johansson *et al.* [62] used XPS to study the interactions between alkyd resin binders and kaolinite. Sorption and desorption studies were both carried out on the pure kaolinite with a soybean alkyd and linseed oil. The interactions were studied by quantifying the change in the C (1s) peak, Si (2p 3/2) and Al (2p 3/2) peaks as the alkyds were added. They found that the alkyd resins were absorbed strongly onto the kaolinite and that there was a specific interaction between the fatty acid double bonds in the alkyd resins and the aluminium groups or hydroxyl groups next to the aluminium in the kaolinite. In another publication Wickman and Johansson [63] stated that after washing and desorption tests, analysis using the XPS instrument showed that 81% of the alkyd resin was still attached to the kaolinite.

### 2.3.5 XPS for analysis of paper surface treatments

XPS has also been used extensively in determining whether surface treatments to paper have been successful in changing their surface chemistry, for example Rentzhog showed that increasing corona dosage to PE coated board resulted in an increased O/C ratio and a higher surface energy [64].

Pykonen *et al.* [65] have used XPS to study the degradation in the plasma and corona activation of paper with time (Figures 15–18). Surface sized and coated papers were treated with laboratory and pilot scale atmospheric plasma treatment and also conventional corona treatment. Changes in the surface energy were assessed directly after the treatment, and for three months after this. XPS measurements and contact angle measurements using the KSV CAM 200 showed that the treatments caused an increase in the

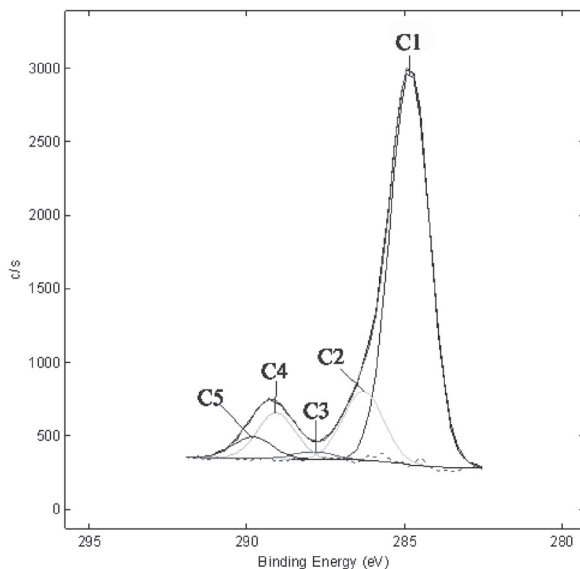


**Figure 15.** High resolution C1s spectrum and deconvolution for the untreated pigment coated paper.

oxidation of both paper surfaces and also the surface energy. During the aging process the surface energy was found to decrease initially during the first few weeks, but then the rate of decrease slowed considerably, approaching a stable level (Figure 18). The oxidation level however did not decrease and remained stable throughout the 12 weeks. These differences were explained in terms of the orientation of some polar species. These may have been rotated by the plasma process, but then rotated back into the material with time. There may also be some recontamination of the surface where low surface energy constituents in the paper may have migrated to the surface of the paper with time.

In a later publication Pykonen *et al.* [66] studied the changes in surface energy and chemistry which occurred on plasma treatment and the impact of these changes on the offset printability of surface sized and coated papers. Contact angle measurements and surface energy determination showed that the plasma treatment had resulted in an increase in the polar surface energy due to the formation of oxygen containing molecular groups such as carboxyl and ester groups with laboratory plasma treatment and alcohol, aldehydes and ketones with pilot scale plasma treatment. When a hydrophobic surface

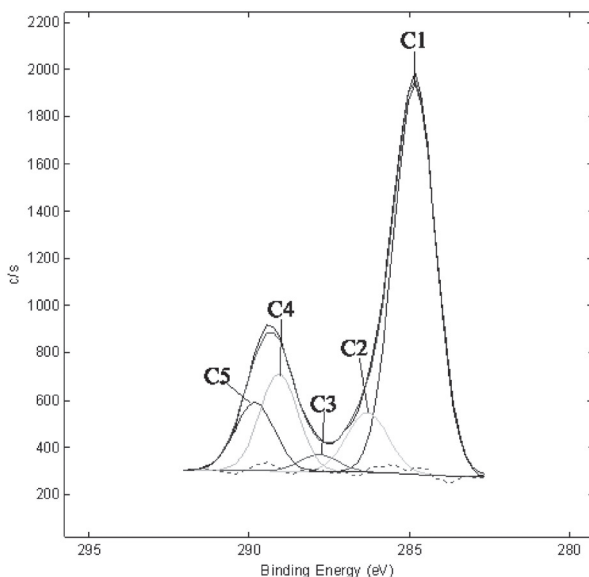


**Figure 16.** High resolution C1s spectrum and deconvolution for the laboratory scale plasma treated pigment coated paper.

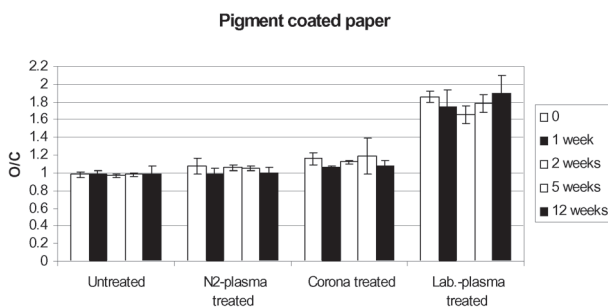


**Figure 17.** O/C ratio for pigment coated paper.

sized paper was treated with the plasma, the damping water absorption was changed impacting ink transfer, print density and gloss.

More detailed evaluation of the changes in surface chemistry occurring on plasma and corona treatment of coated and pigmented papers showed that the plasma treatment oxidised the long polymer chains present in surfactants

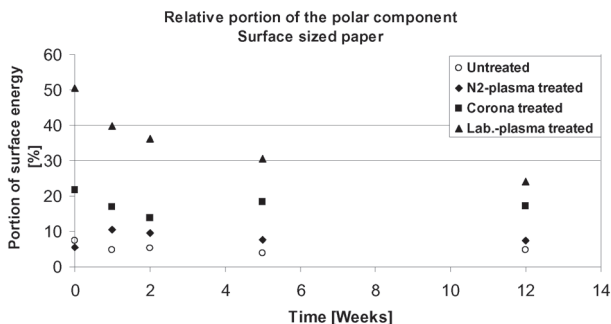


**Figure 18.** Polar component of surface sized paper.

and other paper chemicals. The CO<sup>+</sup> groups were distributed unevenly in the pilot scale treatment, but were more even in the laboratory treatment. The treatment also increased the micro-scale roughness for the coated papers and this resulted in an increase in the wettability [67].

## 2.4 Secondary Ion Mass Spectrometry (SIMS)

SIMS uses an energetic beam of primary particles (commonly oxygen, caesium or gallium) targeted onto the substrate surface. The beam causes the substrate to disintegrate at the very surface, releasing molecular fragments characteristic of its composition. These fragments are identified by measuring their molecular mass in a mass spectrometer and are separated as a function of their charge to mass ratio [68]. These species can then be analysed to give a positive or negative SIMS spectrum.

The energy transferred by this bombardment causes atoms, ions and electrons to be ejected, or sputtered, from the surface. The ejected species may be uncharged, positively, or negatively charged. The species can be atoms, clusters of atoms or molecular fragments. The system operates under a vacuum, and separates the fragments as a function of their molecular mass and charge. The ions can be passed through an energy filter before being detected, so that ions with a specific range of kinetic energies are analysed. The mass analyser can be a quadrupole, magnetic sector, or a time of flight analyser (TOF).

The SIMS process involves two main stages; the emission of the particle (sputtering) and ionisation. The particles may be sputtered or ejected from the surface by direct collision with the incident beam, or from knock-on collisions to neighbouring particles. At high primary beam densities a thermal spike may cause transient vaporisation of atoms in the impact region.

Only a proportion of the particles emitted from the surface are ionised and analysed. After the bombardment of the surface with the primary particle beam, the crystalline structure of the solid is considerably disrupted. It is therefore not likely that the electronic structure is that of a perfect solid. It has been suggested that the area of emission is amorphous with a continuum of energy states [69].

SIMS analysis is concerned with the yield of secondary ions from a surface which can be described by the following expression:

$${}_iM_s = i_{pr} S R^+ \theta_M \mu \quad (3)$$

where  ${}_iM_s$  is the secondary ion current of an element of species M

$i_{pr}$  is the primary particle flux (number of ions or particles per s)

S is the sputter yield for M

$R^+$  is the ionisation probability to positive secondary ions

$\theta_M$  is the fractional coverage of M

$\mu$  is the transmission of the analysis system which is determined by the ion collection / mass spectrometer used.

S and  $R^+$  are important parameters for the amount of ions produced.

There are a number of different variants of SIMS, e.g. Static SIMS (SSIMS), imaging SIMS and depth profiling SIMS. In the early 1970's Benninghoven [69] demonstrated that by reducing the primary bombarding beam intensity, species emitted from the surface monolayer could be collected without destruction of the surface. This is known as static SIMS and is often used to map the chemistry of a surface. This technique is very surface sensitive and will analyse the topmost single atomic layer. Static SIMS uses low-energy (100eV to 10keV) and low-flux density (<5 nA/cm<sup>2</sup>) primary ion beams to bombard the sample. A dose of less than 10<sup>12</sup> atoms cm<sup>-2</sup> will ensure that the ion cascades do not overlap and come only from the virgin surface and this is generally regarded as the static SIMS limit [70]. The most intense mass peaks correspond to the most stable ions formed. The SIMS sensitivity therefore varies depending upon the species being detected. The highest sensitivity elements detected for positive ions are the group 1 elements Li, Na etc. In Imaging SIM a compositional image of the surface is produced. Dynamic SIMS experiments use higher current density primary ion beams to give faster sputter rates and to release secondary ions. This mode is mainly used for smaller samples (due to increased sensitivity of the SIMS) and for depth profiling [23],[71], [72]. As the secondary ions are released, rapid erosion of the surface occurs and it is possible to determine the changes of elemental composition with depth. The depth resolution is very high, around 20 nm,

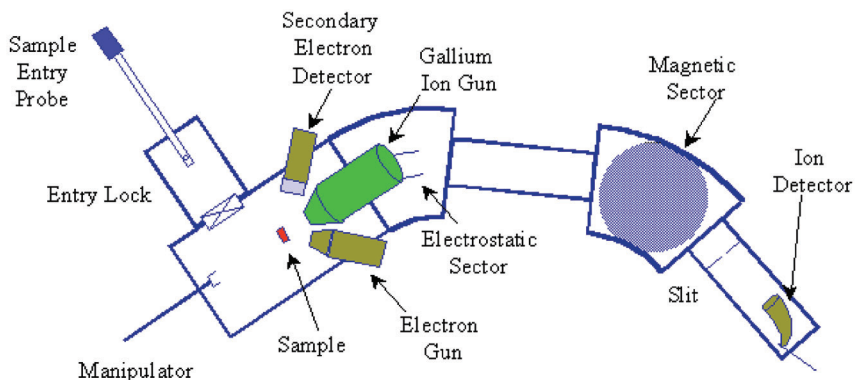


Figure 19. Schematic diagram of magnetic sector SIMS (from Heard [73]).

but is dependent upon such factors as the uniformity of etching by the incident beam, the absolute depth below the surface at which the etching is being carried out, and the nature of the ion beam being used. The nature of the substance being analysed will also affect the resolution achieved.

SIMS usually uses a quadrupole or sector mass analyser. The most recent breakthrough has given rise to time-of-flight (TOF) mass analysers [74]. These have several advantages over conventional techniques, for example, due to the greater transmission of ions through the TOF analyser there is increased sensitivity. Also the mass assignment accuracy and lateral resolution is improved giving easier quantification of results and better imaging capabilities [71]. Mass resolutions of  $10^{-3}$  to  $10^{-4}$  amu (sometimes quoted as 100–1000  $M/\Delta M$ ) are possible, which allows peaks which were previously seen as overlapping, to be resolved. This high sensitivity also allows surface species as low as ppb to be detected.

SIMS has several advantages over other analysis techniques. Detailed chemical information can be achieved with an analysis depth of around 1–2nm. This shows increased sensitivity over other techniques such as XPS. SIMS can also identify all elements, including H and He, at a much lower concentration, e.g. dopants in semiconductors[75]. The main advantage of SIMS is the ability to gain chemical information on functional groups and molecular fragments such as radicals [23]. There are however some drawbacks. It is not very straightforward to quantify the peaks in a mass spectrum due to the high surface sensitivity. Contaminants can also be a huge problem, and can lead to an inaccurate spectrum. Further, the beam range diameter is also fairly limited (1–200 microns). This means that the sensitivity of the

experiment is lowered as the beam diameter is reduced. This is due to the fact that fewer ions are ejected from the surface of the sample [75].

#### *2.4.1 Applications of SIMS in paper*

SIMS can be used to solve practical problems for which both spatial resolution and chemical information are required [43], [75]. For example Brinen *et al.* used SIMS to map the position of inorganic paper additives and surfactants [76], and Brinen and Proverb mapped fluorinated organic surfactants on paper fibre surfaces [77]. Sodhi *et al.* [78] used TOF SIMS combined with Principal Component Analysis (PCA) to analyse the surface and z direction distribution of ink into coated paper. They were able to follow the distribution of both dye and pigment based inkjet inks. In the case of the pigment based inks, the separation of the ink vehicle, binder and pigment could all be determined. Depth analysis was achieved by mapping the cross sectioned coating and ink layers, and the authors suggest that this is more realistic than using depth profiling by sample sputtering in dynamic SIMS. They say that this can destroy the substructure of the sample, rendering the chemical information meaningless. However in their technique, the cross sections were achieved using a freeze fracture process and this is likely to also distort or destroy the surface of the sample. Sun *et al.* [79] presented a similar study in which cross sections of printed papers were analysed with TOF SIMS and the data processed using principal component analysis.

Preston *et al.* [80] studied the distribution of fount solution within a double coated paper sample, and compared this to the pick strength and position of failure which occurred when this paper was assessed using a wet pick test. The sample was “printed” with CsCl labelled fount solution and then passed through a heated oven attached to the laboratory printing press (Prufbau multipurpose printing unit). The dried paper was then embedded in epoxy resin and sectioned using an ultra microtome. The block with the cut face was then placed in the static SIMS and ions indicative of the different layers were mapped.

In Figure 20 the ion map is constructed for the single side double coated paper prior to fount solution addition. The fibres were imaged using the Na<sup>+</sup> peak and are coloured green, the calcium carbonate filler and coating layer topcoat were assessed using Ca<sup>+</sup> and are coloured red. The Al<sup>+</sup> represents the kaolin and is in blue.

In Figure 21 all of the paper ions have been coloured grey, and only the Cs<sup>+</sup> is coloured red. The position of the fount solution can be easily seen from this image. It has passed through the calcium carbonate topcoat and is entering the kaolin layer. Examination of the pick failure using a SEM

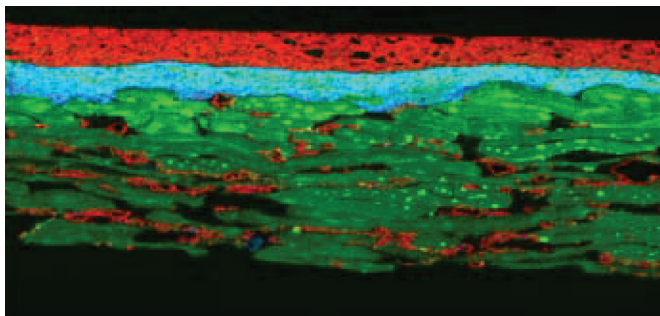


**Figure 20.** Colour overlay of SIMS mapping, through single side, double coated paper.

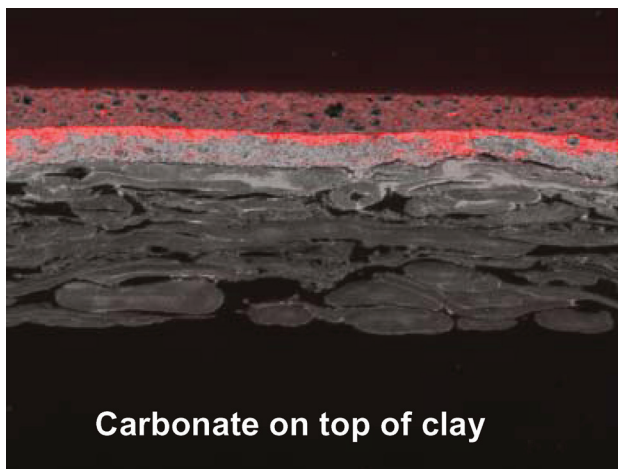


**Figure 21.** Cs+ found on double coated paper.

showed that the failure occurred just below the interface between the calcium carbonate and the kaolin (Figures 22 and 23).

A similar technique was used to assess a section through a commercially coated paper which was printed on one side [72]. In this work, both dynamic SIMS and static SIMS were used to determine whether there was any penetration of ink into a coating layer. In Figure 24, the ink layer can be seen as a very faint red line on the downwards facing coating layer. The sectioned

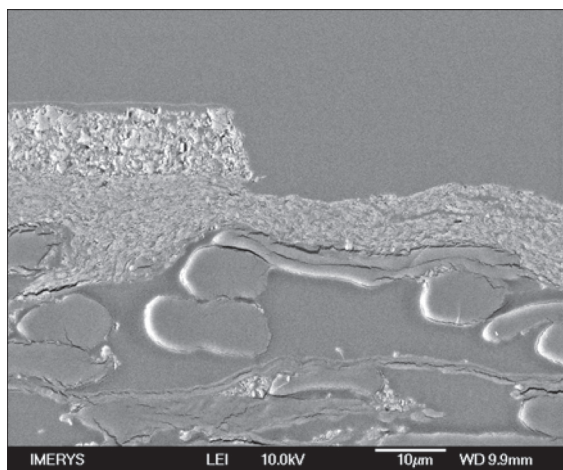


Figure 22. Position of pick failure.

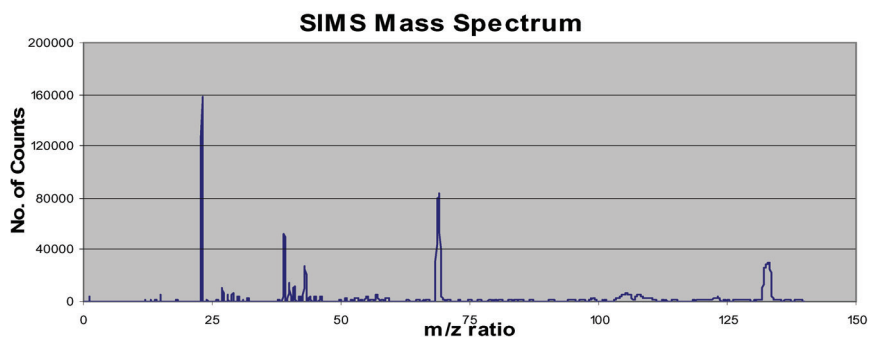
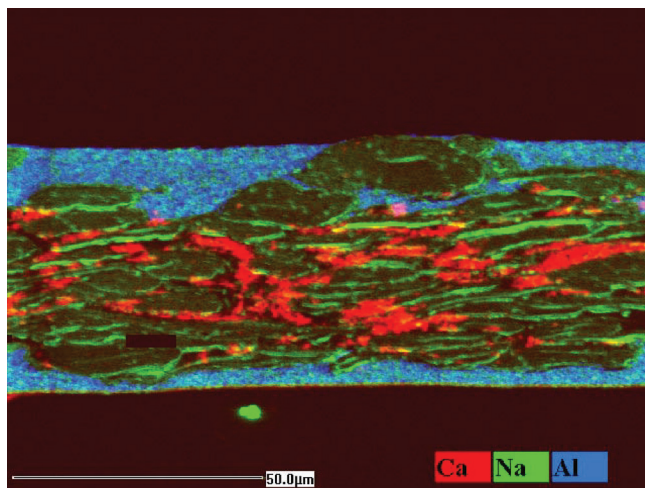


Figure 23. This shows the SIMS spectrum of a paper coating printed with CsCl. The 3 main peaks are shown at approximately  $m/z$  23,  $m/z$  69 and  $m/z$  133. These can be attributed to Na, Ga (from beam) and Cs ions respectively [80].

paper when imaged using static SIMS, clearly shows the distribution of filler within the sheet, however the spatial resolution was not sufficient to show details of the ink distribution.

TOF-SIMS with etching and subsequent re-measurement was initially used to try and determine if there were differences in the distribution of ink components throughout the printed ink layer. This showed that a resin layer covers all of the ink components. As the sample was etched and re-measured an increase in the ink pigment ( $\text{Ca}^+$ ) could be seen. As the etching exposed the ink paper interface,  $\text{Ca}^+$ ,  $\text{Al}^+$  and  $\text{Si}^+$  ions were all detected [81].



**Figure 24.** Section through coated paper with a fine printed ink layer on the underside (red line). Colour overlay of ion maps.

Dynamic SIMS with continuous sample etching gave more detailed information about the depth of the ink layer (Figure 25). Point to point variations in the ink film thickness were seen as differences in the time taken to reach the ink / paper interface. The ink film thickness determined by the SIMS was roughly proportional to the amount of ink printed on the paper initially. The measured concentration of  $CN^-$  or  $O^-$  ions across the interface between the ink and the paper coating was shown to be due to the micro-roughness of the coating layer. This was further evidence that the ink pigment had not penetrated into the coating layer, but was following the micro-roughness profile of the surface.

The techniques of SIMS and XPS have been used in the study of paper and print surfaces by a number of different researchers [85]–[92]. However, most of these studies centred on the investigation of industrial problems.

Zimmermann *et al.* [82] used TOF-SIMS to investigate the difference between a high quality paper sample and a mottled print sample. From SIMS analysis it was found that the signals for Ca ions (due to the presence of calcium carbonate pigment) and hydrocarbon fragments (from latex) were not evenly distributed throughout the sample in the mottled paper. Other authors have also suggested that uneven binder distribution is linked to print mottle [83].

More recently Koivula *et al.* [84] used TOF-SIMS to characterise the

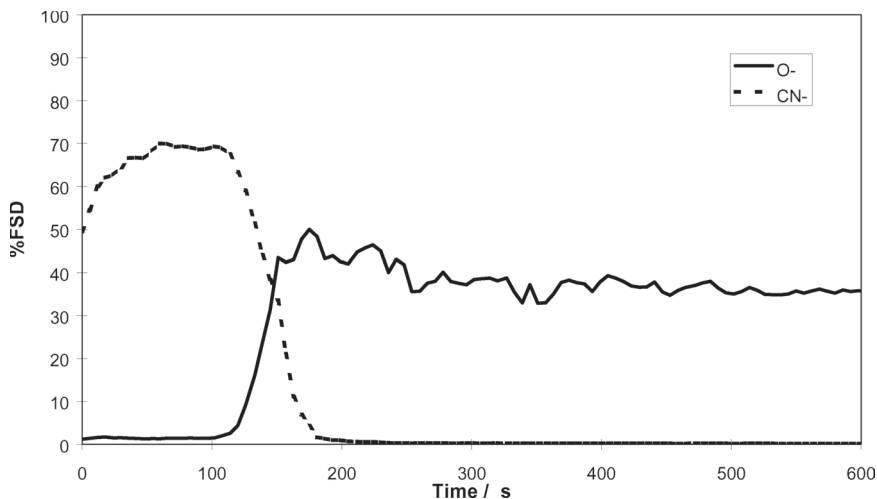


**Figure 25.** Magnetic sector SIMS depth profile of clay coating printed with 1.5  $\mu\text{m}$  ink using negatively charged fragments ( $\text{CN}^-$  to depict the ink and  $\text{O}^-$  the coating layer) at  $\times 5000$  magnification (area 26  $\mu\text{m} \times 20 \mu\text{m}$ ).

distribution of dispersant on pigment particle surfaces. They found that the resolution of the technique was sufficiently high to see that the dispersant was concentrated around the edges of the kaolin particles, but the calcium carbonate particles were too small to see differences in dispersant distribution.

Brinen and Kulick [85] used ESCA (XPS) and TOF SIMS to detect the presence of high mass aggregates on 'hard to size' bleached sulphite paper fibres. The poorly sized areas were found to be associated with the build up of high mass fragments, sometimes present as aggregates. Tentative assignment of peaks suggested that there was a range of high molecular weight contaminants as a homologous series of  $\text{C}_x \text{H}_{2x+1} \text{NO}$ . Seppanen [86] also used TOF-SIMS in conjunction with XPS to study the spreading of AKD and ASA sizing agents on uncoated papers. The XPS was used to determine its chemical state and the SIMS, its lateral distribution. Seppanen showed a strong relationship between the drying conditions used in the papermaking and the spreading and redistribution of AKD sizing agent on the paper surface. Spreading of the AKD continued to occur via an autophobic monolayer precursor. The rate of spreading increased with increasing temperature, and decreased with a higher melting point AKD. The spread of AKD was enhanced by the presence of extractives from the furnish, when in water and was not hindered by either hydrolysed AKD or the presence of PCC filler.

In another publication Kulick and Brinen [87] showed the use of TOF

SIMS in identifying two different type of 'fish eye' (transparent area of paper) contaminants in paper. One type of fish eye was found to contain fragments of calcium and silicone, as a result of poor dispersion of the calcium carbonate filler and agglomeration of a silicone based defoamer. Another fish eye area also contained black specks. The SIMS showed the presence of alum (peak at mass 27) and a strong peak at 149; a phthalate fragment from PET plastic.

West outlined the use of SIMS and XPS in analysis of packaging interfaces and showed its use in understanding the impact of contaminants on the surface chemistry of interfaces that had failed [88]. The migration of low molecular weight organic compounds and surface active monomers, such as methacrylates caused a failure at the organic / metal interface. After detection and identification of the migrated contaminants, they were able to be eliminated, solving the problem.

Istone [89] described the use of SIMS and XPS to determine changes in the surface chemistry of paper which lead to defects in the final product. Examples included chemical migration, which decreased surface energy and led to a lack of adhesion between polyethylene and paper, and contamination of xerographic paper causing to black streaks. Istone suggests experimental conditions which can be used to overcome the problems of charging and sample degradation, both of which are common problems with surface analysis of paper. Burrell [90] used a combination of XPS and static SIMS to study the changes in surface energy that occurred when polycarbonate film was exposed to UV radiation. This change manifested itself in a decrease in the ink adhesion to the substrate. Filtering out the short wavelengths (<300 nm) resulted in a significant decrease in the photo oxidation. Work carried out by Swift and West [91] has concentrated on the use of SIMS and XPS to study adhesion failure at interfaces, for example, identification of problematic species which cause adhesion failure of inks, coatings and adhesives in multi-layer systems. Pachuta and Staral [92] showed that TOF-SIMS was suitable for non destructive analysis of pen inks.

## 2.5 UV analysis of surface binder content

A number of authors have used ultra violet (UV) spectroscopy for determination of surface binder content of paper coating layers. Whalen-Shaw and Eby [93] for example correlated variations in surface latex content with the occurrence of backtrap print mottle. The technique was described by Fujiwara and Kline [94], and consists of an x-y stage onto which the sample to be scanned is placed. A light source (visible and UV light) was placed above the sample at 90 degrees, and a detector was placed at an angle of 45degrees. The

spot size used was  $0.4 \times 0.4$  mm. The SB latex had an ultraviolet absorption peak at 220nm and 260–270nm due to the presence of the double bonds in the butadiene. The authors found that the surface latex content increased when the dwell time between the blade and the drier was decreased. Binder migration also decreased with strong Infra Red drying. Kline [95] used UV mapping of coating surfaces to determine migration of binders and pigments during drying. Inoue *et al.* [96] investigated many different properties of the colour formulation with respect to binder migration, using the UV/Visible method including latex Tg, co-binder type, solids content, pigment content, and drying regime. A similar study was reported by Malik and Kline [97]. Matsubayashi *et al.* [98] used reflected and transmitted visible light to study coat weight distribution for single and double coated samples using the same instrumentation. The double coated paper was treated with OsO<sub>4</sub> which caused the coating layer to blacken as the Os attached to the double bonds in the latex. High wavelength light reflected from the surface gave a map of the coat weight distribution and the UV absorption, an indication of the latex distribution.

### **3 ELECTRON MICROSCOPY**

#### **3.1 Scanning Electron Microscopy (SEM)**

The first SEM was developed in the 1950s and was used to examine topographical features of a paper sheet in 1958 [99]. Since then this technique has been the standard way to gain morphological information through scales ranging from the microstructure formed by individual pigment particles ( $\sim 0.1\mu\text{m}$ ) to the larger scale of coating distribution (millimetres), and fillers and fibres for uncoated papers [100],[101],[102],[107]. An excellent recent review of modern microscopy techniques and their application in the field of paper is given by Chinga-Carrasco [103]. The instrument works by producing a beam of electrons from an electron gun which are focussed by a series of lenses and electromagnetic fields. The beam passes vertically through a vacuum and onto the surface of the sample. After striking the surface secondary electrons, backscattered electrons, auger electrons and X-rays are emitted, which can be detected with different detectors present in the instrument.

Further developments in SEM technology have allowed more detailed information to be extracted from a coated paper sample. Examples include cryogenic SEM (Cryo-SEM), which allows the study of frozen and immobilized liquids. The environmental SEM (ESEM) works at a lower vacuum allowing liquid samples to be studied. Field emission SEM (FE-SEM) has

higher magnification capabilities compared to conventional SEM. Another advantage is that low accelerating voltage (<1 kV) with FE SEM reduces the requirement of conductivity. These techniques allow samples to be studied while frozen, at lower vacuums (hence the ability to study the effect of moisture) and at higher magnification respectively [23]. These instruments have been used in studying the microstructure of paints drying, and cement for example. Figure 26 shows a cryogenic micrograph of a coating colour containing kaolin and 12 wt.% of a SB latex of Tg 20°C. This was drawn down on a plastic base, and the wet coating layer rapidly frozen in liquid Nitrogen slush. The latex can be seen prior to film formation as a series of small spherical particles about 100–200 nm in diameter.

New methods for improving the resolution and decreasing artefacts produced by mechanical sectioning are being sought. Erfman *et al.* [104] presented a precise method of sectioning and polishing samples for SEM analysis using argon beam milling. This technique was found to have the advantages of being able to section both soft and hard materials simultaneously with minimum distortion and disruption of the sample.

### 3.1.1 Examples of SEM use in paper

Oliver and Mason [105] adapted the SEM so that drops of different fluids and polymer melts could be introduced into the electron microscope and studied with respect to their spreading and contact angle on different substrates. They

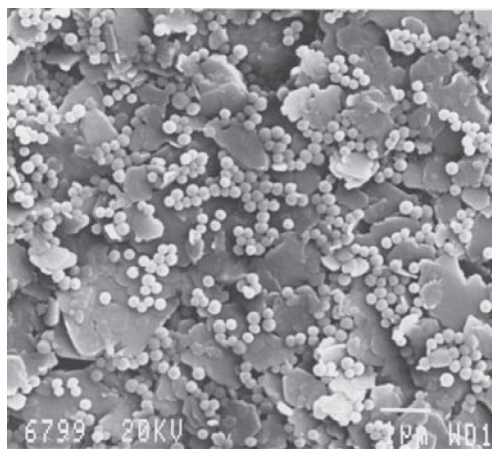


**Figure 26.** A Cryo SEM Image of a coating colour showing a mixture of unfilm formed latex particles and kaolin platelets – from Husband & Hooper.

showed the significant influence of surface roughness and shape and orientation of these roughness features on the spreading of the different fluids. One drawback to the technique was that the substrates had to be coated with gold immediately prior to studying to prevent charging, and this removed any influence on the substrate surface energy on the contact angle.

Morseburg and Chinga-Carrasco[106] have reported a combination of SEM and FE-SEM for analysis of clay and nanofibrillated cellulose in layered TMP sheets. Synergistic effects were seen by inclusion of the nanofibrillated cellulose, which allowed an increase in optical performance with the filler addition without loss in strength. Laser profilometry was also used to assess the surface topography of the sheets.

SEM has been used extensively to provide both surface images of a paper coating, and of sections through it [107],[108]. Chinga and Helle [109] used SEM in secondary and backscatter electron imaging (SEI, BEI) mode to study the surface porosity of coated papers. For different areas of the paper, the pore area fraction and the mean pore diameter were quantified, using image analysis. It was found that there was a correlation between the variation in size of the closed areas of coating and print mottling; surfaces which had larger closed areas having higher mottle. This is probably linked to the poor accessibility for the ink oils. Print gloss was also shown to be influenced by pore size and also pore geometry, a finding supported by Preston *et al.* [110]. In these studies Chinga *et al.* developed a combination of paper coating staining methods to show the location of the binder in the coating layer in combination with image processing and analysis routines to obtain a good description of the coating layer topography and porosity characteristics such as the shape of the pores, their size and orientation.

### *3.1.2 SEM for topography analysis*

Kugge *et al.* [111] carried out an extensive study looking at the topography of coatings in the SEM and Environmental SEM (ESEM) which varied in their pigment content (calcium carbonate and kaolin), their latex glass transition temperature, the thickener type (carboxymethyl cellulose (CMC), ethyl hydroxyl ethyl cellulose (EHEC)) and thickener molecular weight. The colloidal interactions taking place between the different coating components were shown to have an impact on the morphology of the surface layer. This was shown as differences in the roughness, particle orientation and surface porosity, which in turn influenced the final gloss of the coating layers. Drying experiments in the ESEM appeared to give a different surface structure to those coatings prepared by the mechanical bench coater, so were of limited use.

Scanning electron microscopy can also be used to give a micro-roughness

parameter as described by Santos *et al.* [37]. They correlated their roughness index (SRI) with sheet gloss. Another key technique is the use of SEM in backscattering mode (BSEM). This can increase the contrast between the coating layer and base paper and can provide details of coating coverage and coat weight [112].

### 3.1.3 Staining and cross sections

Staining techniques may enhance and extend the usefulness of SEM and a number of these were outlined by Chinga-Carrasco in reference [103]. Amongst these are the use of bromine gas to stain lignin containing papers. The technique is very easily carried out and has been used to improve the quality of backscattered images. These have been used to see the distribution of lignin in pulp after different refining processes or in the presence of moisture, e.g. by Gregersen *et al.* [113] and Reme *et al.* [114].

Another staining method often used in this field is that of  $\text{OsO}_4$ . This osmium tetroxide attaches to double bonds, as described for the UV technique in section 2.5 and can be viewed in SEM – BSI mode. This staining technique has often been used to determine the position of latex throughout a coating paper, for example as shown by Chinga-Carrasco in Figure 27, Dahlstrom in Figure 28 [115] and by Preston in Figure 29.

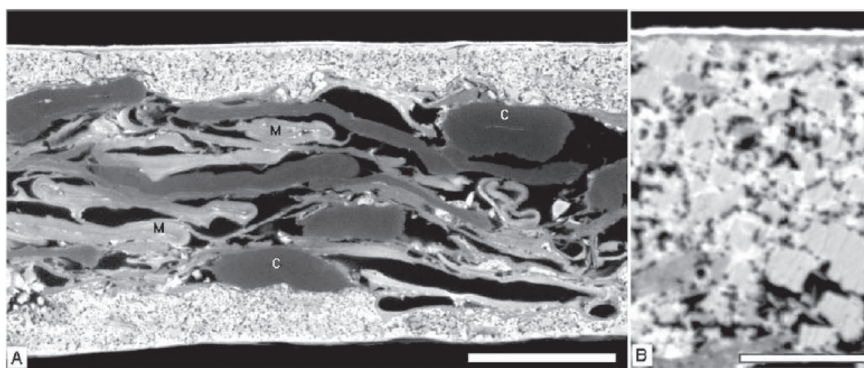


**Figure 27.** BSE images of coated paper reacted with  $\text{OsO}_4$ . A) Mechanical pulp fibres (M), and chemical pulp fibres (C) can be distinguished in the low magnification image (Bar: 25  $\mu\text{m}$ ). B) High magnification image of the coating layer. Top: Gold sputtering establishes a bright borderline between the (grey) printing ink and the (black) epoxy. Main part: The binder films are observed as bright areas surrounding the (grey) pigment particles and (black) voids, filled with epoxy (Bar: 5  $\mu\text{m}$ ). Courtesy of Chinga-Carrasco & reproduced from [107].

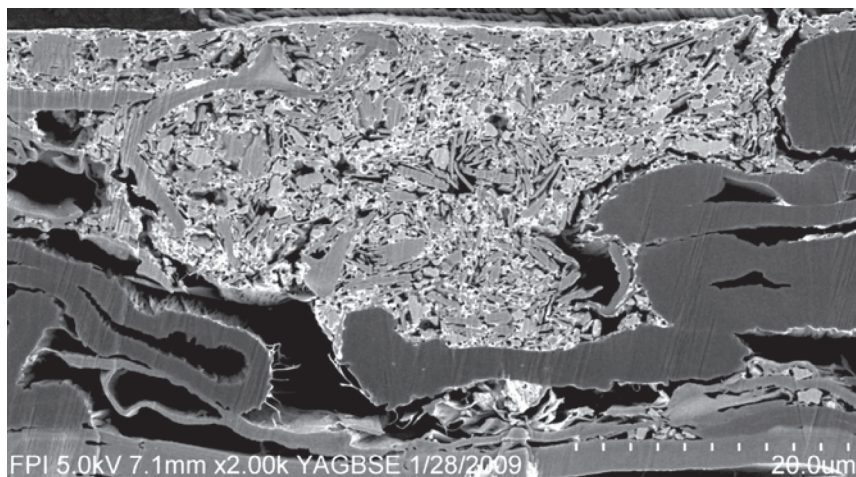


**Figure 28.** OsO<sub>4</sub> treated coating. The white areas are the latex, grey the pigment particles and black, the pores.

The osmium tetroxide technique has also been used by Pohler [116] *et al.* to analyse the pore structure (size, pore volume and pore orientation) of paper coating sections produced using different minerals and binder levels. The porosity and pore sizes achieved using image analysis of the SEM sections was compared to mercury porosimetry of the coated papers and a qualitative although not quantitative agreement was observed. The study also used SEM images of the surface to quantify the coating surface porosity, pore size distributions and pore area. The surface porosity had more impact on the printability than did the bulk porosity characteristics.

### 3.1.4 SEM and image analysis

Chinga *et al.* [117] published a good description of the surfaces of supercalendered paper filled with kaolin and calcium carbonate, which was assessed using a combination of SEM and laser profilometry and image analysis. Gold coating was applied to the surface of the papers prior to measurement and this was shown to reduce artefacts commonly encountered when measuring with the profilometer (Figure 30). An Image J (image analysis) plug in was used in development of a gradient analysis of the profilometer data and parameters such as a gradient magnitude, orientation and surface area were obtained.

Bandpass filtering was used to break down the image into a series of different

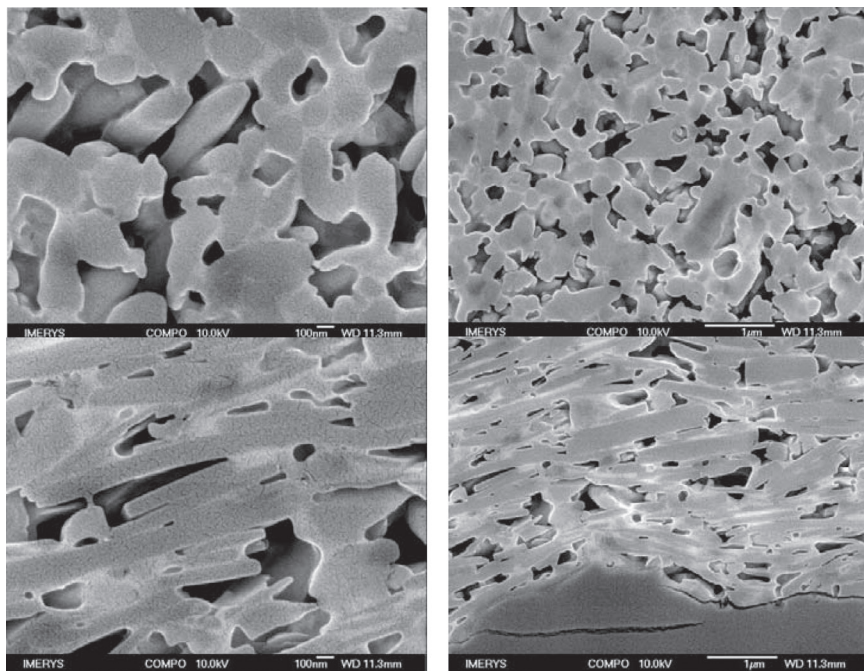


**Figure 29.**  $\text{OsO}_4$  treated PCC and kaolin coatings at two magnifications, which have been sectioned without embedding resin and then analysed in the SEM using backscattered electrons. The latex appears as white edges to the pigment particles (Preston unpublished work).

wavelengths and the magnitude of roughness at these different wavelengths assessed. The PPS (Parker Print Surf) roughness commonly used for paper assessment correlated best with surface features of between 80 and 160  $\mu\text{m}$  whereas the gloss correlated best with micro-scale features below 12  $\mu\text{m}$  in size.

The technique of bandpass filtering of images to show variations at different length scales has also been used by several authors for study of variations in gloss and print mottle for example [118]. Non-uniformity on the scale of 0.1–10 mm in size has been reported as important for paper as this is the scale of paper flocs and fibres and of human perception [119]. Johansson *et al.* suggest that a size of 1–8 mm is the region of interest when studying print mottle [120].

SEM has been used by Dahlstrom *et al.* [121] to analyse sections through coated paper in order to determine how the base sheet properties influence

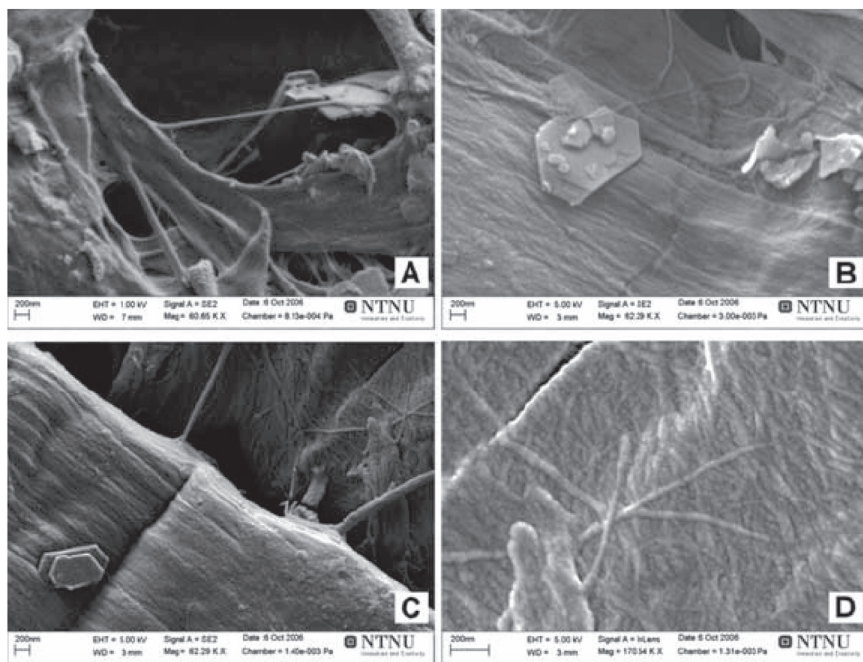


**Figure 30.** Field-emission SEM micrographs of untreated samples (A), and treated with 30 s (B) and 120 s (C) gold sputtering. The upper-right area of C has been magnified to better visualize the microfibrils (D). Reproduced from Chinga [117].

the coating thickness uniformity at different length scales. SEM was used in backscattered mode to obtain a number of images covering a 6 mm length of paper. Image J was used to stitch the images together and then the coating thickness, coating surface profile, base sheet thickness, surface height (base sheet profile), mass length and pore length were measured (Figure 31). It was found that the surface height variations in the base sheet controlled the coating uniformity at shorter length scales. At short wavelengths, the coating filled the micro pores and micro roughness of the surface causing a levelling effect. Studying a larger area of paper revealed contour coating which followed the base sheet surface.

In another subsequent publication Dahlstrom and Uesaka [122] once again used SEM sections and showed that coating thickness distribution resembled random deposition with local levelling. At length scales of the order of fibre widths, strong levelling occurs and the coating thickness distribution is strongly influenced by the basepaper surface profile. At longer length scales

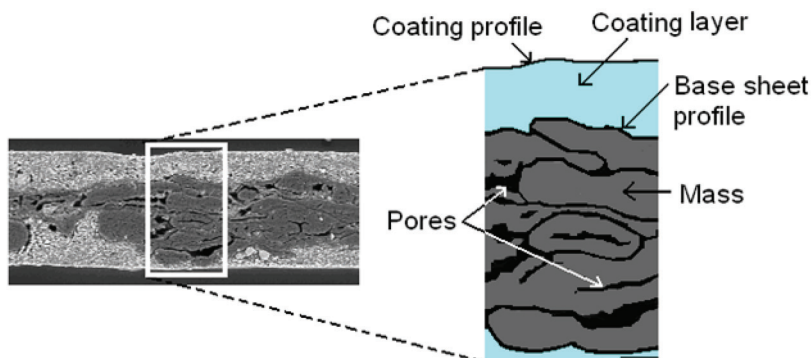


**Figure 31.** Schematic of paper section measurement positions, from Dahlstrom [121].

coating thickness variations diminish in intensity but still retain a significant correlation with base sheet structure, particularly formation, and a contour coating situation results. Differences of opinion in the literature probably arise from the different length scales studied by authors and the different resolutions of the techniques used.

### 3.1.5 Dispersive X-Ray analysis EDX on SEM

One useful attachment to the SEM is Energy Dispersive X-Ray Analysis (EDX), which allows both analysis and mapping of elements in the specimen. In this technique, the SEM electron beam causes electrons from the inner shells of the atoms to be ejected, forming ions. To stabilise the system, an electron from the outer shell then drops back to the inner shell and in doing this energy is emitted as an x-ray. The x-ray has a characteristic energy which enables identification of the element. It is possible to detect elements down to beryllium in atomic number. Semi quantitative analysis is possible by comparing the peaks with known standards, although matrix effects must also be taken into account. Gibbon [123] gives a good overview of how SEM and EDX can be used in the analysis of coated papers. The importance of careful sample preparation and measurement especially for fractured samples is emphasised, for example the need to analyse from at least two different positions if a rough and uneven sample is studied.

Kuang *et al.* [124] presented a simple method for determination of styrene-butadiene latex distribution in a latex containing paper. The paper was treated with bromine which attached to the double bonds in the latex. The sample was then cross sectioned and the distribution of bromine detected

using the EDX attachment to a SEM. The technique was able to show differences in latex distribution due to differences in paper density, degree of sizing and latex charge.

This technique has been used widely to study the filler distribution throughout a filled sheet [102]. In the example below (Figure 32), the image is an average of 6 scanned areas. The filler can be seen to be evenly distributed through the thickness of the sheet [125].

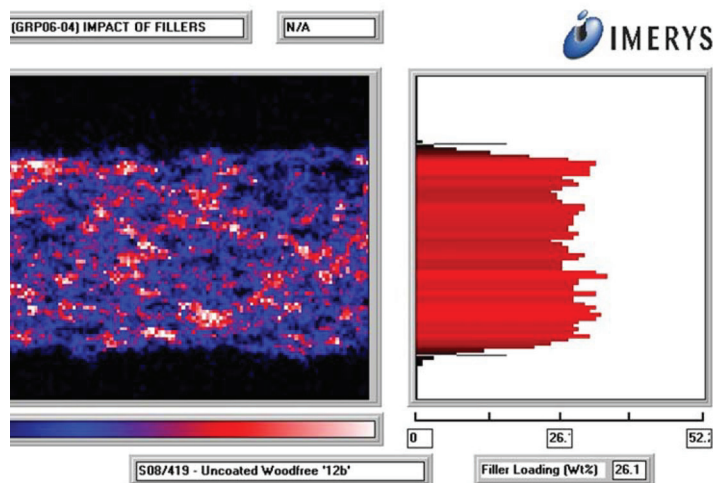


**Figure 32.** EDX composite map, showing filler distribution in an uncoated Wood Free (WF) filled sheet.

### 3.2 Transmission Electron Microscopy (TEM)

Transmission electron microscope is often used for high resolution images of thin sectioned materials. The draw back of this technique is the fact that only thin sections of samples can be used (typically 50–100nm) as the beam needs to penetrate through the sample, and this often involves time consuming embedding and cross sections using an ultra microtome. In the field of paper it has been used to look at the structure of paper coating layers and ink as shown in Figure 33. It also has application in the study of particle morphology, and a shadowing technique has been applied to particles of kaolin in order to determine their aspect ratio, as shown in Figures 34 and 35.

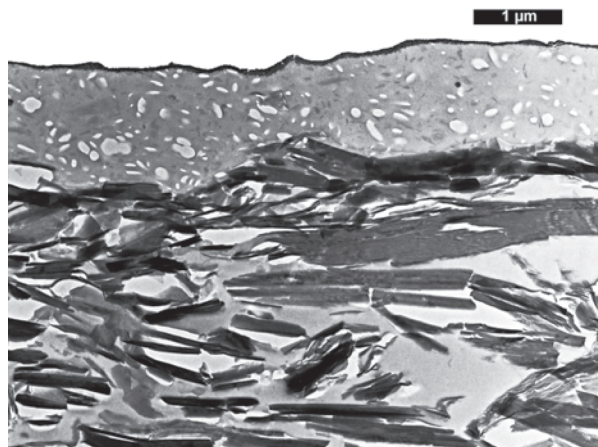


**Figure 33.** TEM thin section through a printed kaolin coating.

Climpson and Taylor [3] carried out work looking at pore structures of kaolin layers prepared using a transmission electron microscope. The kaolinite layers in various stages of flocculation were flaked off a plastic substrate and were embedded in epoxy resin. After ultra-microtoming to obtain ultra-thin cross sections, the samples were etched with hydrofluoric acid. The subsequent micrographs were analysed using an image analyser and the pore system modelled as a series of oblate spheroids. These were then used in light scattering calculations and were found to be in good agreement with the experimental measurements.

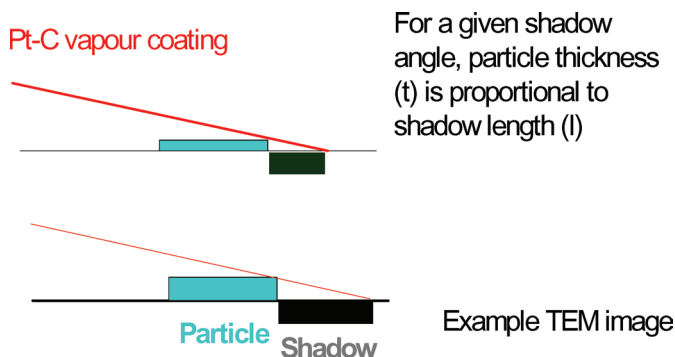


**Figure 34.** Schematic of TEM particle shadowing technique.

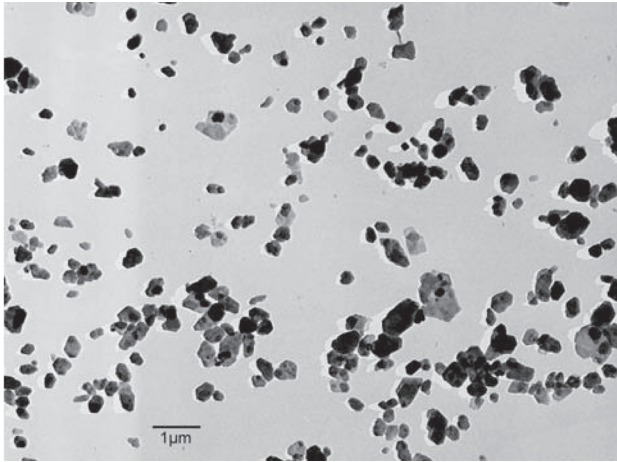


**Figure 35.** Shadowed particles viewed in the TEM used for determination of particle aspect ratio.

## **4 PAPER TOPOGRAPHY**

The study of paper topography is vital for many important aspects of paper's optical appearance, gloss and surface finish and also its printability. In the section below a number of different ways for measuring the topography are outlined in the order of increasing resolution.

### **4.1 Air leak methods**

The substrate topography is another important parameter for controlling the optical and print properties of a paper and there are many references covering this field. A good review of the different methods of measurement is given by Barros [126].

The most common instruments used in the field of paper science are the air leak instruments, for example the Parker Print Surf [127],[128], the Bekk smoothness tester [129],[130], the Bendtsen tester [131] and the Sheffield/Gurley Hill [132]. These instruments have the advantage that they are standardised, easily and quickly used and are relatively inexpensive. They have also shown some correlation with printing roughness. The basic principle involves forcing air between the surface of the paper sample and the measuring head and determining how quickly the air can pass through this junction. The

different instruments have a range of backing materials and design of measuring head.

## 4.2 Profilometry & interferometry

Laser and stylus profilometry have often been used to map the surface topography of different paper samples [149],[133],[134],[135]. The stylus profilometry however is limited in its resolution of roughness by the diameter of the stylus tip, which is typically 5–10  $\mu\text{m}$ . The macroroughness of the sheet is made up of features of a large range of length scales and it is often useful to treat the raw data with a Fourier or Walsh transform in order to quantify the magnitude of roughness at each wavelength as described by Kent *et al.* [136]. This was used to determine roughness contributions from the basepaper fibres and from coatings with pigments which immobilised differently and had different coverage over the basepaper. I'Anson [137] used 3-d laser surface profiling to describe the topography of paper and board samples. Fast Fourier transform (FFT) filtering of the data allowed the periodic marks, such as those from the wire or felt to be subtracted from the stochastic variations occurring in the paper (due to formation or roughness of the paper during drying). The contribution of each type of roughness on the final appearance of the paper could then be identified. Mercier *et al.* [138] have reviewed the different techniques used to analyse paper surface topography, with specific reference to different data treatment methods, including Fourier Transform, autocorrelation and wavelet transform. Laser profilometers have some advantages compared to stylus profilometers in that they do not cause any marking of the sample. A comparison between laser and stylus profilometers is given by Wagberg and Johansson [139]. They measured papers of area  $20 \times 20$  mm and found that larger scale roughness features correlated well between the profilometers. However when finer length scales were measured, of the order of the size of pigments, fibres and floccs, some differences were observed; with the optical profilometer giving much higher roughness than the mechanical profilometer. The optical sensor was disturbed by the fine scale 'noise', whereas the large stylus tip was relatively insensitive to it. It was concluded that the real roughness was somewhere between the two.

White light interferometry is a method of imaging a surface based on the difference in optical path of a reference beam and the sample light beam, and analysis of a fringe pattern. The instrument is similar to a microscope, but the beam of light illuminating the sample in reflectance mode is split into the reference beam and that passing to the sample. After recombining the beam, the resulting constructive and destructive interference patterns are analysed in order to generate a 3-d interferogram. A commercial example of such an

instrument is a Wyko Interferometer, and this has been used by many researchers to determine the topography of paper, printing plates etc. (Figures 36 and 37). A comparison between white light scanning interferometry and white light confocal chromatic microscopy and other methods of surface topography are given by Soysouvanh *et al.* [140].

The OptiTopo is an instrument developed at STFI-Packforst AB which will quickly and easily determine the topography of a paper substrate. The technique is based on a photometric stereo principle where a camera picks up 2 images from the same area on the paper which has been illuminated from two grazing angle light sources from opposite directions. The light sources are carefully calibrated and the position of the highlights and shadows obtained from both light sources allows the topography to be calculated. The technique is described fully by Hanson and Johansson [141],[142]. The technique has been used widely for studying the surface topography of paper with respect to print defects; for example the occurrence of missing dots, which

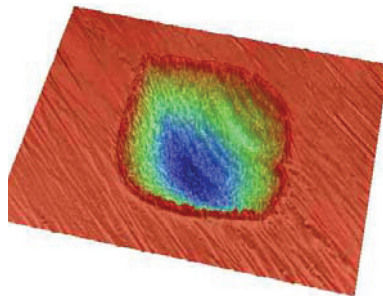


**Figure 36.** A 3-d representation of a rotogravure cylinder cell – Swansea University.

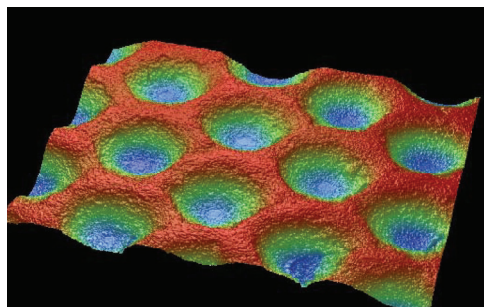


**Figure 37.** A Wyko Interferometer image of a flexographic printing anilox roller surface – Swansea University.

were found to correlate spatially with dips in the paper surface. Land used the device to study the waviness caused by application of moisture to paper held under tension [143]. In a similar study the OptiTopo was used by Nordstrom *et al.* [144] to quantify the waviness present after heatset offset printing of light weight coated papers. The instrument results were shown to correlate well with human perception and ranking. The technique was refined by Barros [126], who subsequently used it to determine the reason for uncovered areas (UCA) in a flexo printed board. He found a strong correlation between the UCA and depressions in the surface, detected by the OptiTopo[145].

### 4.3 Imaging reflectometry

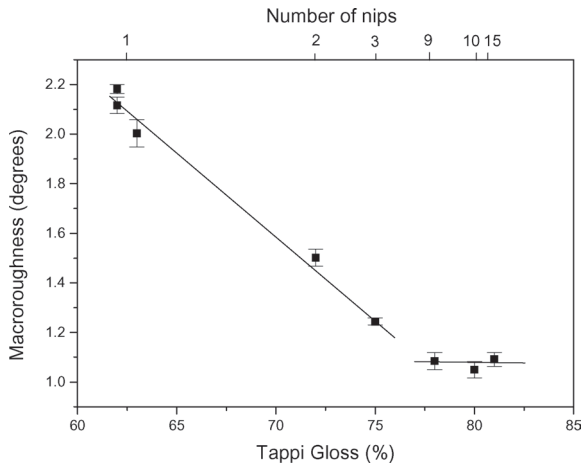
The Imaging Reflectometer [146] is an instrument which can give information concerning gloss and topography of paper surfaces and is based upon an instrument developed by Gate *et al.* [147], [148], [149]. An imaging detector is used to measure the intensity distribution of light forward scattered from a paper surface. By using light polarized perpendicularly and horizontally with respect to the surface, and at two wavelengths, it is possible to derive effective refractive index, microroughness (surface roughness smaller than the wavelength of light), macroroughness (surface roughness greater than the wavelength of light), plus various gloss and reflectance parameters. The technique has been used in many instances to determine differences in topography and surface porosity of different coating structures [150], [151] and also changes occurring with time, such as ink drying [152], [153].

Figure 38 and 39 show data from a laboratory calendering exercise where a clay coating was systematically calendered with increasing number of nips. Figure 39 shows changes in refractive index and microroughness as a function of number of nips. The first couple of passes through the calender compress the base sheet (seen as a large decrease in macroroughness Figure 38), but produces relatively small changes in refractive index and microroughness. A larger number of nips begin to compress the coating layer as well resulting in compaction (increasing RI) and orientation of the clay (decreasing microroughness). A decrease in both the micro and macro-roughness results in an increase in gloss [151].

A comparison of the reflectometer with other gloss measuring devices, for the study of ink drying with time has been made by Koivula *et al.* [154].

### 4.4 Confocal laser scanning microscopy

Light is emitted from a point source and passes through an objective onto the sample. It is then reflected from the surface of the sample and passes through



**Figure 38.** Macro-roughness versus number of nips and Tappi gloss. The first few passes through the calender compress the basesheet and have a significant effect on the macroroughness. The larger number of nips does not affect basesheet smoothness.

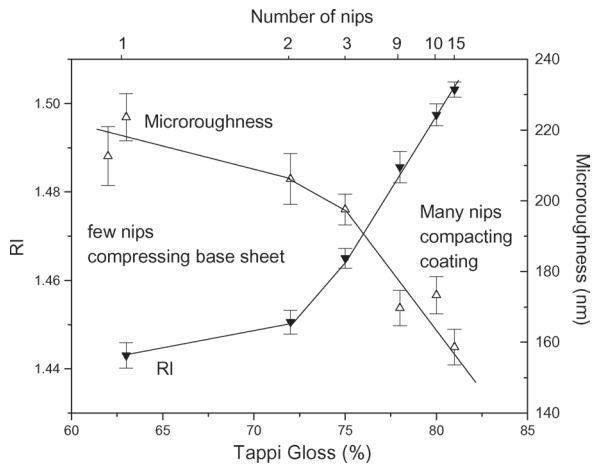


**Figure 39.** After the basesheet compression, further calendaring compresses the coating layer resulting in a lower micro-roughness, a denser, higher RI surface layer and a higher gloss.

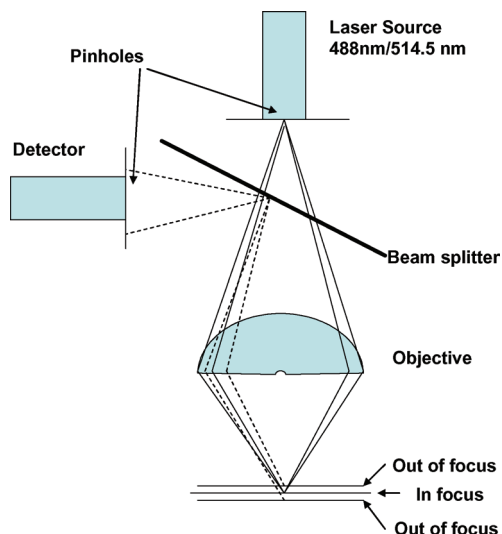


**Figure 40.** Schematic of a confocal laser scanning microscope – reproduced from [170].

a beam splitter to reach the detector. A small pinhole, variable in size, allows only light coming from the focal plane to reach the detector, thus allowing only a thin slice of the sample to be imaged. The focal plane can be moved up or down by a few millimetres allowing some depth profiling to be carried out in the sample.

The resolution for this technique is approximately  $0.2\text{--}0.7\ \mu\text{m}$ , and this decreases with increasing depth of study in the  $z$  direction. There is also a relatively low contrast between different components in a paper. On the positive side, the technique may be automated to allow a series of images to be captured as a function of depth and reconstructed into a 3-d image, or a map of the surface topography, and also the technique does not require any high vacuum allowing wet samples to be studied [103].

#### 4.4.1 Examples of confocal laser scanning microscopy in paper – Topography

Mangin and Beland [155] used the technique to look at paper surface topography. In this reference the authors also used the technique of optical sectioning to determine the coating thickness of two layers of coating in a triple coated paper. The topography results have been related to variations in the local gloss of the paper [156], [157].

The instrument can also be operated in a fluorescence mode, where

fluorescent light is detected at the focal plane. A combination of surface maps in standard mode and fluorescence mode has been used to determine the distribution of black ink (not fluorescent) over a paper surface, together with the topography of the paper for the same area. This gives a good idea of the influence of topography on ink distribution [158].

Smoothness of paper under compression is vital for transfer of ink from the printing cylinder to paper in rotogravure printing [159]. The smoothness under compression was measured by Mangin *et al.* [160] using Confocal Laser Scanning Microscopy (CLSM). An increasing static force was applied to the surface of the paper and the topography of the surface measured as a function of the applied pressure.

Jarnstrom *et al.* [161] used a combination of confocal microscopy and AFM to analyse the roughness features of coating layers which were prepared using plastic pigment and kaolin, and then compare this topography to the gloss of the coating layers. The roughness was analysed at a wide range of length scales using a method based on a two point correlation, where both the amplitude and lateral spacing of the roughness was taken into account. A clear connection was seen between the autocorrelation length and the RMS roughness. It was seen that a small amount of the plastic pigment was able to cover the surface significantly and change its topography and gloss, but that the kaolin coatings had a different response. The most useful image sizes for correlation with measured gloss was between 6,000 and 10,000 nm. Image sizes below 2,000–3,000 were found to be of no relevance to gloss.

#### *4.4.2 Examples of confocal laser scanning microscopy in paper – Coating analysis*

Hirai and Bousfield [162] characterised the penetration of coating colour and coating coverage over a paper substrate using a combination of CLSM and image analysis. Rhodamine-B dye was used to stain the samples after coating, to determine the presence of the dry coating layer. The same stain was added to the wet coating colour to determine the position of the water phase after coating. A second stain, Nile Blue A was used to stain the basepaper. Both techniques were able to give some information concerning coating thickness distribution; however the confocal staining technique does overestimate the coating thickness compared to the SEM (by roughly 3  $\mu\text{m}$ ). There were some difficulties deciding the threshold level, as thicker coatings had attenuated signals due to scattering in the sample.

In a similar publication Ozaki *et al.* [163] also used Rhodamine-B dye and confocal laser scanning microscopy to study the distribution of coating on

basepaper and relate this to backtrap mottle. It was seen that coatings with a more uneven coating thickness distribution were more prone to backtrap mottle. The penetration of ink resin was also followed by detection of fluorescence from a dye and the backtrap mottle was also shown to correlate with uneven resin penetration. Ozaki *et al.* [164] also used this technique to quantify and image the penetration of UV curing offset ink vehicle into uncoated papers. An oil immersion objective lens was used to follow the penetration of the vehicle into the coatings and a series of 2-d images were reconstructed into a 3-d image. Differences in vehicle penetration were observed for different surface sizing strategies, and the ink vehicle was found mainly associated with the fillers in the sheet.

For uncoated paper, the technique has a wide area of application. Drying of fibre webs and shrinkage and collapse of the fibres were followed using CLSM and were reported by Nanko and Ohsawa [165], and Nanko and Wu [166]. This technique has been used by Jang *et al.* for quantification of the cross sections of pulp fibres for determination of wall thickness [167], and to study fibre rigidity and collapse with refining energy [168]. However if a statistically significant number of fibres are to be analysed, then a different approach is needed and Reme *et al.* [169] describe a technique where a large number of fibres are aligned, bundled together, embedded in epoxy resin and cross sectioned. They were subsequently studied using SEM in a back-scattered mode.

A good review of the use of both CLSM and atomic force microscopy is given by Beland [170], and has also been reviewed by Wygant *et al.* [171].

#### 4.5 Atomic Force Microscopy (AFM)

Atomic force microscopy was first introduced in 1986 by Binnig, Quate and Gerber [172]. This technique is extremely useful [173], [174]. A good introduction to the technique is given by Hanley and Grey [175].

The technique uses a very fine stylus which is scanned over a surface in a raster pattern [170], [176]. A 3-D image of the surface can be made up by monitoring the motion of the stylus, by measuring the deflection of a laser beam from the tip surface. More detailed information can also be gathered such as the height and width of the surface features using the data from line profiles [177]. There are many variations of the technique; these being, contact force microscopy, lateral force microscopy, non-contact force microscopy, force modulation mode and tapping mode. Each variation uses a slightly different technique to obtain an image of the sample. These can be read about in detail elsewhere [175].

Advantages of AFM include:

- Measurements of horizontal and vertical length scales are possible.
- Is a non-destructive technique [178]
- Ability of 3-dimensional magnification.
- Range of sample environments (ambient air, vacuum, fluid environment & low temperatures).
- Requires no sample preparation.
- Has resolution at the nanometre scale. The range of sample size possible for the measurement is from around  $10 \times 10 \text{ nm}^2$  to  $100 \times 100 \text{ }\mu\text{m}^2$  [170].
- Can give information about topography, but also micro magnetic fields, friction forces, sample stiffness and localised electrostatic fields [170].
- Can use AFM in tapping mode to resolve the structure and differentiate between binder and mineral particles.

These advantages have allowed the study of a wide range of materials and processes, including biological molecules, electrochemical processes *in situ* and surface properties of polymers [175]. Although this technique is fairly new, there are already many other applications [179] of AFM particularly in the field of nanotechnology [180], [181].

#### *4.5.1 Examples of use of AFM in paper*

A common use of AFM is in the visualising of the sub micron structure of paper coatings [182]. The images obtained can show the particle size and shape of the components but on a very small area of the sample. Haunschild *et al.* [183] used AFM to explore coated paper surface roughness and structure. They showed that calendering induces an asymmetric deformation of the coating, flattening the hills and leaving the valleys relatively unaffected. During the first nip, the valley depth decreased by 25%, while the peaks are flattened to 50% of their original height.

Larsson *et al.* [184] used AFM to study the topography of coatings prepared with blends of clay and GCC. The pigment slurries alone produced very micro-smooth coating layers. However addition of latex and CMC thickener resulted in a significantly increased micro-roughness.

Jarnstrom *et al.* [185] studied the topography of coatings prepared with increasing levels of PCC onto a synthetic rough substrate. Topographical images at 3, 10 and 50  $\mu\text{m}$  length scales were obtained. A relatively low coat weight smoothed the surface when studying at a larger scale (50  $\mu\text{m}$ ), but increased the RMS roughness when looking at a 3  $\mu\text{m}$  length scale. The surface topography was then related to the gloss of the coating layers.

Wallstrom *et al.* [186] used AFM to study the ordering and particle packing of polystyrene particles in the presence of different thickeners (CMC and

EHEC). In this work, topographical images of the coating surfaces were achieved using the AFM. Image analysis was then used to process the data and a pair distribution function (in 2-d) was used to determine the ordering (correlation length which is related to the size of the domains) of the particles. As the thickener concentration increased, so did the disorder in the coating layer. This also related to depletion and bridging flocculation of the coating mixtures. In reference [187] the work was extended to look at the effect of a water swellable emulsion and poly vinyl alcohol on the ordering and rheology of a polystyrene coating. The final coating microstructure appeared to relate more to the concentration of water soluble polymer during the final stages of consolidation and drying than the initial viscosity of the colour. Finally the work was extended to look at PCC containing coatings [188], but the pair distribution function was not able to predict ordering in this system. Instead the surface structure was described by a nematic structure where the particles were seen to be aligned in the machine direction. A particle orientation parameter and number of particles per unit area were used to describe the surface.

In a recent publication by Chinga *et al.* [189], the 3D characterization of 25 coated papers was described by using the techniques of laser profilometry, atomic force microscopy and X-ray microtomography. The different techniques were complimentary describing different aspects of the coating layer structure, topography and gloss. They also found that features smaller than  $1\mu\text{m}$  in size had little impact on the paper gloss, that the facet orientation polar angle is a function of the roughness and that skewness did not describe the surface features responsible for the gloss of the coatings. The AFM analysis showed that root mean square roughness (Sq) had a good correlation with the paper gloss when looking at features greater than  $1\mu\text{m}$  in size. The best correlation was found for wavelengths of between 2 and  $8\mu\text{m}$  which corresponds to features of approximately  $1\text{--}4\mu\text{m}$  in size. This was agreement with the findings of Jarnstrom *et al.* [161].

Related to paper, Gelinás & Vidal [190] developed and automated the AFM to analyse the aspect ratios of different platy minerals such as kaolin and talc samples. The results were different in magnitude than for other published values, but ranked the pigments in a similar order.

#### 4.5.2 *Studies of latex coalescence*

AFM has been used extensively in the study of latex for example by Santos *et al.* [191] who studied the morphology and electrical potential patterning of different SB latex films using both AFM and Scanning Electric Potential Microscopy (SEPM). They showed that different packing, cubic and

hexagonal arrays, occurred in neighbouring regions. Granier *et al.* [192] used AFM to study the adhesion and ordering of latex particles on model inorganic surfaces. They varied the chemical nature of the surface and the drying conditions and then used the acid – base theory to discuss the latex interactions and spreading.

A similar study was reported by Unertl [193] who used scanning force microscopy to study the wetting of styrene-butadiene particles on cleaved calcite surfaces. Images from the SFM were used to show the contact angles of the latex particles and showed that the latex particles spread with a slight anisotropy. This resulted in a variation of the contact angle around the edge of the latex particles of  $\pm 6^\circ$ .

Carlsson [194] used AFM to study the coalescence of latex particles with different viscoelasticities. Lin and Meier [195] concentrated on the physics of latex film formation and used AFM to obtain corrugation height data, as a function of the latex properties, temperature and time. They showed that the rheological properties of the latex and the film formation kinetics were directly related, and that the capillary pressure from the water meniscus in wet latex is the dominant driving force for film formation. Meineken and Sander-son [196] used AFM images to study the coalescence of structured (core-shell) latices and latices of different particle sizes with time at different temperatures. Film formation was observed to be influenced by both latex particle size and morphology as predicted, however the core-shell ratio of latex particles appeared to play no role in the kinetics of the film formation.

Backfolk *et al.* [197] studied the influence of a linear anionic dodecylbenzene sulphonate (SDBS) and a non-ionic fatty alcohol ethoxylate (AE) surfactant on the surface morphology of a medium carboxylated styrene/ butadiene latex film. AFM was used to study the localisation of the surfactant on the latex film and the changes in the surface topography caused by aging the latex.

#### 4.5.3 *AFM in print evaluations*

Strom *et al.* [198], used AFM scans at two different magnifications/ length scales, to show that when applying ink to the surface of a coating, the ink will cover the micro-roughness features in the paper, thus increasing the gloss, but generally will not cover the macro-roughness features of the paper (Figure 41).

Bassemir [199] has reported the use of AFM in determination of the topography of printing blankets (offset), and printing cylinders for roto-gravure printing. In the area of printing Naito *et al.* [200] carried out work looking at transfer of sheet fed offset ink to cast coated paper. The size of the

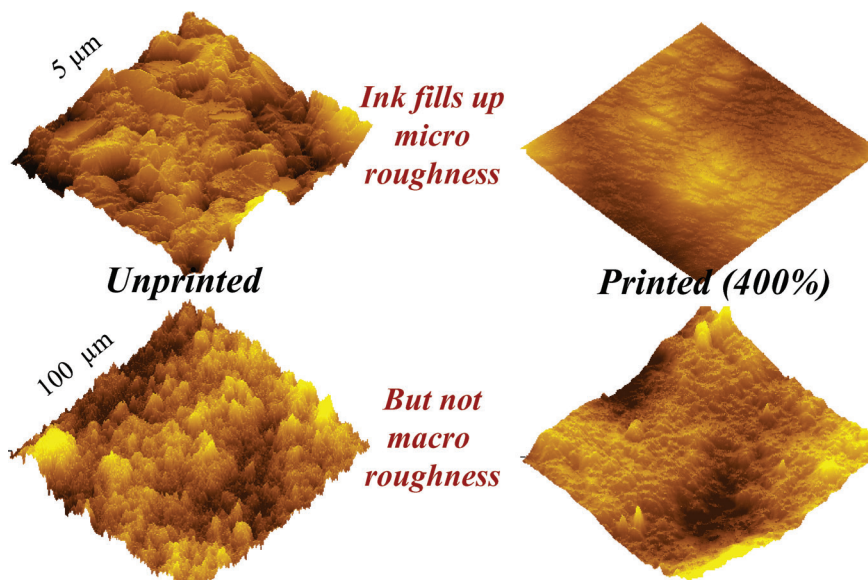


**Figure 41.** AFM images of unprinted and printed coating layers at 2 magnifications from Strom *et al.* [198].

ink particles with increasing ink transfer amount were measured, as well as the topography of the dots, which were shown to be elevated by around 0.7mm above the plane of the paper. Pits in the ink were observed due to emulsification of the fountain solution.

Tag *et al.* [201] used AFM and surface energy measurements to study the influence of surface roughness on the wetting of coated offset papers. Wetting was studied using contact angles of different liquids and was found to be significantly influenced by the microscale topography. The authors derived a roughness parameter describing the ratio between the effective and the real surface area, which is a measure for the roughness compared to an ideally flat surface.

## 5 OTHER PHYSICAL ANALYSIS

### 5.1 Optical microscopy

Optical microscopy has also been used to study the characteristics of coating layers and paper for example by Elton *et al.* [202]. A good overview of the use of the optical microscope in studying coated papers, defects and

identification of unknown contaminants is given by Quackenbush [203]. Sections through coated and printed papers are often studied using optical microscopy in order to determine the position and penetration of ink into the surface [204].

The depth of penetration of inkjet dye based inks into surface treated papers using sample cross sectioning and optical microscopy has been reported by Muck and Novak [205]. De Almeida *et al.* [206] reported on the printing of pigment based inkjet inks onto inkjet media and a study of the coverage and optical density of the printed patches. SEM, TEM and optical microscopy were all employed to determine the coverage, and ink film thickness of the inkjet inks on the surface.

Wiltshie *et al.* [207] presented an automated slice based concept for 3D paper structure reconstruction. In this process an automated microtome is used to section through paper and an optical microscope can be moved accurately in the x, y and z directions in order to obtain digitised images.

## **5.2 Focussed Ion Beam (FIB)**

FIB is a technique which is primarily used in the semi-conductor and materials science fields but has only recently been used with paper. FIB uses a gallium ion beam which is focussed by electrostatic lenses to cut through and image the sample.

Gallium is a metal which is near its melting point at room temperature. The liquid metal wets and flows over a fine needle. A high potential electric field is established between the tip and an extractor system, leading to an intense beam of positive ions being emitted of between 7nm (at 1pA beam current) and 300nm (at 12nA) in diameter at 30keV energy. A platinum organometallic gas injector allows ion beam assisted deposition of platinum over selected areas of the sample and this may be used to protect the top surface of the sample during ion milling. For sample sectioning, a large ion current is used initially to remove a staircase-shaped trench. A finer beam of lower current was then used to ‘polish’ the larger vertical face of the trench by scanning the beam in a line and moving it progressively up to remove further material. The sample is then tilted to 45° and the polished face imaged using the same ion beam, generally at a much lower beam current to achieve high resolution.

Another advantage of FIB is its resolution capability of a few nanometres giving a precise cut, as shown in Figure 42 [208]. This removes the need for embedding, reduces the risk of damage to the coating layer and also avoids any heat generated thermal degradation.

Figure 43 shows the geometry of the FIB ‘trench’ and the images are taken from the rear wall of this trench, viewed from above at an angle of 45°.

### 5.2.1 Examples of FIB use in studying coating structure and ink penetration

One main application in the paper industry is the investigation of ink penetration into coated paper [209], [210]. Ink penetration is not desirable and can cause several problems, the most obvious being the reduced amount of ink at the surface. Other major issues are that of “scuffing” [211] (where the printed paper marks unprinted paper after printing), picking and piling [212], show through, ink strike through and press runnability. Techniques to study the distribution of the ink in the paper have been explored by many authors for example Vucak *et al.* [213], Uchimura *et al.* [214] and Glittenberg *et al.* [215].

It has been found that ‘organic rich’ components such as the ink absorb the gallium rendering them more conductive, so they are easily imaged. However the coating layer does not absorb the beam to any great extent and the particles are not imaged without a conductive coating. Hence the ink layer can be seen, but the pores and the particles in the coating layer are not visible [216]. The images are captured using the ion-induced secondary electrons whose energy distribution peaks at a few electron volts. If the potential of the sample rises by a few volts, then this signal is severely curtailed and the image will appear dark. For the potential of the sample to rise by a few volts as a result of a 4–10pA ion current impinging upon it, the resistance of the sample to ground must be  $> 10^{10} \Omega$ . It appears that this was the case for the coating material in the work reported in reference [216], while for the ink the resistance was less than this, and its appearance was light. The high contrast therefore achieved between ink and coating has been used to visualise rotogravure, sheet-fed offset and UV cured offset inks and finally water based pigmented inkjet within coated paper surface layers [217], [218].

Figures 43 and 44 show the penetration of rotogravure ink into the pigment particles of a kaolin rich coating layer, and this was found to correlate with the dot size of the prints and the measured print density. Coatings containing higher aspect ratio kaolins resulted in bigger dots and a higher print density [216]. The preparation of thin sections of paper using the focussed ion beam (FIB) technique was presented by Uchimura *et al.* [219] and these authors showed that it was possible to obtain a thin section of printed paper that could subsequently be analysed by the EDX attachment on a SEM. The paper sample did not suffer from the usual structural changes or artefacts associated with resin embedment. In a more recent paper [220], a combination of FIB and EDX to differentiate between ink pigment and ink resin was used by first treating the printed paper with osmium tetroxide. They showed that in screen printing the ink pigment was held on the surface of the substrate, but that the ink vehicle penetrated into the centre of the paper, through the small pores in the paper and along the inside of the fibrils. The

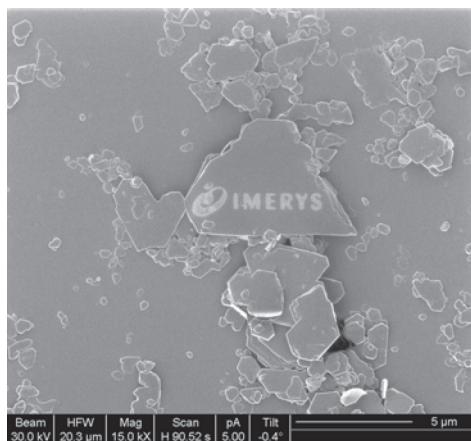
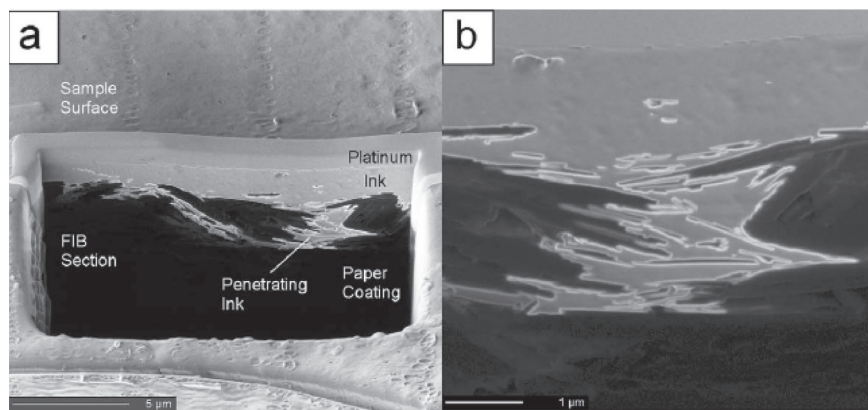


Figure 42. FIB etched kaolin particle, indicating the precision of controlling ion beam.



Figures 43 and 44. This shows a blocky clay coating in both low (a) and high (b) magnification. Ink penetration can be seen clearly in both images.

FIB was used by Uchimura *et al.* [214] to prepare thin sections of inkjet papers printed with dye containing inkjet inks. The distribution of ink was observed using a combination of SEM, optical microscopy and an Electron Probe Micro Analyser (EPMA). However the FIB instrument itself was not used to visualise the printed paper.

To determine which ink components were responsible for the penetration

Koivula *et al.* [212] used the same technique more recently to investigate separate ink components (linseed oil, mineral oil, ester solvent when alone and when combined with a viscous varnish). The results showed that linseed oil penetrated the coating layer to a depth of  $\sim 3\mu\text{m}$  and the ester solvent penetrated to a depth of  $1\text{--}2\mu\text{m}$ . Mineral oil could not be seen in the coating layer using the same technique, however, using a modified TLC plate it was found that mineral oil penetrated the coating layer rapidly, before evaporating due to its volatile nature. When combined with a viscous varnish there appeared to be reduced penetration of all the components [212].

These experiments provide insight into how FIB can help investigate paper coating and printing problems. Figures 45 and 46 are 3-d reconstructions of a series of cuts through a printed PCC and kaolin coating. The increased depth of penetration into the PCC coating is easily observed when compared to the kaolin.

In a recent publication, FIB images of varnish filled coatings were combined with image analysis to provide a description of the pores within coating layers prepared with different morphology pigments [221]. An image analysis technique incorporating a “Maximal Inscribed Sphere” (MIS) algorithm was used to characterise the experimental PCC and GCC 2-d sections. The technique partitions a void space of porous material into an unambiguously

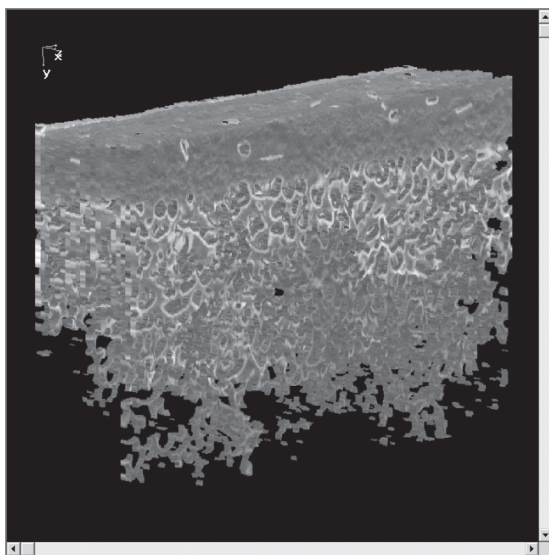


**Figure 45.** 3-d FIB image of ink penetration into a PCC coating layer.

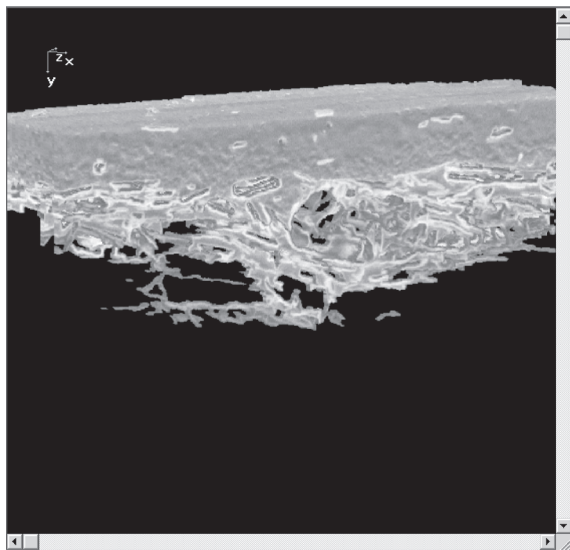


**Figure 46.** 3-d FIB image of ink penetration into a kaolin coating layer. Note that the ink remains mainly on the surface.

defined collection of individual pores and throats connecting them. The results show differences in the pore structure as created by the different pigment particle geometries, including distributions of pore size, pore surface area, pore connectivity, pore surface-to-volume ratio, throat-to-surface area ratio as well as fractal structural parameters. In a similar study Okayasu *et al.* [222] used a FIB instrument to produce cross sections of double coated paper. The sections were then imaged visually in SEM and image analysis was used to analyse the pore size distribution. The authors used polycarbonate membranes with known pore dimensions to show that the porosity determined using this technique was accurate and in good agreement with mercury porosimetry. The FIB cutting technique was found not to destroy the microstructure of the sample, unlike conventional microtoming.

### 5.3 XRD

X-ray diffraction has been used historically to identify crystalline minerals such as kaolinite [223]. An x-ray beam with fixed wavelength is aimed at the sample. Angles at which x-rays diffract from the sample are a function of the inter-atomic spacing associated with the crystalline components [224].

The diffraction patterns produced are characteristic of the crystal structure and these can be used for identification using tables compiled by the Joint Committee on Powder Diffraction Standards (JCPDS) [225]. The relative intensity of patterns can be used to indicate relative abundance.

X-ray diffraction has been used to investigate the surface texture and orientation of crystalline materials [226], [227], [228] and to determine the alignment of kaolin particles in a coated paper [229], [230]. Samples of coatings are mounted in an open Eulerian cradle and during the measurement are tilted and rotated with respect to the x-ray beam. When the kaolinite in the coating is orientated horizontally along the basepaper surface, there is a strong [001] peak, as used by Kraske [231]. The X-ray diffractometer is set up to measure this [001] kaolinite peak, then the specimen is tilted with respect to the goniometer axis to produce a distribution of [001] intensity with tilt angle ( $\chi$ ), as shown in Figure 47. A coating with more aligned particles will have a small peak width with change in tilt angle. The samples were measured for change in tilt angle in both the machine and cross machine directions.

The distribution can be approximated by a pseudo Voigt function (as described by Elton *et al.* [229], [230]), and a measure of alignment can be obtained by determining the full width of the peak at half maximum height

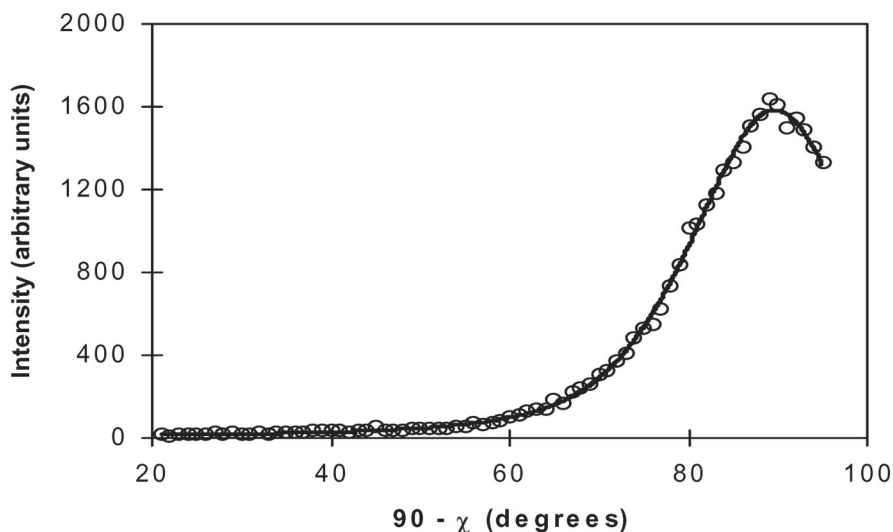


**Figure 47.** A Portion of a Pseudo Voigt Function from which the Measure of FWHM is Obtained (from Elton [230]).

(FWHM). The smaller the FWHM, the more clay plates are aligned parallel to the paper surface.

The technique of XRD particle alignment is a surface biased method but as the X-rays penetrate several microns into the coated surface, it also has some contribution from the bulk. The ATR alignment method is more surface specific and measures the contributions from approximately the top 0.5  $\mu\text{m}$  only (section 2.1.1)

## **5.4 Fluid absorption**

Droplet absorption of fluids into paper and coatings has been used by many authors to simulate absorption of ink and fount and also to determine the surface energy of a surface using two or 3 different fluids of known surface tension [81], [232], [233]. Instruments such as the Fibro DAT dispense a drop of fluid of approximately 2–6  $\mu\text{l}$  in size onto the surface of the paper. A high speed camera captures the image of the droplet on the surface typically 50 times in the first second after application. Image analysis of the captured frame allows determination of change in the drop volume, drop height, contact angle and spreading, via the diameter of the droplet base. Measuring the dimensions of suspended droplets also allows the surface tension of the fluid to be determined, as carried out by Wickman *et al.* [234]. The technique has been used extensively to determine the surface energy of the coating layers for example by Rousu [25], [217]. Different methods of determination of surface energy have involved other techniques not included in this review such as the use of Inverse Gas Chromatography as reported by Lundqvist [235] and Felix & Gatenholm [236].

The Micro-Dat as described by Svanholm [237] has the advantage over the Fibro-DAT in that the volume of fluid applied to the paper is significantly smaller and this will not cause flooding of the pore structure in the coating layer. However Marmur [238] in his review of the theory and practice of measuring contact angles suggests that the droplet size needs to be large.

## **5.5 Mercury porosimetry**

Mercury porosimetry is a technique developed by Ritter and Drake [239] in 1945 which allows the volume and size of macropores and mesopores in porous materials to be measured. Micropores smaller than 500  $\text{Å}$  are best measured by gas absorption.

The paper sample is placed in a glass chamber of accurately controlled size and evacuated to remove the air. Mercury is gradually forced into and then

withdrawn from the sample at increasing and decreasing pressure, and the volume of mercury measured.

The technique is based upon the property of mercury to behave as a non-wetting liquid i.e. the contact angle with the solid surface is greater than  $90^\circ$ . Spontaneous absorption of mercury into pores due to surface tension forces, will therefore not occur, but application of external pressure will force the mercury into the pores.

If the pores are assumed to be cylindrical, and the solid does not deform under the pressure, the pore radius can be expressed in terms of the mercury surface tension, contact angle  $\theta$ , and the absolute applied pressure, according to Laplace equation [3].

$$p r = - 2 \gamma \cos \theta \quad (3)$$

where  $r$  = pore radius

$\gamma$  = mercury surface tension

$\theta$  = contact angle

$p$  = absolute applied pressure in  $\text{kg/cm}^2$

**NB** The contact angle of mercury has been measured for a range of different solids and varies between  $125^\circ$  and  $152^\circ$ . The average of  $141.3^\circ$  is usually used, although a value of  $140^\circ$  was used by Larrondo *et al.* [240]. The surface tension of the mercury is taken as  $480 \text{ mNm}^{-1}$ .

Application of mercury porosimetry to coated paper presents certain practical difficulties. Some of the problems result from the fact that paper is a compressible material, which might alter in its pore structure when intruded with mercury under high pressure. Other difficulties arise because not all of the pores in a paper coating are connected and accessible to mercury intrusion. Ink bottle pores are sealed at one end and may not allow mercury to be fully intruded into them. A fuller description of the problems of mercury porosimetry of paper is given by Kettle *et al.* [241],[242]. In these references, the authors describe two methods of overcoming problems such as compression and shielding of large pores by smaller pores. Commercially available packages for compensation of sample compression (PorComp™) and shielding effects (Pore-Cor™) are suggested. The Pore-Cor™ package models a porous material as a three dimensional structure which has a mercury intrusion curve and porosity value in close agreement with experimental measurements. This model is described briefly in references [241] and [242], and more fully in Matthews *et al.* [243] and Kettle and Matthews [244]. The problems of mercury porosimetry measurement and a comparison of this method with a stain imbibition method are discussed by Larrondo *et al.* [240].

In many cases it is preferable to measure coatings with the base-paper in situ, as the final coating structure is dependent upon the application and drying conditions [245],[246]. Industrial problems often demand measurement of the coating porosity on commercially available papers. A particular challenge posed by this is to determine the pore size and pore volume of the coating layer alone, independently of the base-paper. The base-paper will generally have larger pores than the coating layer, however there is often some overlap between the two. In some cases the basepaper is run separately and then subtracted from the coated paper curve, however this will not take into account the surface pores at the interface of the coating and basepaper. Curve fitting programs are often utilized to separate the coating layer from the basepaper. In general, most of the pore volume of the paper sample derives from the base-paper, and the coating layer gives rise to a small inflexion in the cumulative volume curve around  $0.1 \mu\text{m}$ . A cumulative volume trace for a coated paper which has been calendered at a range of different pressures is shown in Figure 48. It can be seen that as the calendering pressure is increased, the total pore volume of the whole paper is reduced. A good description of the analysis of mercury porosimetry in paper is given by Ridgeway and Gane [247].

Other techniques have been employed in order to study the porosity of paper coatings including NMR [248]. Lehtinen *et al.* [249] presented a

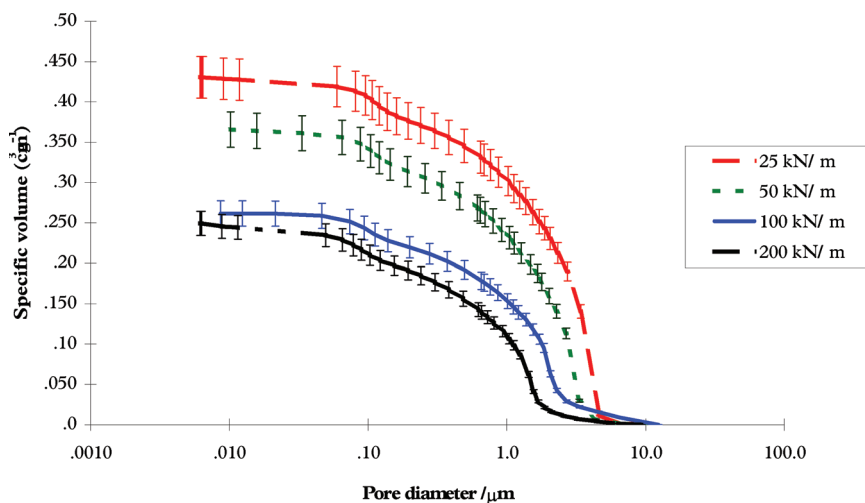


**Figure 48.** Cumulative volume mercury porosimetry curves for clay coated paper, calendered at a range of pressures 81.

comparison of mercury porosimetry, NMR cryoporometry and thermo porosimetry in characterising the porosity of compressed calcium carbonate structures. Both the NMR and thermo techniques were suitable for giving information about the pores involved in the imbibition of fluids, whereas the mercury porosimetry describes the pore structure under non-wetting conditions.

## 6 COMBINATION OF TECHNIQUES

A few authors have used a combination of many surface analytical techniques complimentary to each other to elucidate the structure of paper or problems caused by defects and failure positions. Pykonen *et al.* [250], for example, used a combination of XPS and FTR-IR measurements to determine surface chemistry changes which occurred when pigmented papers were plasma treated (Figure 49). AFM was used to determine any topographical changes which had occurred (Figure 50) and contact angle measurements to show the changes in surface energy which had occurred on plasma treatment. The papers and polymer films were then inkjet printed and the print quality and rub correlated in the changes in surface energy. In all cases the treatment caused an oxidation of the surface and an increase in the base and polar component of the surface energy. The printability of the paper substrates changed very little but it was shown that the quality of printed PE film improved, whilst that of the PP film became worse.

In a later publication Pykonen *et al.* [251] used XPS, TOF SIMS, FIB and print testing to study the influence of plasma treatment on the absorption of

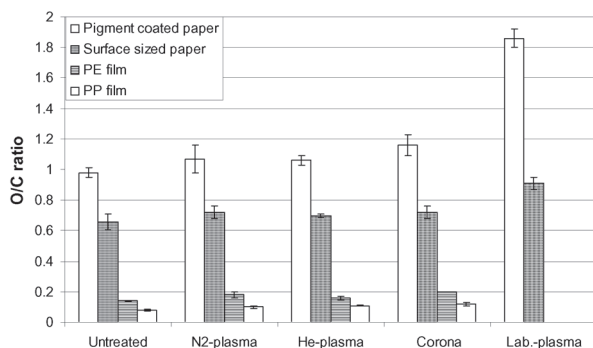


**Figure 49.** XPS determination of the O/C ratio for different substrates and plasma treatments, showing increased oxidation of the surface.

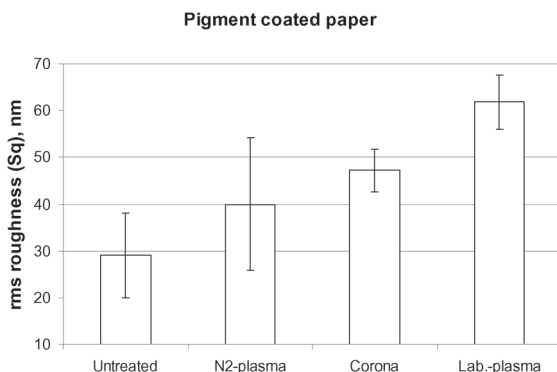


**Figure 50.** AFM RMS roughness showing roughening due to the plasma treatment.

damping water and ink components into coated paper surfaces. Mercury porosimetry was also used to characterise the coatings which contained different pigments. Coatings containing different types of pigments were found to respond differently to the plasma treatment; the talc containing paper being influenced by the treatment to a far greater extent than the calcium carbonate containing coating. Increasing the surface energy and polarity of the coatings decreased the ink setting rate of the polar linseed oil based inks probably due to increased acid-base interaction between ink oil and polar plasma treated coating, but increased the setting speed of the mineral oil based inks. Too intensive plasma treatment resulted in a loss of surface strength of the coating and micro-picking in the surface layers could be observed with the FIB and SEM analysis (Figures 51 and 52).

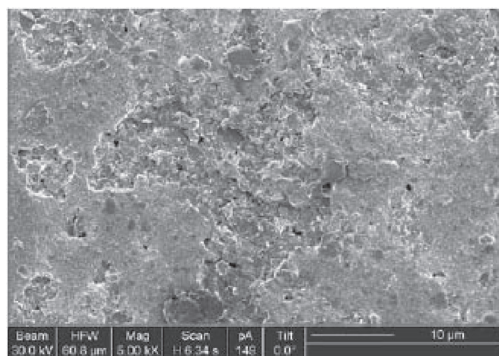


**Figure 51.** FIB imaging to show micro-picking.

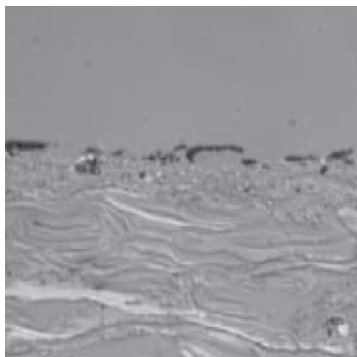


**Figure 52.** Optical microscope section through the coating.

Pykonen *et al.* [252] studied the use of hydrophobic plasma coatings containing fluorocarbon, organosilicone and hydrocarbon depositions, on the absorption of water based damping solutions used in offset printing, by using a combination of XPS, contact angles and ToF-SIMS. These hydrophobic treatments prevented the absorption of the damping water into the coatings, despite the fact that the topography and porosity were unaffected. The best print characteristics were observed when the coating was hydrophobic and oleophilic.

Nutbeem *et al.* [253] presented how a range of topography, porosity and reflectometry techniques could be used in combination to characterise base-paper, coated paper and finally the printed product to determine the cause of print mottle.

Tag *et al.* [254] also used a combination of SIMS, AFM and surface energy determination by contact angle measurement to study the changes in chemistry and topography of a coated paper after application of isopropyl alcohol-based and isopropyl alcohol-free surfactant based model fountain solutions. With the surfactant based fount solutions, AFM analysis showed an increase in the RMS roughness which was ascribed to the presence of surfactants on the coating surface. The surface energy and in particular the polar component, was found to increase. The TOF-SIMS measurements showed that the IPA based fount solution did not change the elemental composition of the surface, but that there was a clear change with the surfactant based fount solution.

TOF SIMS imaging combined with XPS was used by Brinen [255] to study the distribution of sizing agents on internally and surface sized papers. The imaging SIMS was suitable for obtaining the spatial distribution of these

compounds on the surface of the paper, and the TOF SIMS was also good for determination of the chemical structures present. The XPS was also able to detect the presence of the size.

Gustaffson *et al.* [256] used a combination of AFM and XPS to study the surface properties of TMP, and more precisely the chemistry of the surface and morphology of the cell wall structures. Finnish and French spruce samples were studied which had been defibrilliated at two different temperatures, and two stages of refining were also studied. XPS analysis of the cellulose content of the surface showed that the non-cellulosic content of Finnish spruce was higher. Refining resulted in cleavage taking place either within the secondary cell wall or at the interface between the primary and secondary cell wall.

In a similar study Fardim *et al.* [257] used a combination of XPS, TOF-SIMS, chromatography and AFM to study the composition, distribution and nanostructure of extractives on the fibre surfaces of a birch bleached kraft pulp (BKP) and a recycled deinked pulp (DIP). They found that estimations of extractive surface coverage by XPS were consistent with the qualitative observations by TOF-SIMS and AFM.

Lozo *et al.* [258] also investigated a range of spectroscopic and microscopic techniques for depth profiling and assessing the spread of dye and pigment based ink on inkjet printed papers. Amongst the techniques used were confocal Raman, UV Raman, CLSM and FTIR. Raman spectroscopy was good in determination of the chemical components in the ink and their distribution throughout the paper. The dye based ink was found to penetrate to a greater extent, whereas the pigmented ink formed a dense layer on the surface. The high powered laser however burned the paper. Confocal microscopy (CLSM) had a good correlation with the Raman and confirmed the ink distribution in the z direction. The FTIR was able to determine the ink distribution at low depths into the surface, and UV Raman was useful for the surface analysis of prints.

Ozaki and Uchida [259], used a combination of XPS, TOF-SIMS and electron probe micro analysis to study the distribution and absorption of rotogravure ink onto coated papers. The amount of pigment on the surface could be analysed using XPS and the TOF SIMS was utilized in determining the distribution of the thin surface layer of ink vehicle using the ion fragment 135 amu.

## 7 SUMMARY

The comprehensive surface analysis of paper requires a wide range of tests covering visual, physical and elemental analysis and a careful assessment of the resulting information. In order to successfully undertake such an exercise, it is important to know what techniques are available, their limitations and how best to use their combined output.

This review covers: Chemical Structure Analysis using the main spectroscopy techniques of Infrared, Raman, X-Ray, Secondary Ion Mass and UV; Microscopy utilising, Scanning Electron, Dispersive X-Ray, Transmission Electron, Optical, Focussed Ion Beam, Atomic Force and Confocal Laser; Paper Topography through Air Leak methods, Profilometry and Interferometry and Imaging Reflectometry; Physical Analysis by X-Ray Diffraction, Fluid Absorption and Mercury Porosimetry and finally how a combination of techniques can be employed to give an understanding of paper surface properties. For each technique, a description is given covering the main scientific principles, the paper property determined, quality of data and pros and cons.

The main part of the review contains examples of how these techniques have been used by researchers for a wide variety of purposes including quality control and identification of failure mechanisms and problems at interfaces, product development of new coating formulations and an improved understanding of the interactions between different coating components. Many of the instruments can be used for identification of unknown paper constituents and contaminants and lend themselves to competitive analysis.

The large number of surface analytical techniques available to the researcher differ widely in the type of information that they will deliver. A number of considerations will dictate the choice of technique used, not least of these being the instrument availability. Some of the main benefits of using these techniques are for determination of species which may cause failure at interfaces, for example the migration of certain organic species to a surface preventing ink adhesion or correct converting of the sample, e.g. lamination. Factors such as the size of the features of interest and the physical nature of the material will also influence the choice of analysis technique [260]. Certain techniques are specific for chemical analysis and others for physical. For example the XPS and TOF SIMS may be the techniques of choice to study the chemistry of the very surface of the sample, whereas Confocal Raman may be of use if a depth profile into the sample is required. Mercury porosimetry and the topography measurements give detailed information of the physical structure of the paper and the choice of these also depends upon the size of the features studied. AFM for example gives very detailed

information on pigment scale topography, whereas interferometry and profilometry will give the topography over larger areas of the paper and are more useful for looking at fibre distribution.

By its very nature paper is variable from point to point and from sample to sample, and so it must be emphasised that for a rigorous analysis of a surface it is often necessary to analyse many areas to obtain a statistical representation of that surface. Other difficulties may arise because of the many synthetic and natural chemicals used in the process, many of which will be similar in chemistry, (often with a high organic content) and difficult to analyse. This is another reason why a wide range of complimentary techniques is the only way to correctly identify various species distributed throughout the paper.

## 8 ACKNOWLEDGEMENTS

Thanks are extended to Neil Norouzi, Roger Wygant, Marie Ernsstrom, Gary Chinga Carrasco, Jouko Peltonen for help in providing references.

Many thanks are extended to John Husband, Tony Lyons, Graham O'Neill, Karen Leaity, David Preston and Richard Bown for proof reading this document.

## 9 GLOSSARY OF ABBREVIATIONS

$\beta$	Ratio of peak intensities $I_{3695} / I_{3620}$ (ATR IR Particle Alignment)
$\delta$	Macro-roughness
$\varepsilon$	Porosity (void fraction of paper coating)
$\phi_{XPS}$	XPS spectrometer work function
$\gamma$	Surface tension
$\eta$	Viscosity
$\lambda$	Wavelength of light
$\lambda_x$	The mean free path of the photoelectrons in the sample(XPS)
$\mu$	Transmission of analysis system determined by the ion collection of the mass spectrometer (SIMS)
$\mu_2$	Second moment of the wave amplitude distribution for Walsh function
$\nu$	Frequency of exciting radiation
$\theta$	Contact Angle (of fluid).
$\theta_x$	An angular efficiency factor based upon the angle between the photon path and detected electron (instrumental arrangement) (XPS)

$\theta_m$	Fractional coverage of elemental species M
$\rho$	Fluid density
$\rho_m$	Coating density
$\sigma$	The standard deviation of the roughness about the mean plane of the surface (microroughness)
$\sigma_x$	The photoelectric cross section for the atomic orbital in $\text{cm}^2$ (sensitivity – or probability of electron in orbital being ejected in XPS)
$A$	Area
AFM	Atomic force microscopy
ATR IR	Attenuated total reflectance infra red
$A_x$	Area of the sample from which the photoelectrons are detected, (XPS)
BE	Binding energy
C	Constant related to the total pore volume and capillary length, $C = V_o / \pi L$
CMC	Carboxy methyl cellulose
CPVC	Critical pigment volume concentration
CSLM	Confocal scanning laser microscopy
$d$	Thickness of paper
$dp$	Depth of penetration of evanescent wave into sample
$dSIMS$	Dynamic or depth profiling SIMS
$e$	Charge on the ion
EDX	Energy dispersive X-ray mapping
ESCA	Electron Spectroscopy for Chemical Analysis
ESEM	Environmental SEM
FIB	Focussed Ion beam
FTIR	Fourier Transform Infra Red Spectroscopy
FWHM	Full width of peak at half maximum height
$f_x$	The x-ray flux in photons / $\text{cm}^2 \text{sec}^{-1}$ (XPS)
FESEM	Field Emission SEM
GCC	Ground calcium carbonate
GDP	Gross Domestic Product
$h_p$	Planck's constant
HREELS	High resolution energy electron loss spectroscopy
$H$	Magnetic field strength
$I$	Intensity of reflected light (gloss goniophotometry)
IRAS	Infra red reflection absorption spectrometry
$i_{pf}$	Primary particle flux
$I_{3620}$	Intensity (height) of IR peak at $3620 \text{ cm}^{-1}$
$I_{3695}$	Intensity (height) of IR peak at $3695 \text{ cm}^{-1}$
$iM_s$	Secondary ion current of an element of species M

$I_x$	The number of photoelectrons per second in a specific peak (XPS)
$KE$	Kinetic energy
$LIMA$	Laser Ionisation Mass Analysis. This has a small analysis area, so is good for quick analysis of small spots. The laser also has a higher penetration depth of approximately 1 $\mu\text{m}$ and so can be used for looking at substances under the immediate surface. The laser is slightly damaging to the surface and so only simple and low mass structures can be detected.
$L_p$	Wavelength of disturbance (distance between roughness peaks)
LWC	Light weight coated (paper)
$m$	Particle mass
$M/Z$	Mass / charge (Daltons)
$M_c$	Mass of coating layer
$M_{tot}$	Mass of coating plus basesheet
$n$	Complex refractive index (measured)
$n_x$	The number of atoms of the element per $\text{cm}^3$ of the sample (XPS)
PCA	Principle component analysis
PVOH	Poly vinyl alcohol
$p$	Pressure
SNMS	Sputtered Neutral Mass Spectrometry
PCC	Precipitated calcium carbonate
$Pe$	External pressure applied at entrance to capillary tube
$r$	Pore radius
$R+$	The ionisation probability to positive secondary ions
$r_c$	Radius of curvature
RI	Refractive index
S	Sputter rate for elemental species M (SIMS)
SEM	Scanning electron microscope
SIMS	Secondary Ion Mass Spectrometry
$t$	Time
TEM	Transmission electron microscope
$T_g$	Glass transition temperature
TLC	Thin layer chromatography
TOF	Time of flight
$T_x$	The detection efficiency for the electrons emitted from the sample (XPS)
UV	Ultra violet
UPS	Ultraviolet photon electron spectroscopy
$V_{AC}$	Accelerating voltage applied to the mass spectrometer chamber
Wt.%	Weight %
XPS	X-ray photoelectron spectroscopy (sometimes known as ESCA)

- XRD X-ray diffraction  
 $\gamma_x$  The efficiency in the photoelectron process for formation of photoelectrons of the normal photoelectron energy. (polydispersity of energies around the mean photoelectron energy) (XPS)

## 10 REFERENCES

1. Roberts J.C., **The Chemistry of Paper** RSC ISBN 0-85404-518-x 1996
2. Alinec B., Lepoutre P., Porosity and optical properties of clay coatings, *J. Coll. Int. Sci.*, **76**, 439–444, 1980
3. Climpson N., Taylor J., “Pore size distributions and optical scattering coefficients of clay structures”, *Tappi J.*, **59**, (7):89–92, 1976
4. D.J. Priest, in **Technical Applications of Dispersions, Surfactant Science Series**, (Ed. R.B. McKay), vol.52, Chapter 7., Dekker, New York, 1994
5. O’Neill G.P., Poor Economic Efficiency – to be Overcome by Optimisation, or Innovative Solutions? In *Proc. 2008 PTS Papermaking Symposium*, Sept 2008, Munich, 2008
6. Lindqvist U., Moilanen P., Business from hybrid media and printed functionality, *Advances in Printing and Media Technology*, vol. XXXV, Ed. Enlund & Lovrecek *Proc. 2008 IARIGAI* Valencia Spain, pp 101–106, 2008
7. Pekarovicova A., Hrehorova E., Fleming P.D., Rotogravure for printed electronics, *Advances in Printing and Media Technology*, vol. XXXV, Ed. Enlund & Lovrecek *Proc. 2008 IARIGAI* Valencia Spain, pp 289–298, 2008
8. Jabrane T., Jaaidi J., Dube M., Mangin P., Gravure printing of enzymes and phages *Advances in Printing and Media Technology*, vol. XXXV, Ed. Enlund & Lovrecek *Proc. IARIGAI 2008* Valencia Spain, pp 279–288, 2008
9. Bonev S., Wurnitzet B., Security printing for product packaging in industrial applications, *Advances in Printing and Media Technology*, vol. XXXV, Ed. Enlund & Lovrecek *Proc. IARIGAI 2008* Valencia Spain, pp 307–312, 2008
10. Ernstsson M., Warnheim T., “Surface analytical techniques applied to cleaning processes”, Chapter 4 in **Handbook for Cleaning / Decontamination of Surfaces**”, I. Johansson and P. Somasundaren (Ed.s), Elsevier, pp 747–789, 2007
11. Swift A.J., West R.H., Surface and Interface Analysis in the Characterisation of Coatings and Inks, *Paint & Ink International*, pp 86–88, March/April 1998
12. Perry S.S., Somorjai G.A., “Characterization of Organic Surfaces”, *Analytical Chemistry* **66**, (7), pp 403–415, April 1994
13. Hubbe M, Pawlak J., Koukoulas A.A., Papers appearance: a review, *BioResources*, **3**(2), pp 627–665 2008
14. Huang, F.R., and Kline, J.E., An application of infra-red spectroscopy to the studies of binder migration in paper coatings, *Unknown Journal.*, pp 93–98
15. Groves, R., Matthews, G.P., Heap, J., McInnes, M.D., Penson, J.E., and Ridgway, C.J., “Binder migration in paper coatings – A new perspective”. *12<sup>th</sup> Fundamental Research Symposium, Oxford*, September 2001, pp 1149–1181, 2001

16. Leclerc, D.F., and Ouchi, M.D., Rapid characterisation of dirt specks in Kraft pulp by infer-red spectrometry, *J. Pulp & Pap. Sci.*, **22**(3): J112–117, 1996
17. Tatsumi, D., Yamauchi, T., Murakami, K., FT-IR spectroscopy in the evaluation of dry handsheets with an acrylamide-based dry-strength resin, *Nordic Pulp & Paper Sci.* No.2. p 94. 1995
18. Colthup, N.B., Daley, L.H., and Wiberley, S.E. . **Introduction to Infrared and Raman spectroscopy**, Academic Press, New York 1975
19. Coleman, P.B., ed. **Practical sampling techniques for Infrared Analysis**, CRC Press, Inc. Boca Raton, FL. 1993
20. Pelletier, I., Pellerin, P., Chase, D.B., and Rabolt, J.F., New developments in planar array Infra-Red spectroscopy, *Applied spectroscopy*, **59**(2), pp 156–163. 2005
21. Harrick, N.J. **Internal Reflectance Spectroscopy**, p 30. Interscience Publishers, New York. 1967
22. Kortum, G. **Reflectance Spectroscopy**, p. 316. Springer-Verlag, Berlin. 1969
23. Vyorykka, J., Fogden, A., Daicic, J., Ernstsson, M., and Jaaskelainen, A-S., Characterization of paper coatings – review and future possibilities, In *Proc. Tappi Coatings Fundamentals Symposium*, Turku, Finland 8–10 February, 2006, pp 43–66.
24. Acholla, F., Brown, J.T., and Mukkamala, R., Application of photoacoustic fourier transform infer-red spectroscopy for coat weight measurement in paper coatings enriched with organic polymers, *Proc. Tappi Coating Conference*, Toronto, Canada, April 17–20, 2005
25. Rousu S., “Differential absorption of offset ink constituents on coated paper”, PhD Thesis, Abo Akademi University 2002
26. Wickman M., Sundin M., Nordstrom J-E., A new method for the direct measurement of ink setting on coated paper, *Adv. In Printing Sci.,and Technol.*, Vol 24, (Ed J.A. Bristow), PIRA 1998
27. Vikman K., Sipi K., Applicability of FTIR and raman Spectroscopic methods to the study of paper –ink interactions in digital prints, *J. Imag. Sci. Technol.*, **47**(2), pp 139–148, 2003
28. Hiorns, A.G., Husband, J.C., Parsons, D.J., Kent, D.F., Coating surface composition using ATR-IR spectroscopy, *Proc TAPPI Advanced Coating Fundamentals Symposium*, Turku, Finland, 8–10<sup>th</sup> February, pp 67–80, 2006
29. Halttunen M., Loija M., Vuorinen T., Stenius P., Tenhunen J., Kentta E., Determination of SB latex distribution at paper coating surfaces with FTIR/ATR spectroscopy, *Proc 2001 Tappi Coating Conf. and Trade Fair*, San Diego CA pp 203–211, 2001
30. Preston J.S., Daun M., Nutbeem C., Jones A., Attaining print performance through pigment engineering, *Wochenblatt Fur Papierfabrikation*, **5**, pp 252–265, 2000
31. Agarwal, U.P., and Atalla, R.H, Raman Spectroscopy, Paper from **Surface Analysis of Paper** pp 152–181, CRC Press, Boca Raton, New York. 1995
32. Vyorykka, J., Juvonen, K., Bousfield, D., and Vuorinen, T., Raman microscopy in

- lateral mapping of chemical and physical composition of paper, *TAPPI J.*, **3** (9), pp 19–24, Sept 2004
33. Swerin A., Konig A., Brandner B., Andersson K., Lindgren E., The use of silica pigments in coated media for inkjet printing: Effects of absorption and porosity on printing performance and depth-profiling using confocal Raman spectroscopy *Proc. 2008 Tappi Fundamentals Symposium*, Montreal, 2008
  34. Vyorykka J., Vuorinen, T., and Bousfield, D.W., Confocal Raman microscopy: A non destructive method to analyse depth profiles of coated printed paper, *NPPS*, No.2, p 218, 2004
  35. Vyörykkä J., PhD thesis *Confocal Raman Microscopy in Chemical and Physical Characterization of Coated and Printed Papers*, Helsinki University of Technology, Finland 2004
  36. Vikman K., Iitti H., Matousek P., Towrie M., Parker A.W., Vuorinen T., “Kerr gated resonance raman spectroscopy in lightfastness studies of inkjet inks”, *Vibrational spectroscopy Elsevier* in press 2004
  37. Santos, N.F., Kholkin, A., and Velho, J., Coating paper surface analysis using AFM, SEM and Raman Spectroscopy, *Proc. 11th Intl. Printing and Graphic Arts Conference*, vol. 2, Bordeaux, France, October 1–3, 2002
  38. Niemela, P., Hieatala, E., Ollanketo, J., Tornberg, J., Pirttinen, E., and Stenius, P., FT-Raman spectroscopy as a tool for analysing the composition of recycled paper pulp, *Progress in paper recycling*, **8**(4), p 15. 1999
  39. Siegbahn K., Nordling C., Fahlman A., Nordberg R., Hamrin K., Hedman J., Johansson C., Bergmark T., Karlsson S., Lindgreen I., Lindberg B., *WNovo. Acta. Regiae WSOc. Sci., Upsaliensis and Ebser WR*, **20**, 1967
  40. Jenkin J.G., Leckey R.G.C., Liesegang J., *Jour. Of Electron Spectroscopy and Related Phenomena*, **12**, 1–345, 1977
  41. O'Connor D.J, Sexton B.A., St. C. Smart R., **Surface analysis methods in materials science**, Edition: 2, illustrated. Published by Springer, ISBN 3540413308, 9783540413301, 2003
  42. Conners T.E., Banerjee S. (Ed.s), in **Surface Analysis of Paper**, CRC Press LLC New York, 1995
  43. Freire, C.S.R., Silvestre, A.J.D., Pascoal, N. C., Gandini, A., Fardim P., and Holmbom, B., Surface characterization by XPS, contact angle measurements and TOF-SIMS of cellulose fibres partially esterified with fatty acids, *J. Colloid Interface Sci*, **301**, 205–209, 2006
  44. Ahmed A., Adnot A., Grandmaison J.L., Kaliaguine S., Doucet J., ESCA analysis of cellulosic materials, *Cellulose Chem. Technol.* **21**, 483–492, 1987
  45. Moulder J.F., Stickle W.F., Sobol P.E., Bomben K.D., Physical Electronics Division **Handbook of X-ray Photoelectron Spectroscopy**, Ed. G. Chastain, Perkin-Elmer Corporation Publishing, Minnesota, USA.
  46. Dalton J.S., Preston J.S., Heard P.J., Allen G.C., Elton N.J., Husband J.C., Investigation into the distribution of ink components throughout printed coated paper – Part 2: Utilising XPS and SIMS, *Colloids and Surfaces A: Physicochemical and Engineering Aspects*, Elsevier Science., **205**, 199–213, 2002

47. Koljonen K., Effect of surface properties of fibres on some paper properties of mechanical and chemical pulp PhD Thesis Helsinki University of Technology, Series A19, Espoo 2004
48. Johansson, L.-S., Campbell, J.M., Koljonen, K. and Stenius, P Evaluation of surface lignin on cellulose fibers with XPS *Applied Surface Science* 144–145, pp 92–95, 1999
49. Heijnesson Hultén A., Basta J., Larsson P., Ernstsson M., “Comparison of different XPS methods for fibre surface analysis” *Holzforschung*, **60**, 14–19, 2006
50. L.-S. Johansson, J. M. Campbell, P. Fardim, A. Heijnesson Hultén, J.-P. Boisvert, M. Ernstsson, An XPS round robin investigation on analysis of wood pulp fibres and filter paper, *Surface Science*, **584**, 126–132, 2005
51. Istone, W.K., “X-Ray photoelectron spectroscopy”, Paper from **Surface Analysis of Paper** pp 235–268, Ed. Connors T.E., Banerjee S., CRC Press, Boca Raton, New York, 1995
52. Hemminger, C.S., “ESCA analysis as a tool to study surfaces of treated paper”, *Proc. TAPPI Coating Conference*, Tappi Press, Atlanta GA 1985
53. West R., Stevenson P., Characterising paper and coatings using surface analysis, pp 143–148
54. Andersson C., Ernstsson M., Järnström L., Barrier Properties and Heat Sealability / Failure Mechanisms of Dispersion-coated Paperboard, *Packag Technol. Sci*, **15**, 209–224, 2002
55. Strom, G., Carlsson, G., Schulz, A., Chemical composition of coated paper surfaces determined by ESCA, *Nordic Pulp & Pap Res. J.*, **8**(1): 105–112, 1993
56. Brungard N.L., and Cleland, A.J., “Using XPS to estimate relative pigment concentrations on coated paper”, In *Proc. 1994 TAPPI Coating Conference*, Tappi Press, Atlanta GA, 1994
57. Tomimasu, H., Yamasaki, T., Ogawa, S., Ogura, T., and Sakai, Y., ESCA to analyse surface binder concentration of coated paper, In *Proc. 1986 TAPPI Coating Conference*, Tappi Press Atlanta GA, 1986
58. Seppanen R., Sundin M., Swerin A., Brandner B., Purontaus J., Ristolainen M., Relation between surface energy, topography, wettability and detailed surface chemistry by spectroscopy for coated printing papers, *Proc. 2008 Tappi Fundamentals Symposium*, Montreal June 2008
59. Al-Turaif H., Lepoutre P., Evolution of surface structure and chemistry of pigmented coatings during drying, *Prog. in Org Coat.*, **38**, pp 43–52, 2000
60. Al-Turaif H., Lepoutre P., Effect of sintering on surface chemistry and surface energy of pigmented latex coatings”, *Appl Poly. Sci.*, **82**, (4), pp 968–975, 2001
61. Al-Turaif H., The effect of pigment blends on the surface structure and chemistry of pigmented latex coatings, *Tappi J.*, **5**, (8), pp 24–30, Aug 2006
62. Johansson K., Strom G., Stenius P., The interaction between alkyd resin binders and kaolinite, *Colloids & Surfaces*, **56**, pp 313–338, 1991
63. Wickman M., Johansson K., Adsorption of ink binders on paper surfaces, In *Proc. 1992 Tappi Int. Printing & Graphic Arts Conf.*, Tappi Press Atlanta, pp 93–101, 1992

64. Rentzhog M., Fogden A., Effect of corona treatment of PE-Coated Board on water-based flexographic print resistance, submitted to *Nordic Pulp & Paper J.*, but included in M. Rentzhog PhD thesis, KTH, Sweden, 2006
65. Pykönen M., Sundqvist H., Kaukonen O.-V., Tuominen M., Lahti J., Fardim P., Toivakka M., Ageing effect in atmospheric plasma activation of paper substrates, *Surface & Coatings Technology* **202**: 3777–3786, 2008
66. Pykönen M., Sundqvist H., Tuominen M., Lahti J., Preston J.S., Fardim P., Toivakka M., Influence of atmospheric plasma activation on sheet-fed offset print quality, *Nordic Pulp & Paper Res. J.*, **23**(2): 181–188, 2008
67. Pykonen M., Sundqvist H., Jarnstrom J., Kaukonen O.V., Tuominen M., Lahti J., Peltonen J., Fardim P., Toivakka M., Effects of atmospheric plasma activation on surface properties of pigment-coated and surface-sized papers, *Applied Surface Science* **255**: 3217–3229, 2008
68. Briggs D., In **Practical Surface Analysis (2nd edition)**, Vol. 2., John Wiley, Chichester, 367–243, 1992
69. Benninghoven A., Rudenaver T.G., Werner H.W., in **SIMS Basic Concepts, Instrumental Aspects, Applications and Trends**, Wiley-Interscience, 1987
70. <http://www.hiddenanalytical.com/index.php/en/a-sims-primer?start=1>
71. Dettler-Hoskin, L.D., Busch, K.L., SIMS: secondary ion mass spectrometry, Paper from **Surface Analysis of Paper**, CRC Press, Boca Raton, New York, Eds. Connors T.E., Banerjee S., pp 206–234, 1995
72. Preston, J.S., Elton, N.F., Husband, J.C., Legrix, A., Heard, P., and Allen, G., SIMS analysis of printed and coated paper, In *Proc. 2000 Tappi International Printing and Graphic Arts Conference*, pp 101–120, Savannah, USA, Oct. 2000
73. Heard P., Personal Communication
74. Koivula, H., Fardim, P., Toivakka, M., Characterisation of pigment particle surfaces by TOF-SIMS, In *Proc Tappi Coatings Fundamentals Symposium*, Turku, Finland pp. 81–88, 8–10 February, 2006
75. <http://www.siliconfareast.com/SIMS.htm>., “Secondary ion mass spectrometry (SIMS)”, 2005
76. Brinen, J.S., Greenhouse, S., Dunlop-Jones, N., “SIMS (secondary ion mass spectrometry) imaging. A new approach for studying paper surfaces”, *Nordic Pulp & Paper Res. J.*, **2**(6): p 47 1991
77. Brinen J.S., Proverb R.J., SIMS imaging of paper surfaces, Part 2. Distribution of organic surfactants, *Nordic Pulp & Paper Res. J.*, **4**(6): 177–183, 1991
78. Sodhi R.N.S., Sun L., Sain M., Farnood R., Analysis of ink/coating penetration on paper surfaces by Time of Flight SIMS in conjunction with principal component analysis, *The Journal of Adhesion* **84**: pp 277–292, 2008
79. Sun L., Sodhi R.N.S., Sain M., Farnood R., Analysis of ink/coating penetration on paper surfaces by time of flight secondary ion mass spectroscopy in conjunction with principal component analysis, *Proc 2004 Int Printing & Graphic Arts Conf.*, Vancouver, Canada 4–6<sup>th</sup>, pp 95–101, Oct 2004
80. Preston, J.S., Husband, J.C., Norouzi, N., and Heard, P.J., “Pick strength of calcium carbonate and Kaolin coatings and analysis of the distribution of

- fountain solution using CsCl tracers”, *Proc.2008 Tappi Coating Fundamentals Symp.* 2008.
81. Preston J.S., PhD thesis The influence of Coating Structure on the Print Gloss of Coated Paper Surfaces, University of Bristol 2001
  82. Zimmermann, P.A., Hercules, D.M., Rulle, H., Zehnpfenning, J., and Benninghoven, A., “Direct analysis on coated and contaminated paper using TOF mass spectrometry”, *Tappi Journal*, 78(2), 1995, pp 180–186
  83. Kim-Habermehl, L., Wittbrodt, E., Mccoy, B., Langolf, M., Pollock, M., Roper, J., Stolarz, J., Rolf, M., *Proc. 1998 Pan Pacific and Int Printing and Graphic Arts Conf*, Quebec Oct., PAPTAC, CANOPY, Toronto, ISBN 1-896742-39-4, 71, 1998
  84. Koivula H., Fardim P., Toivakka M., Characterization of Pigment Particle Surfaces by TOF-SIMS, *Proc 9th Tappi Coating Fundamentals Symposium*, Turku Finland, pp 81–88, 8–10 Feb 2006
  85. Brinen J.S., Kulick R.J., SIMS Imaging of Paper Surfaces Part 4. The detection of desizing agents on hard-to-size paper surfaces, *Int. Journal of Mass Spectrometry and Ion Processes*, **143**, 177–190, 1995
  86. Seppanen R., PhD Thesis, On the internal sizing mechanisms of paper with AKD and ASA related to the surface chemistry, wettability and friction, KTH, Stockholm, 2007
  87. Kulick R.J., Brinen J.S., Probing paper surfaces with TOF SIMS – a new tool for problem solving, *Proc. 1996 Tappi Papermakers Conference*, pp 325–334, 1996
  88. West R., “Surface analysis of packaging materials”, *Medical Device Technology*, pp 36–38, May 1996
  89. Istone W.K., Static secondary ion mass spectrometry and x-ray photoelectron spectroscopy for the characterisation of surface defects in paper products, *J. Vac. Sci., Technol.*, **A 12** (4), 2515–2522, 1994
  90. Burrell M.C., Tilley M.G., Surface chemistry of polycarbonate film and adhesion of ultraviolet-cured inks, *J. Vac. Sci., Technol.*, **12** (4), 2515–2522, Jul/Aug 1994
  91. Swift A.J., West R.H., Surface and interface analysis in the characterisation of coatings and inks, *Polym. Paint Col. J.*, **188**, (4404), 35–36, 38, 40, May 1998
  92. Pachuta S.J., Staral J.S., Nondestructive analysis of colourants on paper by time of flight secondary ion mass spectrometry, *Anal. Chem.*, **66** (2), 276–284, 1994
  93. Whalen-Shaw M., Eby T., An investigation of factors related to backtrap mottle in coated papers using electron probe microanalysis, *Proc. 1991 Tappi Coating Conf*, Tappi Press Atlanta GA pp 401–409, 1991
  94. Fujiwara H., Kline J.E., SB latex profiles on the pigment coated paper (1) Ultraviolet absorption of SB latex, *Proc. 1987 Tappi Coating Conference*, Tappi Press Atlanta GA, pp 29–34, 1987
  95. Kline J.E., The measurement of binder migration with ultra violet analysis, *Proc. 1990 Tappi Coating Conf*, Tappi Press Atlanta GA pp 201–208, 1990
  96. Inoue T., Kline J.E. Janes R.L., Effect of interaction between binder and pigment on binder latex migration and distribution” 1991 *Eucepta / PTS-Streicherei-Symposium*, München, Allemagne, **121** (19), pp 790–798 (copy from German), 1993

97. Malik J.S., Kline J.E., A study of the effect of water soluble polymers on water holding and binder migration tendencies of coatings, *Proc. 1992 Tappi Coating Conf.* Tappi Press, Atlanta GA, pp 105–113, 1992
98. Matsubayashi H., Saito Y., Takagishi Y., Miyamoto K., Kataoka Y., The influence of coating structure on paper quality, *Proc. 1992 Tappi Coating Conference*, Tappi Press Atlanta GA, pp 161–171, 1992
99. de Silveira, G., Forsberg, P., and Conners, T.E., Scanning Electron Microscopy: A tool for the analysis of wood pulp fibres and paper, Paper from **Surface Analysis of Paper** pp 41–71, Ed. Conners T.E., Banerjee S, CRC Press, Boca Raton, New York, 1995
100. Helle, T., and Johansen, O., “Printing ink distribution on paper as studied by SEM techniques”, In *Proc. 1992 Research Conference of the International Association of Research Institutes for the Graphic Arts Industry (IARIGAI)*, pp 205–216, Pittsburgh, USA, Oct. 1992
101. Peterson, R.A., and Griffith, J.G., “The evaluation of the internal and the surface structure of paper using non-traditional cross sectioning”, *Proc. 1994 Tappi Coating Conference*, Tappi Press Atlanta GA, 1994
102. Modgi, S., McQuaid, M.E., and Englezos, P., SEM/EDX analysis: A technique for z-direction mineral topography in paper, *Nordic Pulp & Pap. J.*, No. 5, p 659, 2007
103. Chinga-Carrasco G. Exploring the multi-scale structure of printing paper – A review of modern technology, In press *J Microscopy* 2009
104. Erdman N., Campbell R., Asahina S., Precise SEM cross section polishing via argon beam milling, *Microscopy Today*, pp 22–25, May 2006
105. Oliver J.F., Mason S.G., “Microspreading studies on rough surfaces by scanning electron microscopy” *J Coll & Int. Sci.* 60, (3), pp 480–487, 1977
106. Mörseburg K., Chinga-Carrasco G., Assessing the combined benefits of clay and nanofibrillated cellulose in layered TMP-based sheets, Accepted for publication in *Cellulose*. DOI : 10.1007/s10570-009-9290-4
107. Chinga,G. and Helle, T. Structure characterisation of pigment coating layer on paper by scanning electron microscopy and image analysis, *NPPS* 17(3): 307–312, 2002
108. Chinga, G., Helle, T. and Johnsen, P.O. Characterization of pigment coating layer structure using SEM and Digital Image Analysis techniques, In *Proc, 2000 Tappi Coating Conference and Trade Fair*, Washington, DC, USA, pp 309–316, 2000
109. Chinga G., Helle T., Relationships Between the Coating Surface Structural Variation and Print Quality, *Journal Of Pulp And Paper Science:* 29(6), pp 179–184, 2003
110. Preston J.S., Elton N.J., Legrix A., Nutbeem C., Husband J.C., The role of pore density in the setting of offset printing ink on coated paper, *Tappi Journal*, 1(3), pp 3–5, 2002
111. Kugge C., Craig V.S.L., Daicic J., A scanning electron microscope study of the surface structure of mineral pigments, latices, thickeners used for paper coating

- on non-absorbant substrates, *Colloids and Surfaces A: Physicochem. Eng. Aspects* **238**, pp 1–11, 2004
112. Dickson, R., Forsström, U. & Grön, J. Coating coverage of metered size press pre-coated paper. *Nord. Pulp Paper Res. J.* 17(4), 434–439, 2002
  113. Gregersen O.W., Skinnarland I., Johnsen O., Helle T. Qualitative Methods for the study of lignin distribution in wood and surface layers of unbleached pulp fibres and paper, *J Pulp Pap Sci* **21**(8), 285–287, 1995
  114. Reme P.A., Johnsen P.O., Helle T., Assessment of fibre transverse dimensions using SEM and image analysis, *J Pulp Pap Sci.* **28**(4), pp 122–128, 2002
  115. Dahlström C., Allem R., Uesaka T., Characterization of Microstructures in Paper Coating using FESEM and Argon Ion Beam Milling Technique, submitted to *Journal of Microscopy* 2009
  116. Pohler, T., Juvonen, K., and Sneek, A., “Coating layer microstructure and location of binder – Results from SEM analysis”, *Proc. Tappi Coatings Fundamentals Symposium*, Turku, Finland 8–10 February, pp 89–100, 2006
  117. G. Chinga, P O Johnsen, R Dougherty, E Lunden Berli & J Walter, The Royal Microscopical Society, *Journal of Microscopy*, **227**, 254–265, 2007
  118. Preston J.S., Hiorns A.G., Elton N.J. Strom G., “Application of imaging reflectometry to studies of print mottle on commercially printed coated papers”, *Proc. 2006 Tappi Coating & Graphic Arts Conf.*, Atlanta, April 06, CD ISBN No.1-59510-122-5, 2006
  119. Waech T.G., *Pan Pacific and Int. Printing and Graphic Arts Conf.*, Quebec Oct. 1998, PAPTAC, CANOPY, Toronto, ISBN 1-896742-39-4, 57, 1998
  120. Johansson P-A., Lundby H., Lindberg S., Nystrom S., In J. Anthont Bristow (Ed), **Advances in Colour Reproduction**. *Proc. 28<sup>th</sup> Res. Conf of the Int. Assoc of Research Institutes for the Printing Information and Communication Industries*. GATF, Pittsburg, PA, USA, 2001
  121. Dahlstrom C., Uesaka T., Norgren M., Base Sheet Structures that Control Coating Uniformity: Effects of Length Scale. In *Proc. 2008 Tappi Coating Fundamentals Research Symposium*, Montreal, 2008
  122. Dahlstrom C, Uesaka T., New insights into coating uniformity and base sheet structures, Submitted to *Industrial & Engineering Chemistry Research* 2009
  123. Gibbon, D.L., “Applications of modern electron beam techniques in the analysis of coated papers”, *Proc. Tappi Coating Conference*, Tappi Press, Atlanta GA, pp 53–64, 1988
  124. Kuang S.J., Ferguson C.A., Rezanowich A., Lepoutre P., “Use of X-ray analysis for measuring the polymer distribution in latex-treated paper”, *Tappi J.*, **67**(8), pp 86–88, Aug 1984
  125. Imerys Internal Test Method
  126. Barros G.G., Influence of substrate topography on ink distribution in flexography, PhD Thesis Karlstad University, Karlstad, Sweden, 2006
  127. Parker J.R., An air leak instrument to measure printing roughness of paper and board, *Pap. Technol.* **6**(2), 126–130, 1965

128. Parker J.R., Development and application of a novel roughness tester, *Tappi J* **54**(6), 943–949, 1971
129. Bekk J., Apparatus for measuring smoothness of paper surfaces, *Paper Trade J*, **94**(26), 41–42, 1932
130. T479 om-91 “Smoothness of paper (Bekk Method), Tappi test methods, 1994–1994, Tappi Press, Atlanta, 1994
131. Bendtsen C., New methods for testing printing paper quality, *Paper Maker* **98**, TS135–TS154, 1939
132. T538 om-88 “Smoothness of paper and paperboard” (Sheffield method) TAPPI Test methods 1994–1994, Tappi Press Atlanta 1994
133. Kent H.J., The fractal dimensions of paper surface topography, *Nord. Pul. Pap. Res. J.*, **4**, 1991–1996, 1991
134. Gane P.A.C., Hooper J.J., Baumeister M., The influence of furnish content on formation and basesheet profile stability during coating, *Tappi J*, **74**(9), 193–201, 1991
135. Gane P.A.C. & Hooper J.J. (1989) An evaluation of interactions between coating colour and basepaper by coating profile analysis pp 871–894 in: *Trans. 9th Fundamental Research Symp., Cambridge*, (Baker & Punton, editors). Mech. Eng. Publications
136. Kent H., Climpson N.A., Coggon L., Hooper J.J., Gane P.A.C., “Application of novel techniques for quantitative characterisation of coating structure”, *Proc. 1986 Tappi Coating Conference*, tappi Press, Atlanta GA pp 103–112, 1986
137. l’Anson S., 3D laser surface profiling of paper and board, *Proc. 1996 PITA annual conference, Paper Technology*, pp 43–49, March 1997
138. Mercier C., Bloch J.F., Baudin P.G., Different techniques to analyze surface topography, *Proc. 2002 Int Print & Graphic Arts Conf*, Bordeaux, Volume 2.
139. Wagberg P., Johansson P.-A., A comparison between optical and mechanical sensing on printing papers, *Tappi J*, **76**(12), 115–121, 1993
140. Soysouvanh D., Eymin-Petot-Tourtollet G., Sabater J., A new tool for fast surface characterization, *Proc. 2002 Int Print & Graphic Arts Conf.*, Bordeaux, France, Volume 2
141. Hansson P, Johansson P.A., A new method for the simultaneous measurement of surface topography and ink distribution on prints., *Nord Pul., Pap Res J.*, **14** (4) 314–319, 1999
142. Hansson P, Johansson P.A., Topography and reflectance analysis of paper surfaces using a photometric stereo method, *Optical Engineering*, **39** (9), 2555–2561, 2000
143. Land C., Laboratory method for the study of moisture-induced waviness in paper, Licentiate Thesis, University of Karlstad, Karlstad, Sweden, 2004
144. Nordstrom J.E., Lindberg S., Lundstrom A., Human perception and optical measurement of HSWO waviness, *Proc. 2002 Int. Print. & Graphic Arts Conf.*, Bordeaux, Volume 2, 2002
145. Barros G.G., Fahlcrantz C.-M., Johansson P.A., Topographic description of Uncovered areas in full tone flexographic printing, *TAGA J*, **2**, pp 43–57, 2005

146. Elton N.J., Preston J.S., “Polarized light reflectometry for studies of paper coating structure: part I Method and Instrumentation” *Tappi J.*, **5**, (7), pp 8–15, 2006
147. Gate, L.F. & Leaity, K. “New Aspects on the Gloss of Coated Paper.” *Proc. 1991 Tappi Coating Conference Proceedings*, TAPPI Press, Atlanta, p 473, 1991
148. Gate, L.F. & Parsons, D.J., The specular reflection of polarized light from coated paper. *Trans. 10<sup>th</sup> Fundamental Research Symposium, Oxford*, 1993, pp 263–284.
149. Gate, L.F, Windle, W. & Hine, M. “The relationships between gloss and micro-texture of coatings.” *Tappi J.*, **56**, 61–64, 1973
150. Preston, J.S. & Gate, L.F. The influence of colour and surface topography on the measurement of effective refractive index of offset printed coated papers, *Colloids and Surfaces A: Physicochem. Eng. Aspects.* 252, 99–104, 2004
151. Elton N.J., Preston J.S., Polarized light reflectometry for studies of paper coating structure – Part II. Application to coating structure, gloss and porosity. *Tappi Journal*, **5** (8), pp 10–16, 2006
152. J.S. Preston, D.J. Parsons, J.C. Husband, C. Nutbeam “Ink gloss development mechanisms at short time-scales after printing. Part 2 – The influence of substrate”. *Proc. 2003 Tappi Fundamentals Conference*. Chicago, May 2003
153. Preston J.S., Parsons D.J., Gate L.F., Husband J.C, Legrix A., Jones M, Ink gloss development mechanisms at short time-scales after printing- Part 1 – The influence of ink film thickness, *Proc. 2002 International Printing & Graphic Arts Conf.* Bordeaux, 2002
154. Koivula H., Jutti M., Bousfield D., Preston J., Silvennoinen R., Peiponen K-E., Toivakka M., Comparison of dynamic gloss measuring techniques, *Tappi J.*, 2009 [http://www.tappi.org/s\\_tappi/bin.asp?CID=9428&DID=562721&DOC=FILE.PDF](http://www.tappi.org/s_tappi/bin.asp?CID=9428&DID=562721&DOC=FILE.PDF)
155. Mangin P., Beland M-C, Three dimensional evaluation of paper surfaces using confocal microscopy Part 1: Research and Development applications, In *Proc. 22<sup>nd</sup> IARIGAI Research Conf. Advances in Printing Sci and Technol.* Munich pp 159–186
156. MacGregor M.A., Johansson P.A., Beland M-C., Small scale gloss variations in prints – Paper topography explains much of the variation. In *Proc. 1994 International Printing & Graphic Arts Conf.*, Tappi Press Atlanta, pp 33–43, 1994
157. MacGregor M.A., Johansson P.A., Gloss uniformity in coated paper – measurements of commercial paper., In *Proc. 1991 Tappi Coating Conf.*, Tappi Press Atlanta, pp 495–504, 1991
158. Beland M-C., Mangin P.J., Three dimensional evaluation of paper surfaces using confocal microscopy in **Surface Analysis of Paper**, (ed. Connors and Banerjee) CRC Press, Boca Raton, USA, 1995
159. Preston J.S., Bollstrom R., Nylander K., Toivakka M., Peltonen J., Rotogravure printability of coated paper samples – development of a new test to measure dynamic contact under the printing nip, IARIAGI conference Valencia Spain, 2008 in *Advances in Printing and Media Technology* vol. XXXV pp 147–155, 2008

160. Mangin P.J., Beland M-C., Cormier L.M., Paper surface compressibility and printing. In *Proc. 1994 International Printing and Graphic Arts Conference*, Tappi Press, Atlanta, pp 19–31, 1994
161. Jarnstrom J., P. Ihalainen, K. Backfolk, J. Peltonen Roughness of pigment coatings and its influence on gloss, *Applied Surface Science*, **254** 5741–5749, 2008
162. Hirai K., Bousfield D.W., Characterization of paper coating penetration by Laser Scanning Microscopy, *Proc. 9<sup>th</sup> Tappi Fundamentals Symp.*, Turku, Finland, pp 101–115, Feb 2006
163. Ozaki Y., Bousfield D.W., Shaler S., Application of confocal laser scanning microscopy to the study of backtrap mottle, *Proc. Tappi 2006 Int. Printing & Graphic Arts Conf.*, Cincinnati, Ohio, 2006
164. Ozaki Y., Bousfield D., Shaler S.M., The 3-d observation of the ink penetration in paper by confocal scanning laser microscope, *Proc. 2004 Tappi Int. Print. & Graphic Arts Conf.* Vancouver, Canada, Oct 4–6 pp 117–122, 2005
165. Nanko H., Ohsawa J., “Scanning laser microscopy of the drying process of wet webs”, *J. of Pulp & Paper Sci.*, **16**(1), J6–J12, 1990
166. Nanko H., Wu J., Mechanisms of paper shrinkage during drying, In *Proc. 1995 Int. Paper Physics Conf.*, pp 103–113, Niagra on the Lake ON, Canada, CPPA, 1995
167. Jang H.F., Robertson A.G., Seth R.S., Optical sectioning of pulp fibres using confocal scanning laser microscopy, *Tappi J.*, **73**(11) pp 267–268, 1991
168. Jang HF, Amiri R, Seth S & Karnis A, Fiber characterization using confocal microscopy – collapse behaviour of mechanical pulp fibers. *Tappi Journal* **79**(4): 203–210, 1996
169. Reme P.A., Johnsen P.O., Helle T., Assessment of fibre transverse sections using SEM and image analysis, *J Pulp, Pap. Sci.* **28**(4), 122–128, 2002
170. Beland, M-C., CLSM and AFM applied in pulp and paper research: A literature review, In *proc. The European conference on pulp and paper*. October 1996, Stockholm, Sweden, 1996
171. Wygant R., Pruett R.J., Chen C.Y., “A review of techniques for characterizing paper coating surfaces, structure and printability”, *Proc. 2005 Coating Fundamentals Symposium*, Dallas, TX, pp 1–15 (1995)
172. Binnig G., Quate C.F., Gerber C., Atomic force microscope, *Physical Review Letters*, **56**(9), pp 930–933, 1986
173. Nilsson, T., “Atomic Force Microscope, a new tool in coating research”, *Nord. Papperstidn.* No 10, Oct 2004, pp 36–37
174. Missori, M., Mondelli, C., De Spirito M., Castellano, C., Bicchieri, M., Schweins, R., Arcovito, G., Papi, M. and Congiu Castellano A. Modifications of the Mesoscopic Structure of Cellulose in Paper Degradation, *Physical Review Letters*, **97**, 238001, 2006
175. Hanley, S.J., and Gray, D.G., Atomic Force Microscopy, Paper from **Surface Analysis of Paper**, Chapter 14, pp 301–324, Eds. Conners T.E., Banerjee S., CRC Press, Boca Raton, New York, 1995

176. Lulevich, V., Honig C., and Ducker, W. A., An atomic force microscope tip as a light source, *Science instrument. Journal*, **76** (12), 123702 (5 pp). 2007
177. D’Orlando, A., “Analysis of Coated Paper”, LOT-Oriel Group, Europe, 2007
178. [http://www.pacificnano.com/nano-roughness\\_single.html](http://www.pacificnano.com/nano-roughness_single.html), “AFM for Nano-Surface Texture/roughness”, 2007
179. [http://www.pacificnano.com/application\\_part.html](http://www.pacificnano.com/application_part.html), “AFM Applications”, 2007
180. Takahashi, H., Numao, S., Bandow, S., and Iijima, S., AFM imaging of wrapped multiwall carbon nanotube in DNA, *Chem. Phys. Lett journal*, **418** (4–6), pp 535–539, 2006
181. Pyo, S., Oh, Y., and Yi, M., Organic thin-film transistors with submicrometer channel length fabricated by atomic force microscopy lithography, *Chem. Phys. Lett journal*, **419** (1–3), pp 115–119, 2006
182. Di Risio, S., and Yan, N., Characterising coating layer z-directional binder distribution in paper using atomic force microscopy, *Colloids and Surfaces A: Physicochem. Eng. Aspects*, 289 65–74, 2006
183. Haunschild A., Pfau A., Schmidt-Thümmes J., Graf K., Lawrenz D., Gispert N., “Surface of coated papers studied by AFM – influence of plastic pigments on microstructure and gloss” *Proc. 1998 Tappi Coating Conference*, Tappi Press, Atlanta GA 1998
184. Larsson M., Vidal D., Engstrom G., Zou X., Paper coating properties as affected by pigment blending and calendaring, *Tappi J.*, **6** (8), 16–22, 2007
185. Jarnstrom J., Sinervo L., Toivakka M., Peltonen J., Topography and gloss of precipitated calcium carbonate coating layers on a model substrate, *Tappi J.*, **6**(5) 23–31 2007
186. Wallstrom A., Jarnstrom L., Hansen P., Peltonen J., Effects of carboxymethyl cellulose and ethyl hydroxyethyl cellulose on the surface structure of coatings drawn down from polystyrene suspensions, In *Proc. Tappi, Advanced Fundamentals Symposium*, ISBN 1-930657-04-8 Tappi Press, Atlanta, 2003
187. Wallstrom A., Jarnstrom L., The influence of thickeners on the surface structure of coatings evaluated by AFM and pair distribution function analysis – relationship between surface structure, colloidal stability and viscosity, *Nordic Pulp & Paper J.*, **20** (4) pp 481–489, 2005
188. Wallstrom A., The consolidation process studied by means of atomic force microscopy, PhD Thesis Karlstad University, 2005.
189. Chinga-Carrasco G., Kauko H., Myllys M., Timonen J., Wang B., Zhou M., Fossum J.O., New advances in the 3D characterization of mineral coatings on paper, *J Microscopy*, **232**, (2) pp 212–224, 2008
190. Gelinas V., Vidal D., Determination of particle shape distribution of clays using an automated AFM image analysis method, Tappi Advanced Coating Fundamentals Symposium, Montreal, 2008
191. Santos J.P., Corpart P., Wong K., Galembeck F., Heterogeneity in Styrene-Butadiene Films, *Langmuir*, **20**, pp 10576–10582, 2004
192. Granier V., Sartre A., Joanicot M., Adhesion of latex particles on inorganic surfaces, *Proc. 1994 Tappi Coating Conference*, Tappi Press Atlanta GA, 1994

193. Unertl W.N., Wetting and Spreading of Styrene-Butadiene Latexes on Calcite, *Langmuir*, **14**, pp 2201–2207, 1998
194. Carlsson R., Effect of latex viscoelasticity on strength development and calendar runnability in coated paper and board production, Licentiate Thesis Karlstad University Studies, **44**, ISBN 91-7063-015-1, 2005
195. Lin F., Meier D.J., Latex film formation – atomic force microscopy and theoretical results, *Progress in Organic Coatings*, **29**, 139–146, 1996
196. Meineken M., Sanderson R.D., Determination of the influence of polymer structure and particle size on the film formation process of polymers by atomic force microscopy, *Polymer*, **43**, 4947–4955, 2002
197. Kaj Backfolk, Caisa Andersson, Jouko Peltonen, Association between a sodium salt of a linear dodecylbenzene sulphonate and a non-ionic fatty alcohol ethoxylate surfactant during film formation of styrene/butadiene latex, *Colloids and Surfaces A: Physicochem. Eng. Aspects*, **291**, pp 38–44, 2006
198. Strom Strom G., Englund A., Karathanasis M., Effect of coating structure on print gloss after sheet-fed offset printing, *Nordic Pulp & Paper Res J.*, **18** (1), pp 108–114, 2003
199. Bassemir R.W., Costello G., Parris J., The use of atomic force microscopy in graphic arts problem solving, In *Proc. Int. Print and Graphic Arts Conf.*, Tappi Press, Atlanta, pp 159–181, 1994
200. Naito I., Deguchi M., Tsumura S., Koga K., Surface analysis of printed matter by using an atomic force microscope, *Advances in Printing Sci & Technol.* **30**, Acta Graphica Publishers, ISBN 953-96276-8-0, pp 111–117, 2003
201. Carl-Mikael Tag, Mikael Jarn, Bjorn, Granqvist, Joakim Jarnstrom, Jouko Peltonen, Jarl Bjorn Rosenholm, Influence of surface structure on wetting of coated offset papers, *Holzforschung*, **61**, pp. 516–522, 2007
202. Elton, N.J., Hooper, J.J. & Gane, P.A.C. Optical Microscopy of Paper: Methodology and Applications, in *Proc. 1990 EUCEPA Conference*, Stockholm, Sweden, May 1990
203. Quackenbush D., The optical microscope as an analytical tool for studying coated papers, *Proc. 1988 Tappi Coating Conference*, Tappi Press, Atlanta, pp 29–46, 1988
204. Svanholm E., An experimental study of inkjet receptive coatings, Licentiate thesis, Karlstad University, ISBN 91-85335-30-4, 2004
205. Muck T., Novak G., Hydrophilic/Hydrophobic surface treatment of sized and unsized base paper for various digital printing techniques, *Wochenblatt fuer papierfabrikation*, **130**, N 14–15, 2002
206. De Almeida P., Pataki T., Peeters D., Van Roost C., Characterization of printed pigment-based inks on inkjet media using cross-sectional electron microscopy, *Materials and Design*, **25** pp 647–654, 2004
207. Wiltsche M., Donoser M., Bauer W., Bischof H., A new slice based concept for 3D paper structure analysis applied to spatial coating layer formation, *13th Fundamental Research Symp. Cambridge*, pp 853–899, 2005
208. Hata, S., Sosiati, H., Kuwano, N., Itakura, M., and Nakano, T., Removing

- focused ion-beam damages on transmission electron microscopy specimens by using a plasma cleaner, *Electron Microscopy Journal*, **55**, (1), pp 23–26, 2006
209. Bristow, J.A., “Print-through and ink penetration – A mathematical treatment”, In *Proc. 19<sup>th</sup> Research Conference of the International Association of Research Institutes for the Graphic Arts Industry (IARIGAI)*, pp 137–145, Eisenstadt, Austria, June 1987
210. Aspler, J.S., Interactions of ink and water with the paper surface in printing, *Nord. Pulp Pap. Res. J.*, 8(1):68–112, 1993
211. Marttila, J., Preston, J.S., and Husband, J.C., Analysis of ink scuff in heatset web offset printed silk papers, *Proc. 12<sup>th</sup> Int. Print. & Graphic Arts Conf*, Vancouver, Oct 4–6<sup>th</sup> 2004
212. Koivula H., Preston J.S., Heard P.J., Toivakka M., “Visualisation of the distribution of offset ink components printed onto coated paper”, *Colloids & Surfaces A: Physiochem. Eng. Aspects* 317, 557–567, 2008
213. Vucak M., Stover H-D., Holzer K., Plattchenformiges PCC: ein einzigartiges Streichpigment für Inkjet-Papier?, *Wochenblatt für Papierfabrikation*, **22**, pp 1370–1374, 2003
214. H. Uchimura, Y Ozaki, Kimura M., “Observation of the ink penetrated into the inkjet printing papers” *Proc. 12<sup>th</sup> Int. Print. & Graphic Arts Conf*, Vancouver, Oct. 4–6<sup>th</sup>, pp 199–205, 2004
215. Glittenberg D, Voigt A, Donigian D. Novel Pigment-Starch Combination for the Online and Offline Coating of High-quality Inkjet papers, *Paper Technology J*, **44**(7) pp 32, 2003
216. P. J. Heard, J. S. Preston, D. J. Parsons and G. C. Allen, “Visualisation of the distribution of ink components in printed coated paper using focused ion beam techniques” *Colloids and Surfaces A: Physicochemical and Engineering Aspects* **244**, 67–71, Aug 2004
217. Dr Sanna Rousu, Dr Janet Preston, Jan Gustafsson, Dr Peter Heard “Interactions between UV Curing, hybrid-UV and sheetfed Offset Inks and Coated Paper – Part 2 Commercial print trials” *TAGA Journal*, **2**, (3), pp 174–189, April 2006
218. Preston J.S., Heard P.J., Lindqvist B Under the microscope – Visualisation of the distribution of inkjet ink on surface pigmented paper using focused ion beams, *European Coatings Journal (ECJ)* 2004, 2007
219. H. Uchimura, Y. Ozaki and M. Kimura. A sample preparation method for printed paper cross-sections using a focussed ion beam, *Proc. Tappi Int. Print. & Graphic Arts Conf*, Quebec, Canada, pp 121–124, 1998
220. Uchimura H, Ozaki Y. and Maruyama S. Observation of Printing Ink transference to and penetration into paper: Application of the cross-section preparation method using the focussed ion beam, *Proc. 11<sup>th</sup> Int. Print. & Graphic Arts Conf.*, Bordeaux, France, 2002
221. Preston J.S., Toivakka M., Heard P.J., “Visualisation, Modelling and Image Analysis of Coated Paper Microstructure: Particle Shape – Microstructure Interrelations” *Proc. 2<sup>nd</sup> IPEC Conference Tianjin China* 9–11<sup>th</sup> May, pp 833–839, 2008

222. Okayasu T., Kusama S., Tozaki E., Miyagawa T., “Analysis of the Real Micro-structure of the cross section of a coated layer prepared by FIB – Novel method for micropore size distribution measurement”, *Proc. Tappi Int. Coat. Graphic Arts Conf.* pp 183–192. 2001
223. Klug, H.P. and Alexander, L.E., **X-ray Diffraction Procedures**, 2nd ed.: Wiley, New York, p 966, 1974
224. Chen, P.-Y., Table of key lines in x-ray powder diffraction patterns of minerals in clays and associated rocks, Geological Survey Occasional Paper 21, Department of Natural Resources, Bloomington, Indiana, p 67, 1977
225. Anon., Mineral Powder Diffraction File Databook Sets 1–42: International Centre for Diffraction Data, Swarthmore, Pennsylvania, p 781, 1993
226. Klug, H.P. & Alexander, L.E. **X-ray diffraction procedures**, pp 555–585. John Wiley & Sons, New York, 1974
227. Wenk, H-R, Measurement of pole figures. pp. 11–47 in: **Preferred orientation in deformed metals and rocks: an introduction to modern texture analysis** (H-R Wenk, editor). Academic Press, Orlando, 1985
228. Bunge, H.J. Preferred orientation in **Deformed metals and rocks: an introduction to modern texture analysis** (H-R Wenk, editor). Academic Press, Orlando. 73–108, 1985
229. Elton, N.J., Gate, L.F. & Hooper, J.J. “Texture and orientation of kaolin in coatings” *Clay Minerals*, **34**, 89–98, 1999
230. Elton, N.J., Gate, L.F. & Hooper, J.J., Texture and orientation of clays in coatings. Mineralogical Society Clay Minerals Group Golden Jubilee Meeting, Aberdeen, 9–11 April, 1997
231. Kraske, D.J. Methods for the analysis of the physical structure of clay-starch coating films, *Tappi J*, **43**, 73–82, 1960
232. T458 om-89 “Surface wettability of paper (angle of contact method) Tappi test methods”, Tappi Press, Atlanta, 1994
233. Etzler F.M., Bobalek J.F., Weiss M.A., “Surface free energy of paper and inks: printability issues” In *Proc. 1993 TAGA Conference Rochester*, p 225, 1993
234. Wickman M., Hallstenson K., Strom G., Effect of printing ink binder composition on emulsification of fountain solutions, *Jour Pulp Pap. Sci.*, **23**, (4), pp J167–J173, April 1997
235. A.Lundqvist, Odberg L., Berg J.C., *Tappi J.*, **78**, 139, 1995
236. Felix & Gatenholm, *Nordic Pulp Paper Res J.*, 1, p 200, 1993
237. Svanholm E., Strom G., “Using the Micro Drop Absorption Tester (MicroDAT) to Study Droplet Imbibition and its Effect on Inkjet Print Quality”, in Svanholm PhD Thesis Karlstad University 2007
238. Marmur A., Soft contact: measurement and interpretation of contact angles, DOI: 10.1039/b514811c, www.rsc.org/softmatter | *Soft Matter*, **2**, 12–17, 2006
239. Ritter, H.L., and L.C. Drake. 1945. Pore-size distribution in porous materials: Pressure porosimeter and determination of complete macropore-size distributions. *Ind. Eng. Chem. Anal.* **17**, pp 782–786. 1945

240. Larrondo L., St. Amour S., Monasterios C., Proc. *TAPPI coating conference*, Tappi Press, Atlanta GA, pp 79–93, 1995
241. Kettle J.P, PhD Thesis “Investigation and computer modelling of the pore structure of paper and of consolidated pigment coatings” University of Plymouth 1996
242. Kettle J.P., Gane P.A., Matthews G.P., Ridgway C.J., Void space structure of compressible polymer spheres and consolidated calcium carbonate paper-coating formulations, *Ind Chem & Eng. Res. J.*, **35**, pp 1753–1764, 1996
243. Matthews G.P., Moss A.K., Spearing M.C., Voland F., *Powder technol.*, **76**, 95–107, 1993
244. Kettle J.P, Matthews G.P., Proc. 1993 *TAPPI Advanced Coating Fund. Conf.*, Tappi press, Atlanta GA, pp 121–126, 1993
245. Gane P.A.C., Watters P., Pigment Particle Orientation, *Paperi ja Puu*, **71** (5), 517, 1989
246. Legrix A., Nutbeem C., Performance solids relationships for engineered carbonates, *Proc. 2001 Tappi Coating Conf.*, San Diego, Tappi Press, Atlanta GA, 127
247. Ridgway, C.J., Gane, P.A.C. (2007): “Complete Determination of Bulk Density and Coating Porosity”, *Proc. 2007 Tappi Coating and Graphic Arts Conference*, April 22–25, Miami, USA, 2007
248. Furo, I. & Daicic, J. NMR cryoporometry: A novel method for the investigation of the pore structure of paper and paper coatings. *Nordic Pulp and Paper Research Journal*, **14** (3), 221–225, 1999
249. Lehtinen E.I., Ridgway C., Valiullin R., Schoelkopf J., Furo I., Gane P., Paulapuro H., Daicic J., On the comparison of NMR Cryoporometry, mercury intrusion and thermo- porosimetry in characterizing pore size distributions of compressed fine ground calcium carbonate structures, In *Proc. 5<sup>th</sup> Int. Paper & Coating Symposium*, p 135, Montreal, Canada, June 16–19, 2003
250. Pykönen M., Hakola L., Eiroma K., Lahti J., Sundqvist H., Kaukoniemi O-V, M Tuominen, J Järnström, J Peltonen, P Fardim, M Toivakka, Effects of Atmospheric Pressure Plasma Activation on Inkjet Print Quality, *NIP23 and Digital Fabrication 2007 Final Program and Proceedings*, pp 404–409, 2007
251. Pykönen M., Silvaani H., Preston J, Fardim P, and Toivakka M. Influence of Plasma Activation on Absorption of Ink Components and Dampening Water in Sheet-Fed Offset Printing, *IARIGAI 2008 – Advances in Printing and Media Technology*, Valencia, Spain, 2008
252. M. Pykönen, K. Johansson, M. Dubreuil, D. Vangeneugden, G. Ström, P. Fardim and M. Toivakka, 2009, An Attempt to Reduce Dampening Water Absorption Using Hydrophobic Plasma Coatings, *TAGA 61st Annual Technical Conference*, New Orleans, 2009
253. Nutbeem C., Preston J.S., Hallam B., Practical Application of Advanced Analytical Techniques for Investigating Mottle Issues in Coated Papers, *Proc. Austria Paper Conference*, Graz, Austria 22nd–23rd May 2007
254. C.-M. Tåg, M.Pykönen, J.B.Rosenholm, K.Backfolk, Wettability of Model Fountain Solutions and their Influence on Offset Paper Properties, *TAGA 60th Annual Technical Conference*, San Fransisco, 2008

255. Brinen J.S., The observation and distribution of organic additives on paper surfaces using surface spectroscopic techniques, *Nordic Pulp & Paper J.*, **1**, pp 123–129, 1993
256. Gustafsson J., Lehto J.H., Tienvieri T., Ciovica L., Peltonen J., Surface characteristics of thermomechanical pulps; the influence of defibration temperature and refining, *Colloids and Surfaces A: Physicochem. Eng. Aspects* **225** pp 95–104, 2003
257. Pedro Fardim., Johanna Gustafsson, Sebastian von Schoultz, Jouko Peltonen, Bjarne Holmbom, Extractives on fiber surfaces investigated by XPS, ToF-SIMS and AFM, *Colloids and Surfaces A: Physicochem. Eng. Aspects* **255** pp 91–103, 2005
258. Lozo B., Vyorykka J., Vuorinen T., Muck T., Non destructive and spectroscopic methods for depth profiling of inkjet prints. *J. Imag Sci & Technol.*, 50(4), pp 333–370, 2006
259. O Ozaki Y., Uchida M., The characterization of water based gravure ink on coated paper – relationship between the distribution of ink and the printability, In *Proc. 2002 IPGAC*, Bordeaux, **2**, 2002
260. Waddilove A., **Surface analysis for materials characterisation**, International Labmate, pp 49–51

## Transcription of Discussion

# THE SURFACE ANALYSIS OF PAPER

*Janet Preston*

Imerys Minerals Ltd.

### ERRATA

Section **8 Acknowledgements** in the paper should have read:

Thanks are extended to Neil Norouzi, Roger Wygant, Marie Ernsstrom, Gary Chinga Carrasco, Jouko Peltonen for help in providing references.

Many thanks are extended to John Husband, Tony Lyons, Graham O'Neill, Karen Leaity, David Preston and Richard Bown for proof reading this document.

### DISCUSSION

*John Roberts*      University of Manchester

Thank you, Janet, for an excellent presentation. Being one on the committee who has always encouraged this topic to be dealt with, I am delighted to see it has arrived. I just have one question and that is, from personal experience, it has always been difficult to find techniques which would determine the precise molecular state of, say, an additive in paper. Examples would be sizing chemicals which may be covalently bound, or maybe wet strength agents which may be cross-linked in some way. Do you see any techniques now or in the future that might solve that problem?

*Janet Preston*

I guess that's quite a tricky thing to do, but I would think from looking at the literature that maybe the XPS would give you the most information, especially concerning the type of the bonding. Infrared techniques may be useful too. I'm looking at Agne Swerin from YKI who might have some other ideas too. Have you got any comments, Agne?

## *Discussion*

*Agne Swerin*      YKI – Institute of Surface Chemistry

Yes, I agree that XPS would be a very good combination with SIMS. But, if you are particularly looking for molecular state and bonding, maybe imaging IR could be useful or a combination with confocal Raman. As for the future developments of chemical mapping, IR is down to micrometre resolution, and I think in the future can possibly go down further. I have a comment also on what you said in one of your slides, and I think it is also in the paper, that Raman is less sensitive towards water, but actually I would say it is the other way around. It is semantics to some degree, but there is a more specific peak for water if you look in the Raman spectrum compared to the IR for water. So, you can actually use Raman spectroscopy to analyze water content.

*Janet Preston*

Yes, I take your point, but I was thinking of it as more of a “contaminant” or interference when you were trying to avoid the moisture in a sample.

*Agne Swerin*

Yes. So in IR, you get more interference from water.

*Janet Preston*

Yes, that is what I was thinking of, and what I gleaned from the literature.

*Agne Swerin*

Thanks for an excellent review.

*Jukka Ketoja*      VTT

In the ink layers, do you observe porosity at any scale ever?

*Janet Preston*

I have not seen any porosity in an offset ink film, or in a rotogravure ink film, but I would say in an ink-jet film, definitely, and a flexo-ink film, possibly. Previously we have used focused ion beam (FIB) to cut through an ink-jet print made with a black HP pigmented ink. The FIB technique had such a good resolution that it was possible to observe the pores within the dried ink layer. However, in an offset ink film I have never observed any pores.

*Kim Tae-Young* KOMSCO

In our dipping process of papermaking, a polyvinyl alcohol (PVOH) solution has been used for impregnation. It is assumed that the inner side PVOH molecules migrate to the surface layer at the drying stage. Could you recommend the best way to estimate the distribution of PVOH at the surface or in a cross-section?

*Janet Preston*

For PVOH, I guess you could use the infrared techniques (ATR-IR), or the Raman technique in a similar manner to the first two latex example results. I would think that would probably give you the best results. It is important to run a spectrum for the binder itself to see and check that there is a peak which does not overlap with the other constituents in your paper or colour. If you can find a peak which is just due to PVOH, then you can make your calibration curve and then look at your production samples. Either of those techniques could be used.